



Cape Peninsula
University of Technology

**AN APPROACH TO VOLTAGE QUALITY ENHANCEMENT IN WIND ENERGY
CONVERSION SYSTEMS**

by

RUAN ESTERHUIZEN

Thesis submitted in partial fulfilment of the requirements for the degree

Master of Engineering in Energy

in the Faculty of Engineering & the Build Environment

at the Cape Peninsula University of Technology

Supervisor: Prof Khaled Aboalez

**Bellville
March 2023**

CPUT copyright information

The dissertation may not be published either in part (in scholarly, scientific or technical journals), or as a whole (as a monograph), unless permission has been obtained from the University

DECLARATION

I, Ruan Esterhuizen, declare that the contents of this thesis represent my own unaided work, and that the dissertation has not previously been submitted for academic examination towards any qualification. Furthermore, it represents my own opinions and not necessarily those of the Cape Peninsula University of Technology.



Signed

7/03/2023

Date

ABSTRACT

Given the obstacles posed by legislation, pollution, and the depletion of nonrenewable energy sources, electricity production is progressively turning toward renewable energy sources such as the sun and wind. Wind energy looks to account for a considerable proportion of power production in developed nations relative to other renewable energy sources. As energy demand grows, the incorporation of renewable energy into the nation's electrical systems is expanding considerably. This has shown a variety of benefits, including meeting demand increases, providing energy security, and contributing to the decarbonization of the energy system. However, as the usage of renewable energy sources increases, the power system becomes more unstable, especially in the event of grid faults. Wind farms must comply with grid code standards to avoid the collapse of the power system. External electrical grid factors, such as the unpredictability of the wind and power electronics in wind turbine applications, may affect power quality. Even though there have been significant technical advancements in wind energy production on a worldwide scale, transmission system operators continue to be concerned about power quality and system stability. Consequently, evaluating the effects of power quality is vital and necessary. Transmission system operators developed rules and grid code standards to analyze the power quality of wind energy prior to incorporating it into the grid. The IEC 61400-21 standard is one of the most widely used and well-known requirements for describing the power quality of wind turbines.

The primary focus of this dissertation is voltage quality, one of the power quality issues that impede the connection of wind energy plants to the electrical grid. The study evaluates the quality characteristics of harmonic distortion, voltage flickering, voltage fluctuation, voltage unbalance, voltage sag, voltage swell, undervoltage, and overvoltage. In addition, a technique for enhancing voltage quality was evaluated in order to mitigate the consequences of voltage quality issues during any occurrence that might disrupt the electrical system. In order to enhance the efficiency of power transmission in power systems, the Flexible AC Transmission System (FACTS) controllers Static VAR Compensator (SVC) and Static Synchronous Compensator (STATCOM) are widely used. Wind energy conversion systems (WECS) have used FACTS controllers to enhance their transient stability, voltage quality, and regulation.

When SVC and STATCOM are connected to the electrical grid, simulation results in the MATLAB/Simulink environment indicate that their reactive power assistance to the electrical grid during fault situations has a significant impact on the voltage profile and reduces the recovery time following any fault. STATCOM operated somewhat faster than SVC under fault circumstances and supplied more reactive power during severe faults when the bus voltage was lower.

ACKNOWLEDGEMENT

I would want to thank my family and parents for their assistance, understanding, and patience while I worked to complete my dissertation.

In addition, I would like to express my appreciation to my dissertation adviser, Professor Khaled Aboalez, for his assistance and encouragement during the writing process.

TABLE OF CONTENTS

| | |
|---|-----|
| DECLARATION | ii |
| ABSTRACT | iii |
| ACKNOWLEDGEMENT | iv |
| TABLE OF CONTENTS..... | v |
| LIST OF FIGURES | vii |
| LIST OF TABLES | ix |
| CLARIFICATION OF BASIC TERMS AND CONCEPTS..... | x |
| CHAPTER ONE: INTRODUCTION..... | 1 |
| 1.1 Introduction..... | 1 |
| 1.2 Statement of the research problem..... | 2 |
| 1.3 Background to the research problem | 2 |
| 1.4 Hypotheses or research questions..... | 2 |
| 1.5 Objectives of the research | 2 |
| 1.6 Research design and methodology..... | 3 |
| 1.7 Delineation of the research | 4 |
| 1.8 Significance of the research..... | 4 |
| 1.9 Expected outcomes, results, and contributions of the research | 4 |
| 1.10 Dissertation organization | 5 |
| 1.11 Summary and Conclusion..... | 5 |
| CHAPTER TWO: LITERATURE REVIEW | 6 |
| 2.1 Introduction..... | 6 |
| 2.2 Renewable energy..... | 6 |
| 2.2.1 Types of Renewable energy: | 7 |
| 2.2.1.1 Wind Energy | 8 |
| 2.2.1.2 Solar Energy..... | 8 |
| 2.2.1.3 Hydro Energy..... | 9 |
| 2.2.1.4 Bio Energy..... | 9 |
| 2.2.1.5 Geothermal energy | 10 |
| 2.2.1.6 Marine energy..... | 10 |
| 2.3 The electrical grid | 11 |
| 2.4 Renewable energy integration | 12 |
| 2.5 Wind energy conversion system (WECS) | 13 |
| 2.5.1 Parts of the HAWT..... | 15 |
| 2.5.2 WECS configurations..... | 16 |
| 2.5.3 Wind turbine power characteristics | 17 |
| 2.6 General power quality issues | 19 |
| 2.7 Power quality characteristic in WECS based on IEC 61400-21 | 21 |
| 2.7.1 Harmonics distortion | 21 |
| 2.7.2 Flicker and voltage fluctuation | 23 |
| 2.7.3 Voltage unbalance | 25 |
| 2.7.4 Voltage sag | 26 |
| 2.7.5 Voltage swell | 27 |
| 2.7.6 Undervoltage | 28 |
| 2.7.7 Overvoltage | 28 |
| 2.8 Grid strength..... | 29 |
| 2.9 Voltage quality enhancement in WECS | 30 |
| 2.9.1 Reactive power/voltage control..... | 31 |
| 2.9.2 Power filters..... | 32 |
| 2.9.3 Low-voltage ride-through capability | 35 |
| 2.9.4 Flexible AC transmission controllers | 37 |

| | | |
|---|--|-----|
| 2.9.4.1 | Static VAR Compensator (SVC) | 38 |
| 2.9.4.2 | Static Synchronous Compensator (STATCOM) | 40 |
| 2.10 | Summary and Conclusion..... | 42 |
| CHAPTER THREE: MATHEMATICAL MODELING | | 44 |
| 3.1 | Introduction..... | 44 |
| 3.2 | Variable pitch wind turbine..... | 45 |
| 3.3 | Induction generator..... | 45 |
| 3.4 | Transformer..... | 48 |
| 3.5 | Transmission line..... | 50 |
| 3.5.1 | Short transmission line | 52 |
| 3.6 | Static VAR compensator (SVC) | 53 |
| 3.7 | Static Synchronous Compensator (STATCOM) | 57 |
| 3.8 | Summary and Conclusion..... | 61 |
| CHAPTER FOUR: COMPUTER MODELING..... | | 62 |
| 4.1 | Introduction..... | 62 |
| 4.2 | Wind turbine induction generator | 62 |
| 4.3 | Static VAR Compensator (SVC) | 64 |
| 4.4 | Static Synchronous Compensator (STATCOM) | 67 |
| 4.5 | STATCOM and SVC monitoring signals | 69 |
| 4.6 | Complete simulation models..... | 70 |
| 4.6.1 | SVC model | 70 |
| 4.6.2 | STATCOM model | 71 |
| 4.7 | Summary and Conclusion..... | 72 |
| CHAPTER FIVE: SIMULATION RESULTS AND DISCUSSIONS | | 73 |
| 5.1 | Introduction..... | 73 |
| 5.2 | Reference WECS modeling with a momentary fault condition | 73 |
| 5.3 | Newly designed WECS modeling with momentary fault conditions | 78 |
| 5.3.1 | Momentary fault conditions without and with FACTS controllers..... | 82 |
| 5.3.1.1 | Line-to-ground fault..... | 83 |
| 5.3.1.2 | Line-to-line fault | 85 |
| 5.3.1.3 | Three-phase fault | 90 |
| 5.4 | Summary and Conclusion..... | 95 |
| CHAPTER SIX: CONCLUSION AND FUTURE WORK..... | | 97 |
| 6.1 | Introduction..... | 97 |
| 6.2 | Objective – Specific conclusions..... | 97 |
| 6.2.1 | Objectives 1,2,3 and 4..... | 98 |
| 6.2.2 | Objective 5 | 98 |
| 6.2.3 | Objectives 6 and 7 | 99 |
| 6.3 | Future work | 100 |
| REFERENCES | | 101 |
| APPENDIX A: Computer modeling components | | 107 |
| 8.1 | Three-phase programmable voltage source | 107 |
| 8.2 | Three-phase mutual inductance Z1-Z0 | 108 |
| 8.3 | Three-phase transformer | 109 |
| 8.4 | Grounding transformer..... | 110 |
| 8.5 | Three-phase PI Section | 111 |
| 8.6 | Three-phase parallel RLC load | 112 |
| 8.7 | Three-phase V-I measurement | 113 |
| 8.8 | Three-Phase Fault..... | 114 |
| 8.9 | Three-Phase Series RLC Load..... | 115 |
| APPENDIX B: Reference model parameters and computer model | | 116 |

LIST OF FIGURES

| | |
|--|----|
| Figure 2.1: RES rate increase of energy generation | 7 |
| Figure 2.2: Classification of renewable energy | 7 |
| Figure 2.3: General layout for an electrical grid..... | 11 |
| Figure 2.4: Wind energy conversion system | 14 |
| Figure 2.5: (a) HAWT and (b) VAWT | 14 |
| Figure 2.6: Wind turbine energy conversion layout | 15 |
| Figure 2.7: Type 3 (a) and type 4 (b) wind turbine configuration | 16 |
| Figure 2.8: Wind turbine power coefficient curve..... | 18 |
| Figure 2.9: Wind turbine power characteristics curve | 19 |
| Figure 2.10: Flow diagram of PQ issues | 20 |
| Figure 2.11: Harmonic waveforms | 22 |
| Figure 2.12: Voltage fluctuations at the load | 24 |
| Figure 2.13: Voltage unbalance in a three-phase system..... | 25 |
| Figure 2.14: Voltage sag caused by a fault | 26 |
| Figure 2.15: Voltage swell..... | 27 |
| Figure 2.16: Undervoltage trend | 28 |
| Figure 2.17: Overvoltage trend | 29 |
| Figure 2.18: Power filters classification | 32 |
| Figure 2.19: (A) Shunt active power filter, (B) Series active power filter, and (C) Hybrid active power filter..... | 34 |
| Figure 2.20: Grid code requirement during fault consists of (a) Ride-through curve and (b) Reactive power support curve..... | 35 |
| Figure 2.21: European grid code requirements of grid-connected wind power plant | 36 |
| Figure 2.22: SVC in WECS..... | 38 |
| Figure 2.23: (a) SVC V-I characteristics curve, (b) SVC V-Q characteristics curve | 40 |
| Figure 2.24: STATCOM in WECS..... | 41 |
| Figure 2.25: (a) STATCOM V-I characteristics curve, (b) STATCOM V-Q characteristics curve..... | 41 |
| Figure 2.26: Output waveforms for square-wave modulation and pulse-width modulation ... | 42 |
| Figure 3.1: Block diagram for the proposed virtual simulation model..... | 44 |
| Figure 3.2: Control system for pitch angle control | 45 |
| Figure 3.3: (a) Squirrel cage induction generator connected to an electrical, (b) Steady-state equivalent circuit in terms of resistances and reactances, and (c) Steady-state equivalent circuit in terms of impedances..... | 46 |
| Figure 3.4: Per-phase transformer equivalent circuit..... | 48 |
| Figure 3.5: ABCD matrix representation..... | 52 |
| Figure 3.6: Short-length line equivalent circuit | 52 |
| Figure 3.7: (a) Basic layout of SVC, where T_C1, T_C2, and C are the switching thyristors and capacitor of the TSC; and T_L1, T_L2, and L are the switching thyristors and inductor of the TCR. (b) Variable susceptance SVC model | 54 |
| Figure 3.8: Control principle of SVC operation | 55 |
| Figure 3.9: TCR susceptance versus firing angle..... | 56 |
| Figure 3.10: STATCOM system overview | 57 |
| Figure 3.11: (a) Phasor diagram of capacitive operation, and (b) Phasor diagram of inductive operation..... | 58 |
| Figure 3.12: STATCOM reactive power control model | 58 |
| Figure 3.13: STATCOM control block diagram..... | 59 |
| Figure 3.14: STATCOM equivalent circuit..... | 60 |
| Figure 4.1: Wind turbine generator block icon..... | 62 |
| Figure 4.2: Wind turbine induction generator detailed model..... | 63 |
| Figure 4.3: Wind turbine generator setup block..... | 63 |
| Figure 4.4: Wind turbine setup block..... | 64 |
| Figure 4.5: SVC block icon..... | 64 |
| Figure 4.6: SVC block setup | 65 |

| | |
|--|-----|
| Figure 4.7: SVC block control model..... | 66 |
| Figure 4.8: SVC signal monitoring blocks..... | 66 |
| Figure 4.9: STATCOM block icon..... | 67 |
| Figure 4.10: STATCOM block setup | 67 |
| Figure 4.11: STATCOM block control model..... | 68 |
| Figure 4.12: STATCOM controller model | 68 |
| Figure 4.13: STATCOM signal monitoring blocks..... | 69 |
| Figure 4.14: STATCOM and SVC monitoring signal blocks..... | 69 |
| Figure 4.15: Complete SVC simulation model..... | 70 |
| Figure 4.16: Complete STATCOM simulation model..... | 71 |
| Figure 5.1: Complete reference model with SVC controller | 74 |
| Figure 5.2: Complete reference model with STATCOM controller | 75 |
| Figure 5.3: Fault location for the reference model | 75 |
| Figure 5.4: Reference model - Voltage profile at B13.8 - Line-to-line fault..... | 76 |
| Figure 5.5: Reference model - Reactive power supplied at B13.8 from the FACTS controllers | 77 |
| Figure 5.6: Reference model settling time..... | 77 |
| Figure 5.7: Complete SVC simulation model..... | 79 |
| Figure 5.8: Complete STATCOM simulation model..... | 79 |
| Figure 5.9: B25 active power – (line-to-ground fault) w/o and w/FACTS controllers | 83 |
| Figure 5.10: B25 reactive power – (line-to-ground fault) w/o and w/FACTS controllers | 84 |
| Figure 5.11: Reactive power provided by the SVC and STATCOM controller during fault condition (line-to-ground fault) | 84 |
| Figure 5.12: B25 positive sequence voltage – (line-to-ground fault) w/o and w/FACTS controllers | 85 |
| Figure 5.13: B25 active power – (line-to-line fault) w/o and w/FACTS controllers..... | 86 |
| Figure 5.14: B25 reactive power – (line-to-line fault) w/o and w/FACTS controllers | 87 |
| Figure 5.15: Reactive power provided by the SVC and STATCOM controller during fault condition (line-to-line fault)..... | 87 |
| Figure 5.16: B25 positive sequence voltage – (line-to-line fault) w/o and w/FACTS controllers | 88 |
| Figure 5.17: B575 voltage for wind turbine generator sets – (line-to-line fault) w/o and w/FACTS controllers..... | 89 |
| Figure 5.18: Tripping condition for the grid w/o FACTS controllers attached – (three-phase fault) | 90 |
| Figure 5.19: B575 voltage for wind turbine generator sets – (three-phase fault) w/o and w/FACTS controllers..... | 91 |
| Figure 5.20: B25 active power – (three-phase fault) w/o and w/FACTS controllers..... | 91 |
| Figure 5.21: Sets of generator rotor speeds – (three-phase fault) w/o and w/FACTS controllers..... | 92 |
| Figure 5.22: B25 reactive power – (three-phase fault) w/o and w/FACTS controllers..... | 93 |
| Figure 5.23: Reactive power provided by the SVC and STATCOM controller during fault condition (three-phase fault) | 93 |
| Figure 5.24: B25 positive sequence voltage – (three-phase fault) w/o and w/FACTS controllers..... | 94 |
| Figure 8.1: Three-phase programmable voltage source icon | 107 |
| Figure 8.2: Three-phase programmable voltage source setup | 107 |
| Figure 8.3: Three-phase mutual inductance Z1-Z0 icon..... | 108 |
| Figure 8.4: Three-phase mutual inductance Z1-Z0 setup..... | 108 |
| Figure 8.5: Three-phase transformer icon | 109 |
| Figure 8.6: Three-phase transformer setup..... | 109 |
| Figure 8.7: Grounding transformer icon..... | 110 |
| Figure 8.8: Grounding transformer setup | 110 |
| Figure 8.9: Three-phase PI Section icon..... | 111 |
| Figure 8.10: Three-phase PI section setup | 111 |
| Figure 8.11: Three-phase parallel RLC load icon..... | 112 |
| Figure 8.12: Three-phase parallel RLC load setup..... | 112 |

| | |
|--|-----|
| Figure 8.13: Three-phase V-I measurement icon | 113 |
| Figure 8.14: Three-phase V-I measurement setup | 113 |
| Figure 8.15: Three-phase fault block icon | 114 |
| Figure 8.16: Three-phase fault block setup | 114 |
| Figure 8.17: Three-Phase series RLC Load block icon | 115 |
| Figure 8.18: Three-Phase series RLC Load setup block | 115 |
| Figure 9.1: Complete reference model without FACTS controller..... | 117 |

LIST OF TABLES

| | |
|---|-----|
| Table 1: Clarification of basic terms and concepts | ix |
| Table 2: Glossary of terms | x |
| Table 2.1: Voltage magnitude and duration for LVRT international grid codes | 37 |
| Table 5.1: Reference model results | 78 |
| Table 5.2: Parameters of the WECS | 80 |
| Table 5.3: Parameters of the FACTS controllers..... | 81 |
| Table 5.4: Parameters of the wind turbine protection system | 81 |
| Table 5.5: Line-to-ground fault results..... | 85 |
| Table 5.6: Line-to-line fault results | 89 |
| Table 5.7: Three-phase fault results..... | 95 |
| Table 9.1: Parameters of the reference WECS model..... | 116 |
| Table 9.2: Parameters of the reference FACTS controllers..... | 117 |

CLARIFICATION OF BASIC TERMS AND CONCEPTS

List of abbreviations

Table 1: Clarification of basic terms and concepts

| Abbreviation | Definition |
|-------------------|---|
| IEC | International electrotechnical commission |
| PCC | Point of common coupling |
| AC | Alternating current |
| TSO | Transmission system operators |
| WECS | Wind energy conversion systems |
| MW | Megawatt |
| RES | Renewable energy sources |
| PV | Photovoltaic |
| CSP | Concentrated solar power |
| °C | Degree Celsius |
| °F | Degree Fahrenheit |
| HAWT | Horizontal axis wind turbines |
| VAWT | Vertical axis wind turbines |
| DFIG | Doubly-fed induction generator |
| VSC | Voltage source convertor |
| kg/m ³ | Kilogram per cubic meter |
| m | Meter |
| m/s | Meter per second |
| rpm | Revolutions per minute |
| PQ | Power quality |
| IEEE | Institute of Electrical and Electronics Engineers |
| Hz | Hertz |
| IGBT | Insulated-gate bipolar transistor |
| THD | Total harmonic distortion |

| | |
|------------------|-----------------------------------|
| RMS | Root-mean-squared |
| GSC | Generator side converter |
| VUF | Voltage unbalance factor |
| p.u | Per-unit |
| SCR | Short-circuit ratio |
| SVC | Static VAR compensators |
| STATCOM | Static synchronous compensator |
| ms | milliseconds |
| LVRT | Low-voltage ride-through |
| TCR | Thyristor-controlled reactor |
| TSC | Thyristor-switched capacitor |
| V-I | Voltage-current |
| V-Q | Voltage-reactive power |
| VA _r | Volt-ampere reactive |
| MMF | Magnetomotive force |
| PLL | Phase-locked loop |
| DC | Direct current |
| PWM | Pulse-width modulation |
| kV | kilovolt |
| MVA | Mega volt-ampere |
| kVA _r | kilovolt-ampere reactive |
| SCIG | Squirrel cage induction generator |
| s | second |
| MVA _r | Megavolt-ampere reactive |

Glossary of terms

Table 2: Glossary of terms

| Term | Explanation |
|---|---|
| Flexible AC transmission systems | A system composed of static equipment used in AC systems to enhance controllability and increase power transfer capability. |
| International electrotechnical commission | An international standard organization that prepares and publishes international electrical and electronic technology standards. |
| Per-unit | Expression of system quantities as a fraction of a reference base quantity. |
| Point of common coupling | The point where a generating station is connected to the local electrical grid. |
| Wind energy conversion systems | Wind energy conversion systems are designed to convert kinetic energy from the wind turbine to mechanical energy that can rotate a shaft within an electrical generator to produce electricity. |

CHAPTER ONE: INTRODUCTION

1.1 Introduction

An electrical power grid is dedicated to providing electrical energy for both small and large-scale consumers. Traditionally, the electrical system is based on establishing large-scale generating power stations to meet the continuously growing energy demand. Fossil fuels and nuclear power plants are common types of conventional power stations. Power system planners and operators aim to provide their consumers with a high degree of reliability and quality of supply. However, with the environmental concerns, a change of energy source for electricity supply is considered. This source comes from renewable energy sources, which have the significant advantage of being replenished or replaced naturally. Solar, wind, hydro, geothermal, marine, and biomass are examples of sources of renewable energy. Incorporating solar and wind power into the electrical system has gained popularity over the last several decades. Even if the incorporation of renewable energy into the electrical grid is on the rise, there are fears that the unavailability of renewable energy sources under certain situations would hinder sustainable electricity generation. Problems occur when integrating renewable energy into the electrical grid due to not accurately predicting and controlling renewable energy compared to the conventional generation. The operation of the electrical power grid also becomes more complex as the generated power flows to consumers and in both directions as consumers also generate power and send the power into the electrical grid. These problems can cause excessive voltage variations and bottlenecks. Therefore, grid modification is needed to compensate for these changes (Sallam & Malik, 2020).

Solar and wind energy are usually referred to as variable energy resources due to the fluctuating output of wind and solar generators across a variety of periods. It has been suggested by a number of integration studies and operator experiences that when these variable energy resources are integrated into the electrical grid, changes may take place in how the electrical grid is planned and run. However, effective approaches to overcoming these effects have been created (Du et al., 2017).

The intermittent nature of wind makes it difficult to maintain power quality under the International Electrotechnical Commission (IEC) 61400-21 standard when wind energy is considered as an energy supply (Aluko, 2018). IEC 61400-21 specifies the power quality characteristics of grid-connected wind turbines for power production, which employs grid codes to evaluate the quality of power output (Jerin A et al., 2018).

This research focuses on the voltage aspects within the power quality characteristics based on the IEC 614200-21 standard. The voltage quality characteristics include harmonic distortion, voltage flickering, voltage fluctuations, voltage unbalance, voltage sags, voltage swells, undervoltage, and overvoltage. Furthermore, approaches are proposed to enhance the voltage quality in any system disturbance that occurs through intermittent wind speeds or grid faults.

1.2 Statement of the research problem

Wind turbines linked to the electrical grid affect grid stability and voltage quality. Voltage quality issues experienced by the grid following the integration of wind turbines need to be researched. Possible mitigation techniques must be proposed to ensure stability and support of the grid during these problems.

1.3 Background to the research problem

Wind turbine generation has emerged worldwide. Therefore, factors that affect the power quality that wind turbine generators deliver to the grid need to be considered. These factors are wind speed fluctuations and the use of electronic components like power converters (Zobaa et al., 2019). Due to the unpredictable nature of wind resources and electronic equipment, power quality concerns are producing difficulties with voltage fluctuations, reactive power consumption, and harmonic distortion (Liang, 2017).

1.4 Hypotheses or research questions

For this research, the primary research question is what voltage quality mitigation techniques are there to enhance voltage quality in grid-connected wind turbines.

Further sub-questions are what the voltage quality challenges that the grid operators face and what possible mitigation techniques can be applied to these challenges to mitigate the effect on the electrical grid. Furthermore, comparisons can be made to identify the best voltage quality mitigation technique.

1.5 Objectives of the research

The objective of this study is to develop a method to improve the voltage quality in wind energy conversion systems. The following are the research objectives:

- Identify the existing voltage quality issues relating to the IEC 61400-21 international standard for grid-connected wind turbines.
- Understand the voltage quality issues in the context of grid-connected wind generation.
- Investigate existing mitigation techniques that are used to control the voltage quality issues.
- Provide a clear summary of the voltage quality issues and mitigation techniques.
- Perform computer simulations to achieve waveforms and see the voltage quality effects of a fault present in the grid without any mitigation technique.
- Perform the computer simulations again, add the mitigation technique to observe how the voltage quality is improved, and compare the results to the computer simulation where the mitigation technique was not present.
- Compare own simulation results to existing literature based on the same research area using MATLAB/Simulink to confirm the results.

1.6 Research design and methodology

To meet the research's objectives, the following methodologies were employed:

- A literature review from accredited journal papers and books to perform studies of:
 - Voltage standards within the IEC 61400-21 international standard.
 - Voltage problems that correlate to the IEC 61400-21 international standard.
 - Flexible AC transmission systems controllers.
- The focusing areas of this study will include:
 - Reactive power compensation.
 - Harmonic distortions, voltage flickering, voltage fluctuations, voltage unbalance, voltage sags, voltage swells, undervoltage, and overvoltage.
- Use computer modeling to perform simulations by:
 - Creating a dynamic model in MATLAB/Simulink computer software to achieve a baseline reference.
 - Introducing grid faults to observe voltage quality effects.
 - Including mitigation techniques to the model and observing how the fault impact is lessened and voltage quality is enhanced.
 - Analyzing and interpreting the simulation results.

1.7 Delineation of the research

This study examines the power quality of wind turbines linked to the grid in wind energy conversion systems. Only the voltage quality relating to the IEC 61400-21 is the focus within the power quality aspects. The following points are covered by the research conducted:

- Wind energy conversion systems.
- Power quality of wind turbines.
- Voltage quality enhancement of wind turbines.
- MATLAB/Simulink modeling.

1.8 Significance of the research

This study's relevance is in improving transmission voltage quality in alternating current (AC) power networks when wind energy systems are present. Likewise, the power quality should be of a high standard during any potential grid fault. This dissertation's study adds to the mitigating effects that assure the improvement of power quality to mitigate the impact of the fault. Using computer modeling and incorporating the investigated mitigation approaches into wind energy may considerably enhance the power quality of wind energy studies, which might contribute significantly to the field.

1.9 Expected outcomes, results, and contributions of the research

Based on the IEC 61400-21 standard, this research studies voltage quality improvement strategies in wind energy conversion systems. On the basis of the simulation findings, it is anticipated that the mitigation approach increases the voltage quality in accordance with the IEC 61400-21 standard and existing literature in the same study field.

Based on the outcomes of the results for including mitigation techniques to enhance voltage quality, some mitigation techniques are expected to perform better than others under different scenarios. A comparative analysis can then be performed to identify the best-performing mitigation technique.

The possible stakeholders to benefit and the contributions this research will offer to is:

- Electricity Supply Commission (ESKOM).
- Cape Peninsula University of Technology (CPUT).
- Individuals undertaking research in the same subject area.
- Wind energy power plants.
- IEC Committee.

- Renewable energy systems.

1.10 Dissertation organization

Chapter one provides an introduction to the research problem with a brief background. Then, the research objective is explained by indicating the research design and methodology. In addition, chapter one describes the anticipated results and contributions of this study.

Chapter two provides an introduction to the literature review for this dissertation. This chapter will identify the standards used for voltage quality in wind energy systems and provide several problems with mitigation methods for voltage quality enhancement in wind energy conversion systems.

Chapter three provides the mathematical modeling for the individual components used in a virtual simulated WECS network.

Chapter four provides a detailed computer modeling of a wind turbine model in MATLAB/Simulink.

Chapter five comprehensively studies the simulated results produced from the wind turbine model during steady-state and momentary fault conditions using the mitigation techniques to compare it to the research received within the literature review.

Chapter six conclude the research work. The objectives are discussed with recommendations for future research work.

1.11 Summary and Conclusion

This chapter introduced the topic for this dissertation. The research origin of the problem statement has been outlined, which derived a detailed scope of this research. Next, a brief background of the research problem was discussed, creating the research questions for this research. Furthermore, this chapter addressed the research objectives, design, methodology, and delineation. Lastly, discussions of the importance of this study, the expected outcomes and results, with the dissertation organization have been discussed.

CHAPTER TWO: LITERATURE REVIEW

2.1 Introduction

With the growth of wind power production, it is vital to solve the challenges related with wind energy integration into the electrical grid. Megawatt-scale wind power facilities are directly linked to the electrical distribution grid, replacing conventional producing stations at the distribution level. To replace the non-renewable traditional power stations, modifications must be made to these large wind power plants. These adjustments include voltage control, elimination of harmonics, and regulation of active and reactive power. Transmission system operators created grid codes and power quality standards that must be met in order to connect wind turbines into the grid (Ahmed, 2017). This literature review will concentrate on voltage-related issues and mitigation techniques based on the power quality concerns of international standard IEC 61400-21.

In this chapter, renewable energy is introduced along with brief explanations of popular forms of renewable energy. The electrical grid is then presented using an example of several generating sources integrating into the grid and showing how power is produced with various voltages from generation to customer. The technical prerequisites for integrating renewable energy into the electrical grid are then described, which opens the door to more concentrated study on wind energy conversion systems. The power characteristics of a wind turbine are examined after various wind turbine layouts, and sections of wind turbines are covered. The final main topic for this dissertation is the IEC 61400-21 standard for voltage quality-related issues that wind turbines need to conform to in order to be linked to the electrical grid. Power quality for wind energy conversion systems is then explored. Finally, various strategies for improving voltage quality in wind energy conversion systems are reviewed.

2.2 Renewable energy

It is anticipated that global energy consumption will increase by more than 33 percent by the year 2035 as global energy demand continues to rise (Bollen & Moreno-Munoz, 2017). As traditional energy supplies such as coal, oil, and natural gas deplete, the need for alternative energy sources rises due to the global dependence on energy. Figure 2.1 indicates that the contribution of renewable energy sources (RES) is increasing annually.

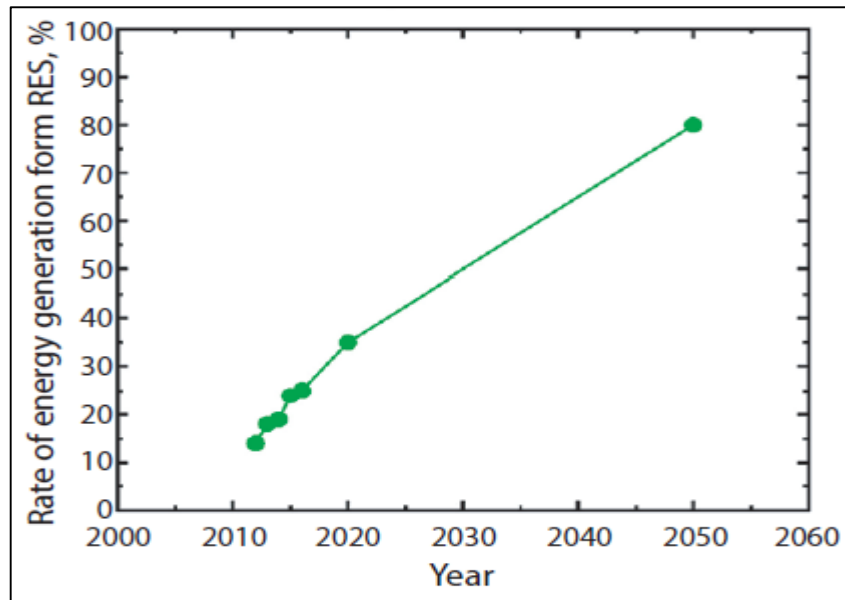


Figure 2.1: RES rate increase of energy generation (Chamundeswari et al., 2021)

Figure 2.2 depicts common forms of renewable energy sources. By using these RES, the world may advance toward a cleaner and safer environment and contribute to a smaller carbon footprint.

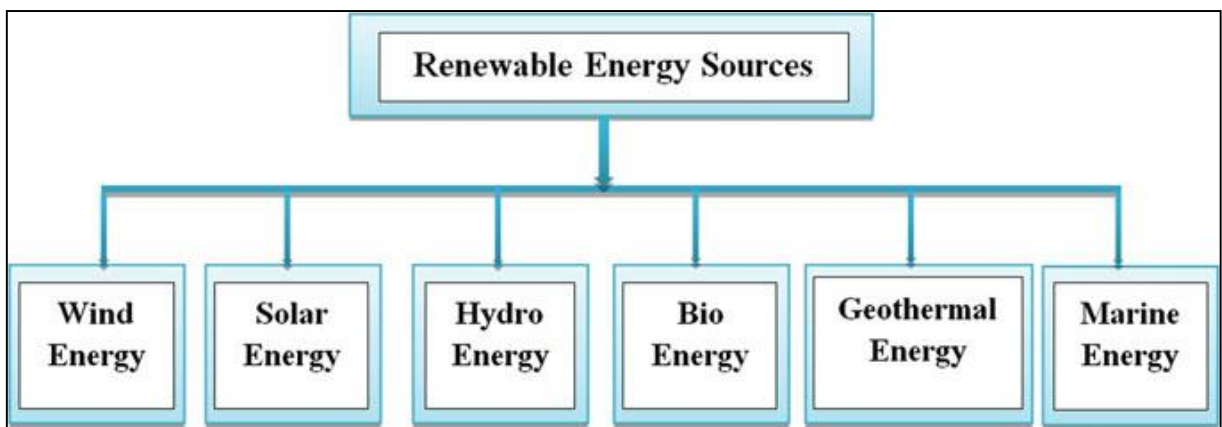


Figure 2.2: Classification of renewable energy (Roy & Das, 2018)

2.2.1 Types of Renewable energy:

1. Wind Energy
2. Solar Energy
3. Hydro Energy
4. Bio Energy
5. Geothermal Energy
6. Marine Energy

The types of RES mentioned above are briefly described.

2.2.1.1 Wind Energy

Wind energy conversion systems (WECS) are among the RES with the quickest growth rate. The power generating size of wind turbines has risen through time, from 0.05 MW with a 15-meter rotor diameter in 1985 to 2-3 MW onshore and 3-5 MW offshore with rotor diameters of up to 167 meters, respectively (Chamundeswari et al., 2021).

Wind energy has a wide range of uses. Originating in the late 19th century, harnessing the wind to create energy has become a major study area, with the amount of producing capacity dependent on the size of the wind turbine, the location of the project, and the length of the rotor blades (Zohuri, 2018; Zare Oskouei & Mohammadi-Ivatloo, 2020).

Wind energy is the energy collected from moving air, with the quantity of energy extracted varying according to the cube of wind velocity (Dey et al., 2019). When air flows, the flowing air exerts a force on the precise design of the wind turbine blade, forcing the blade to rotate. The turbine blade is attached to the generator rotor, and the spinning rotor inside the electrical generator generates power (Roy & Das, 2018).

2.2.1.2 Solar Energy

Solar energy is derived from the sun's energy, which is converted into thermal or electrical energy (Zare Oskouei & Mohammadi-Ivatloo, 2020).

Active and passive solar approaches are grouped as solar energy conversion technologies. Active solar technology employs photovoltaic (PV) cells, solar heating systems, and concentrated solar electricity (CSP). PV conversion converts direct sunlight into energy in a PV cell. In contrast, solar thermal conversion employs concentrated solar energy to heat a liquid in order to generate steam for the turbines of an electrical generator. Passive solar technology utilizes thermal materials and light dispersion qualities to store and release heat when the sun is not present. These methods are well known and are used globally to produce power. Location is the most important aspect of solar energy production (Roy & Das, 2018; Chamundeswari et al., 2021; Zohuri, 2019a).

2.2.1.3 Hydro Energy

Hydro energy is designated as a renewable energy source (RES) since it utilizes the pressure or flow of water to create electricity. Hydroelectricity is the generation of electricity from the gravitational force of falling or flowing water. Coupled to a turbine, the energy of falling or flowing water is turned into mechanical energy. The turbine is attached to the rotor shaft of the electrical generator, which creates electricity when turned (Chamundeswari et al., 2021).

Standard hydroelectric power plants store water in a reservoir through a dam or river. The water is subsequently released from the reservoir and runs into the turbine, causing it to rotate and generate power from the generator. A pump storage plant is an additional frequent form of a hydroelectric power station. The water is kept in an upper dam or reservoir, released to the generator, and then collected in a lower dam or reservoir when the energy has been created. Then, at night or during periods of low energy consumption, the generator may function as a motor to run a pump that returns water to the higher reservoir. Based on their functioning, there are three kinds of hydroelectric schemes: run of the river, storage, and pumped storage (Zohuri, 2018; Roy & Das, 2018).

2.2.1.4 Bio Energy

Bio energy is derived from agricultural waste, living organisms, waste wood, plants, trees, animals, and crops. In addition, bio energy comprises biomass and biofuels that are the result of photosynthesis and the gathering of solar energy (Roy & Das, 2018; Zare Oskouei & Mohammadi-Ivatloo, 2020).

Biomass combustion generates heat by releasing chemical energy. You may either directly burn biomass or convert it into liquid biofuels or biogas to use as fuel (Zohuri, 2018). Moreover, biomass may be utilized directly in steam-electric power plants or converted into biogas that can be burnt in internal combustion engines, gas turbines, and steam generators (Zohuri, 2019a).

The following are sources of biomass energy production (Chamundeswari et al., 2021):

- Wood and processing waste: generation of heat energy from wood waste combustion.
- Agricultural waste is used as a fuel source and turned into biofuels.
- Food and rubbish waste are converted to biogas using landfills or burned directly to generate power.

2.2.1.5 Geothermal energy

Geothermal electricity is heat energy derived from magma conduits, hot springs, or hydrothermal circulation that may be utilized to power electrical steam generators or heat buildings. Geothermal power is cost-effective, environmentally friendly, and reliable but is geographically limited to locations near tectonic plate boundaries (Zohuri, 2018).

Three different sorts of geothermal power plants are commonly used (Roy & Das, 2018; Chamundeswari et al., 2021):

- Dry steam: Subterranean pipes carry steam from wells below the earth's surface straight into the electrical steam generator turbine.
- Flash steam: Water-filled geothermal reservoirs are employed at temperatures over 182 °C (360 °F) for geothermal power production. When the pressure in subterranean wells diminishes, and part of the hot water boils into steam, the hot water rises due to its own pressure. Once the steam has been extracted from the water and employed to power the electrical steam generator turbine, the residual water, and condensed steam are reintroduced into the reservoir.
- Binary steam: Water temperatures in binary cycle power plants range between 107 and 182 degrees Celsius (225 and 360 degrees Fahrenheit). Using the heat from the hot water, a working fluid, such as an organic compound with a low boiling point, is boiled in these facilities. This fluid is transformed into steam in a heat exchanger and supplied to the electrical steam generator turbine. During this cycle, hot water is returned to the soil to be warmed while the fluid is maintained separately.

2.2.1.6 Marine energy

Marine energy, also known as ocean, wave, and tidal energy, is a technology used to draw power from the sea but is not currently developed. Marine energy has large potential over other RES as it is predictable and does not require large areas of land (Roy & Das, 2018).

The ocean produces both heat energy from the sun and mechanical energy through the motion of the tides and waves. Systems that make use of warm surface water temperatures may convert thermal energy to electricity. Mechanical energy is generated by utilizing the ebbing and flowing of the tides caused by the rotation of the earth and the gravitational attraction of the moon.

2.3 The electrical grid

The electrical grid is a network that delivers power from generators to consumers. Power generators produce energy, high-voltage transmission lines move it to distant substations, and distribution lines deliver it to individual users. These components make up the electrical grid. The electricity-generating sources are typically situated distant from densely inhabited regions and close to their principal fuel supply.

Figure 2.3 illustrates a typical electrical grid layout of multiple generating sources and integrates into the electrical grid to supply consumers.

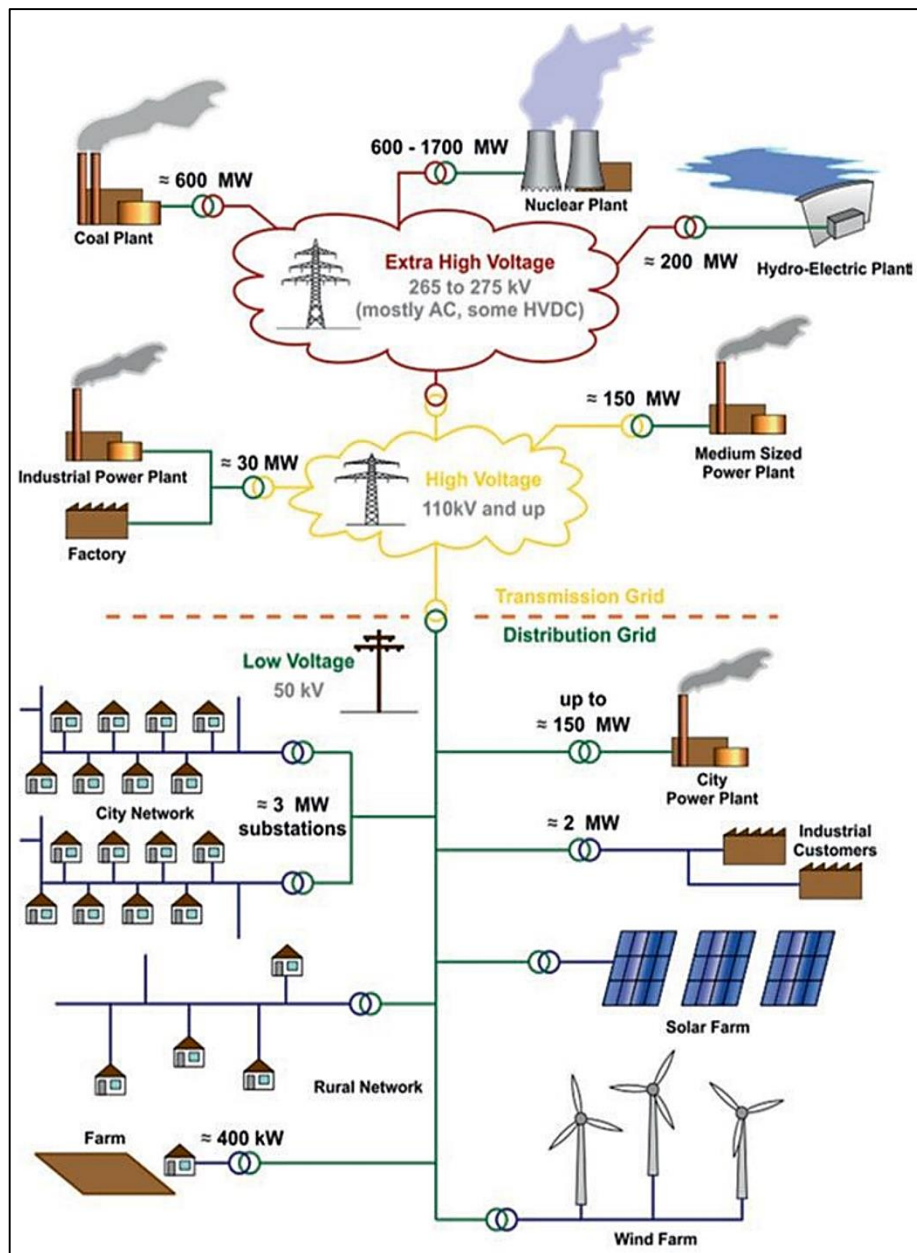


Figure 2.3: General layout for an electrical grid (Zohuri, 2019b)

For the transmission network, the voltage of the generated electricity is increased. In order to minimize power losses over long distances, the voltage is boosted to a high level. The distribution of electricity to its final destinations might occur at substations or even across international boundaries. It originates from a wholesale client that operates a local power distribution system. After receiving electricity from the transmission network, the substation reduces the voltage to the level required by the distribution network. The voltage level is subsequently reduced to the required service level voltage at the substation, where the power is available and linked to a service point's distribution cable.

The electrical grid is synchronized and works at the same frequency. The grid and all associated generators must continue to run in phase and at the same frequency. Local governors adjust the driving torque of spinning generators to maintain a steady speed while the load varies. Parallel generators with load sharing use droop speed control. As electricity is used, the grid must maintain a balance between production and consumption. The generator safety mechanism may disconnect the generator from the grid if the grid frequency deviates even slightly from its nominal value. Therefore, equilibrium is essential. The system frequency falls below its nominal value when the grid is heavily loaded. For consistent power distribution, droop control is used. In order to preserve grid synchronization and create more power within the generator's rated capacity, the governor is altered to increase the machine's speed. When the grid is only lightly loaded, the frequency climbs beyond the normal system frequency, requiring the generators to slow down and reduce their power production (Zohuri, 2019b).

2.4 Renewable energy integration

Integrating RES into the electrical grid needs to follow technical requirements (Zare Oskouei & Mohammadi-Ivatloo, 2020):

1. Voltage and reactive power control:

After the usage of RES, the allowed voltage fluctuation from the nominal voltage at the point of common coupling (PCC) must be within 10%.

2. Frequency and active power control:

Incorporating intermittent RES, such as wind and solar, into the electrical grid would influence system frequency due to the fluctuating nature of RES production, which may result in higher or reduced produced power. After the implementation of RES, the permissible frequency variation from the nominal voltage should be between -5% and +3%.

3. Short-circuit power level:

When incorporating RES into the electrical grid, grid designers must consider power grid stability. When fault conditions occur in different sections of the power system, RES with inverter-based resources may severely damage electric systems. The performance of the conventional protective relay system, which was first created for synchronous generators, is predicted to be impacted by inverter-based resources, which have distinct short-circuit characteristics for the electrical grid (Haddadi et al., 2021). In order to compute short-circuit power levels with and without RES, grid designers must do so. To avoid the power system entering a critical state, the findings need to be analyzed.

4. Power quality issues:

With the utilization of RES, power quality is an important consideration that must be evaluated. Analysis of harmonic orders that result in waveform distortion and short-term fluctuations is a component that contributes to the significance of evaluation. International standards that outline the technical criteria and constraints can be utilized for power quality studies with RES connections.

5. Congestion management:

Power congestion can occur when the electrical grid does not have the infrastructure capacity for newly added RES at the PCC. Congestion may restrict the flow of electricity from the RES at the PCC to other zones within the power grid. Therefore, grid planners should conduct a complete analysis at the PCC to identify weak or undersized infrastructure components that can lead to congestion.

This dissertation focuses on wind energy conversion systems, hence wind energy will be the topic of discussion moving forward.

2.5 Wind energy conversion system (WECS)

WECS are intended to convert wind energy into mechanical energy. Wind turbines use generators to convert mechanical energy into electrical energy. As shown in Figure 2.4, WECS comprises a wind turbine, gearbox, electrical generator, power electronic converter, and transformer.

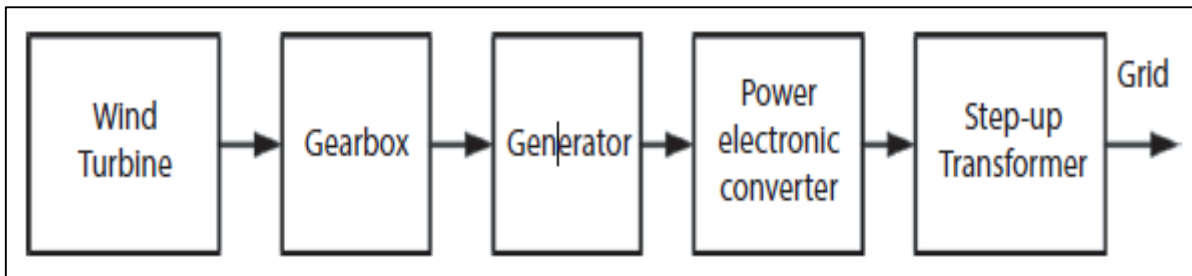


Figure 2.4: Wind energy conversion system (Chamundeswari et al., 2021)

Horizontal and vertical wind turbines are available. Figure 2.5 demonstrates that horizontal-axis wind turbines (HAWT) function with their rotating axis parallel to the ground, whereas vertical-axis wind turbines (VAWT) operate with their revolving axis perpendicular to the ground (Chamundeswari et al., 2021).

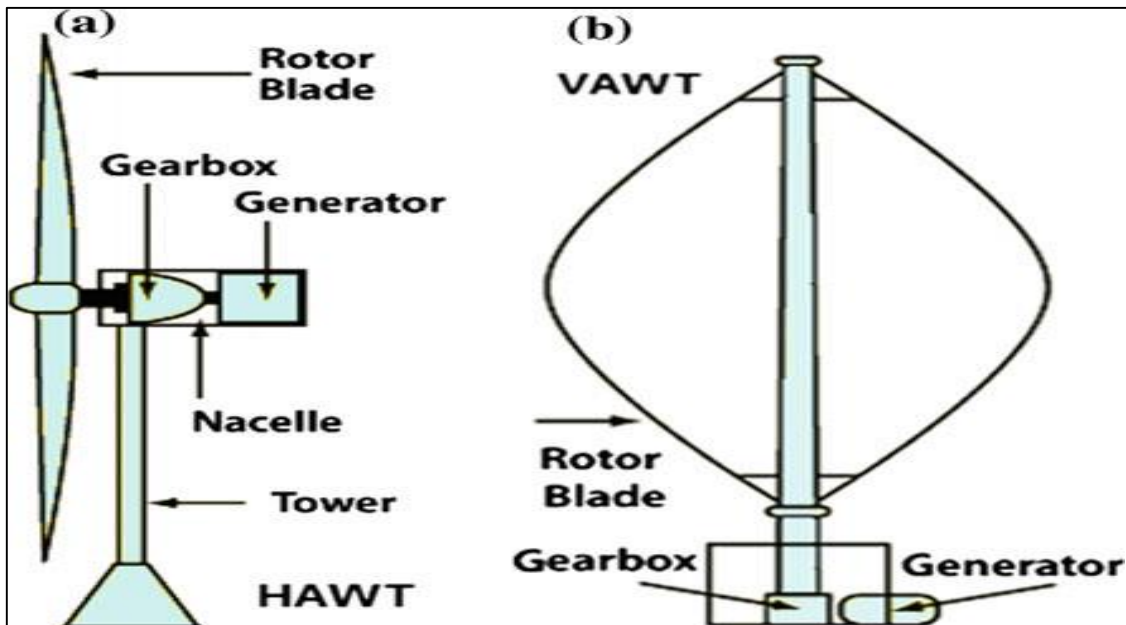


Figure 2.5: (a) HAWT and (b) VAWT (Tawfiq et al., 2018)

The electrical generator for the HAWT is located atop the tower. A gearbox is required to enhance the blades' slow spinning to a suitable speed for the generator. The HAWT towers are tall in order to extract high wind speeds and create more energy. To face the turbine toward the wind, additional control equipment is required. The downside of the HAWT is that the tower needs intricate construction to support the weight of the generator, gearbox, and turbine blades, disrupting natural landscapes.

The electrical generator and gearbox for the VAWT are located at the foot of the tower. Consequently, no extra control equipment is required to face the wind turbine toward the wind. The benefit of the VAWT is that it is simple to maintain and can be deployed in many locations, such as on roadways and building rooftops. As a result of the near proximity of the blades to

the ground, the VAWT has a lower power output than the HAWT. Therefore, HAWT is recommended over VAWT or low-power applications for commercial WECS (Chamundeswari et al., 2021; Tawfiq et al., 2018).

Since HAWT is more preferable for commercial WECS, HAWT will be the focus moving forward.

2.5.1 Parts of the HAWT

Figure 2.6 illustrates a typical HAWT arrangement. The wind turbine consists of the nacelle, the rotor blades, and the tower. The mechanical component of the wind turbine placed atop the tower is called the nacelle. The nacelle has a generator, gearbox, brakes, and control devices. The controlling mechanism is the component that enhances wind energy collection and conversion by either spinning the nacelle into the wind or pitching the rotor blades to achieve the optimal angle of attack. The hub of the rotor blades is attached to the nacelle via a shaft. Consequently, wind flows across the air-foiled rotor blade, causing a mechanical movement on the rotor blade. The generator shaft is coupled to a gearbox to improve its mechanical rotation. The electricity is subsequently linked to the national grid using power electronic equipment and step-up transformers (Roy & Das, 2018).

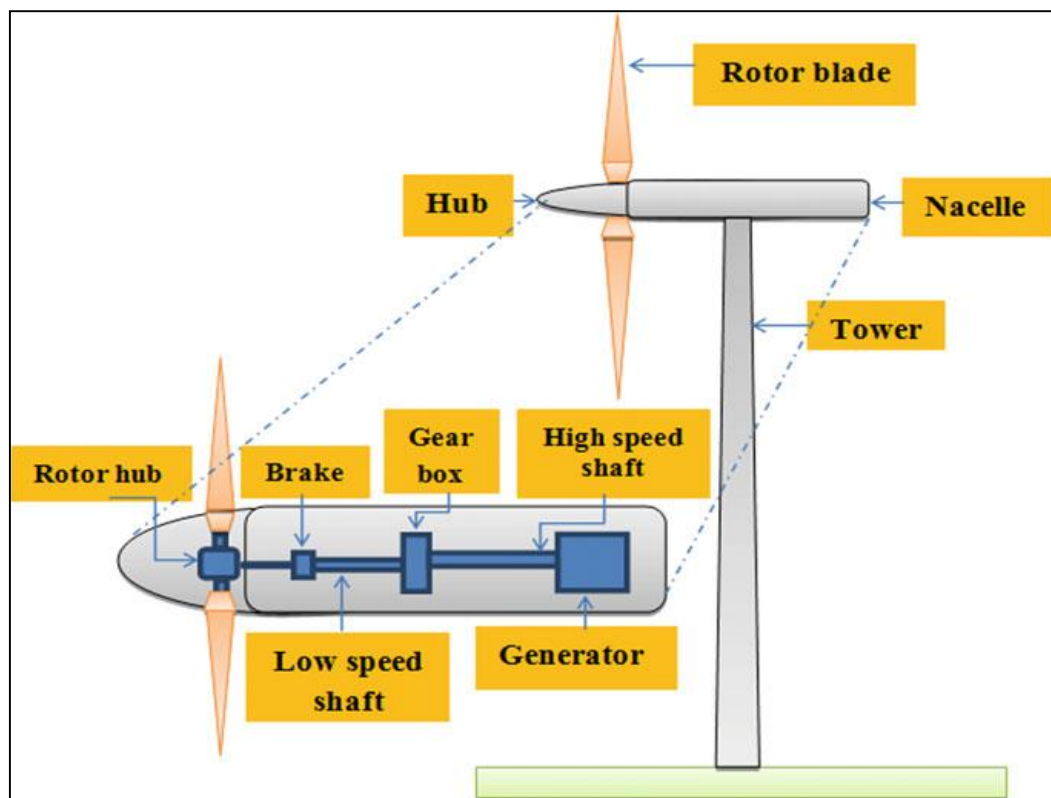


Figure 2.6: Wind turbine energy conversion layout (Roy & Das, 2018)

2.5.2 WECS configurations

Wind turbines in WECS are classified into types of configurations (Bollen & Moreno-Munoz, 2017):

- Type 1: Fixed speed WECS.
- Type 2: Limited variable speed WECS.
- Type 3: Variable speed WECS with partial scale power electronic converter.
- Type 4: Variable speed WECS with full-scale power electronic converter.
- Type 5: Variable speed WECS with mechanical transmission.

Configuration types 1 and 2 are rare in present wind power facilities. These types of configurations make use of induction generators that are directly coupled to the grid and operate at a fixed frequency of the grid without the use of power electronics. Additionally, the wind power facility requires a reactive power compensator or a soft starter. Type 5 is a solution for the future. However, type 3 and type 4 arrangements are often employed.

Illustrated in Figure 2.7 are type 3 and type 4 WECS configurations.

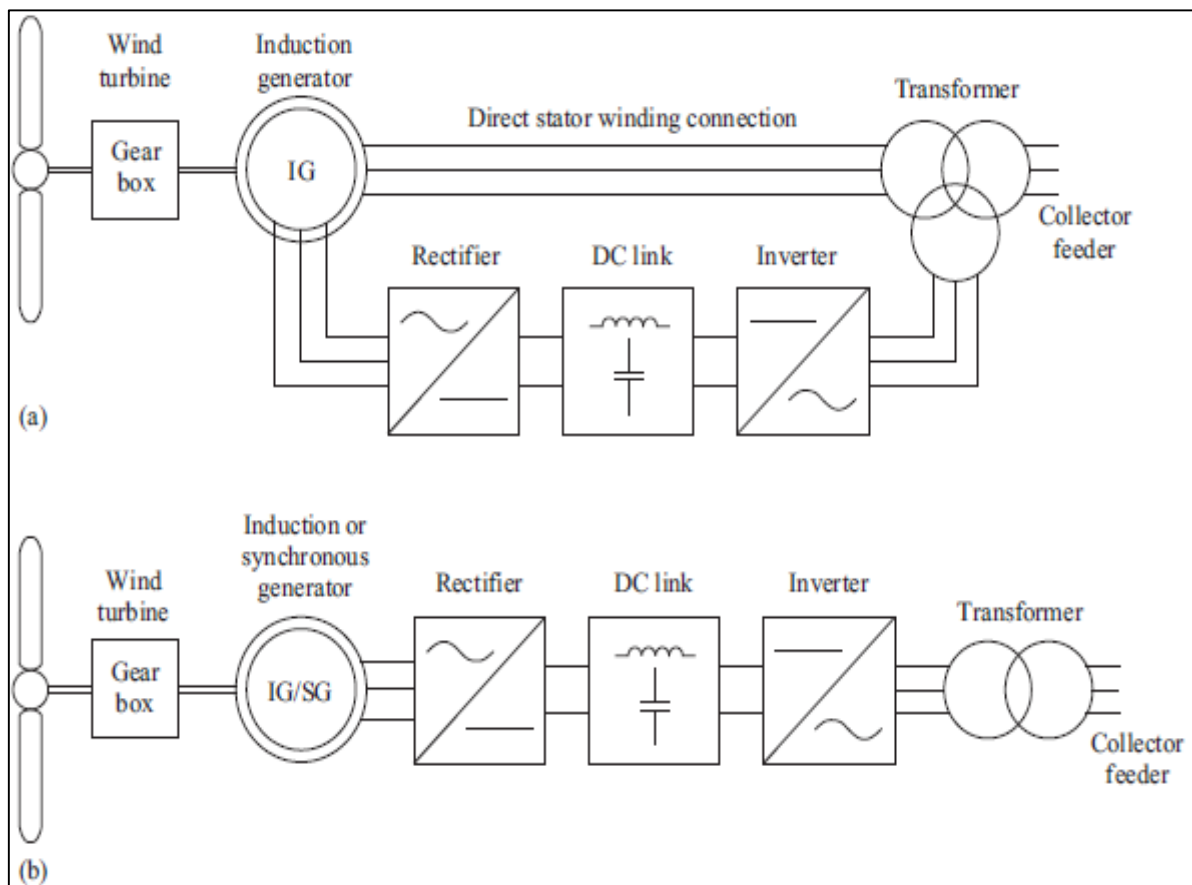


Figure 2.7: Type 3 (a) and type 4 (b) wind turbine configuration (Bollen & Moreno-Munoz, 2017)

The doubly-fed induction generator is the type 3 configuration (DFIG). In this configuration, a partial-scale power converter supplies variable frequency voltage to the generator's rotor winding. The power converter consists of a back-to-back voltage source converter (VSC) that may transmit power to the grid as necessary. Using this partial-scale power converter, greater control can be exerted over the turbine speed, and active and reactive power management may be separated without the need for additional reactive power compensation equipment. In a type 4 configuration, the stator winding is connected through a full-scale power converter. This enables the generator to run at its own variable speed. The power converter receives the variable frequency electricity and synchronizes its output with the grid. The gearbox is not usually required since the generator may function at lower speeds by increasing its poles because of its variable frequency operation. Induction and synchronous generators are employed in types 3 and 4. The power electronic converters employed are very effective and have the capability of delivering reactive power (Bollen & Moreno-Munoz, 2017).

2.5.3 Wind turbine power characteristics

Equation 2.1, which is derived from the formula for kinetic energy, is used to define wind power (Tawfiq et al., 2018; Infield & Freris, 2020),

$$K = \frac{1}{2}mv^2 \quad (2.1)$$

$$P_{wt} = \frac{1}{2}p\pi R^2V^3 \quad (2.2)$$

Where P_{wt} is the amount of energy captured by the wind, p is the air density measured in kg/m³, R is the diameter of the wind turbine blades measured in meters, and V is the wind speed measured in m/s.

Under the power coefficient C_p given by the turbine's ability to create mechanical power may be calculated,

$$P_{mec} = C_p P_{wt} = \frac{1}{2}C_p p\pi R^2V^3 \quad (2.3)$$

Without power losses, wind turbine blades can only capture 59% of the wind's available energy, which is known as the Betz limit and C_p . As a function of C_p , the wind turbine tip speed ratio lambda (λ) is defined by,

$$\lambda = \frac{\omega R}{V} \quad (2.4)$$

Where, ω stands for the rotor's rotational speed (rpm), R for the swept area's radius (in meters), and V for the wind velocity. Using the ratio of tip speed to rotor speed and the power coefficient C_p , the wind turbine performance of any size rotor may be defined.

Figure 2.8 illustrates the C_p - λ relationship for different blade pitch positions (β). The radius of the blade and the wind speed cannot be controlled to modify the tip speed. The only method to alter the tip speed is to alter the rotating speed of the rotor blade, which is ω . By constantly adjusting the rotor blade pitch, torque on the blade can be increased or reduced, affecting the rotor blade's speed. Modern wind turbines are thus built to run at varying speeds in order to retain the maximum C_p and produce the greatest wind turbine production (Infield & Freris, 2020).

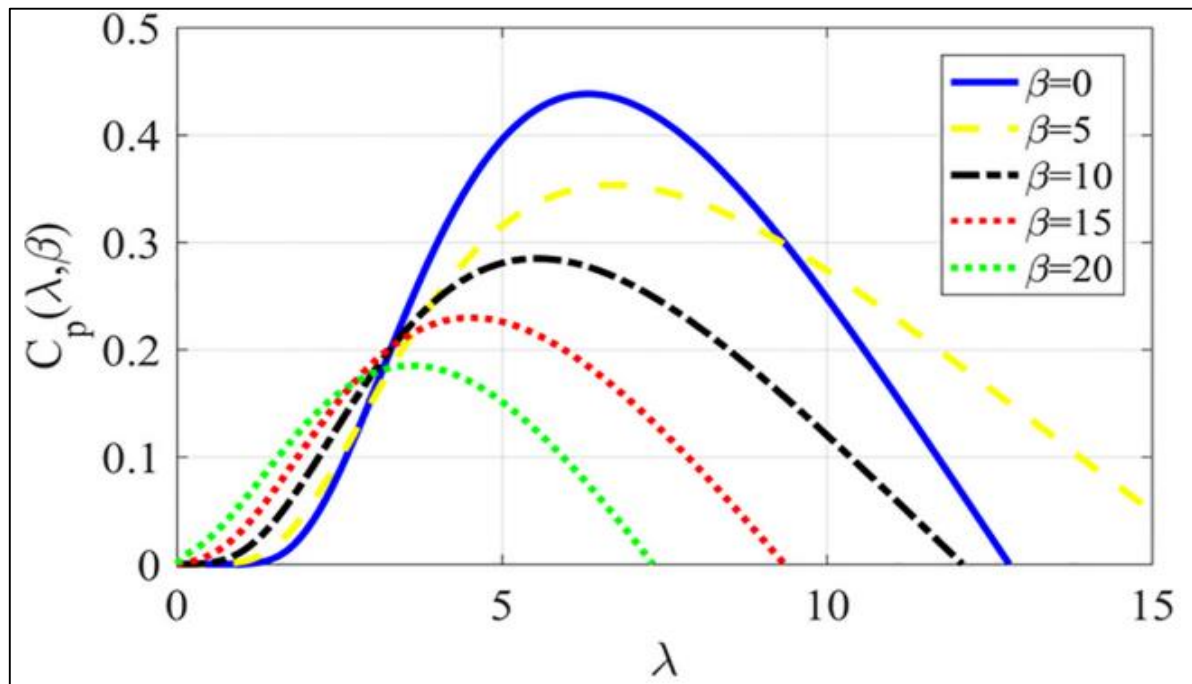


Figure 2.8: Wind turbine power coefficient curve (Fan & Zhu, 2019)

Wind turbines are engineered to generate maximum production at certain wind speeds. Figure 2.9 depicts the power characteristic curve at various wind speeds. If a set wind speed of 9.5 m/s at 1500 rpm was selected, the maximum output power would be limited to that precise wind speed. If the wind speed rises or drops, the maximum power output for that wind speed will not be achieved. Variable-speed wind turbines are thus widely used. By continually altering the pitch of the rotor blades, the greatest amount of torque from the wind on the rotor blade is attained to follow the maximum power point at each wind speed within the wind turbine's rated power output.

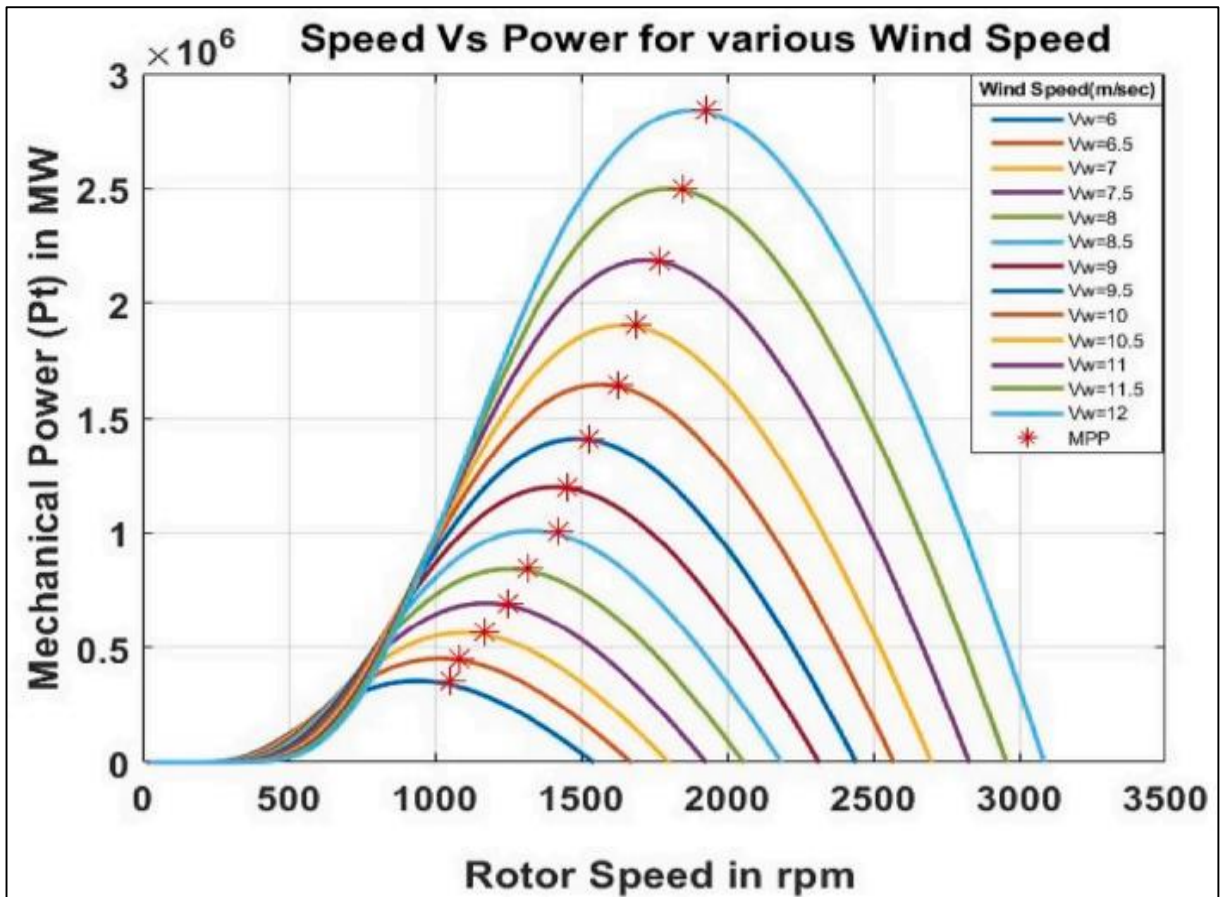


Figure 2.9: Wind turbine power characteristics curve (Gupta & Shukla, 2022)

2.6 General power quality issues

Power quality (PQ) is the comparison of real voltage and current waveforms to their "clean" pure, undistorted sinusoidal waveforms (Siahpoosh, 2019). PQ is a fundamental operational component that must be considered for any power system (Cisneros-Magaña et al., 2018). Electrical utilities must adhere to several stringent criteria pertaining to harmonics, transient states, and voltage sags.

The power quality industry developers must understand the causes of the power quality degradation, the origin of the disturbance, and the effect on electrical equipment (Musoni, 2018).

Steps to evaluate power quality issues are illustrated in the flow diagram in Figure 2.10. The first step in the flow diagram is to categorize the PQ issue. The second step is to characterize the identified PQ issue by getting more data. This information can be data collection or measurements. Receiving the data can determine the impact on equipment, the characteristics, and the causes of the issue. The third step is identifying possible solutions to

fix the PQ issue with an evaluation. The last stage is analyzing the completed solution to the PQ problem to get optimum economic outcomes (Hepsiba et al., 2021).

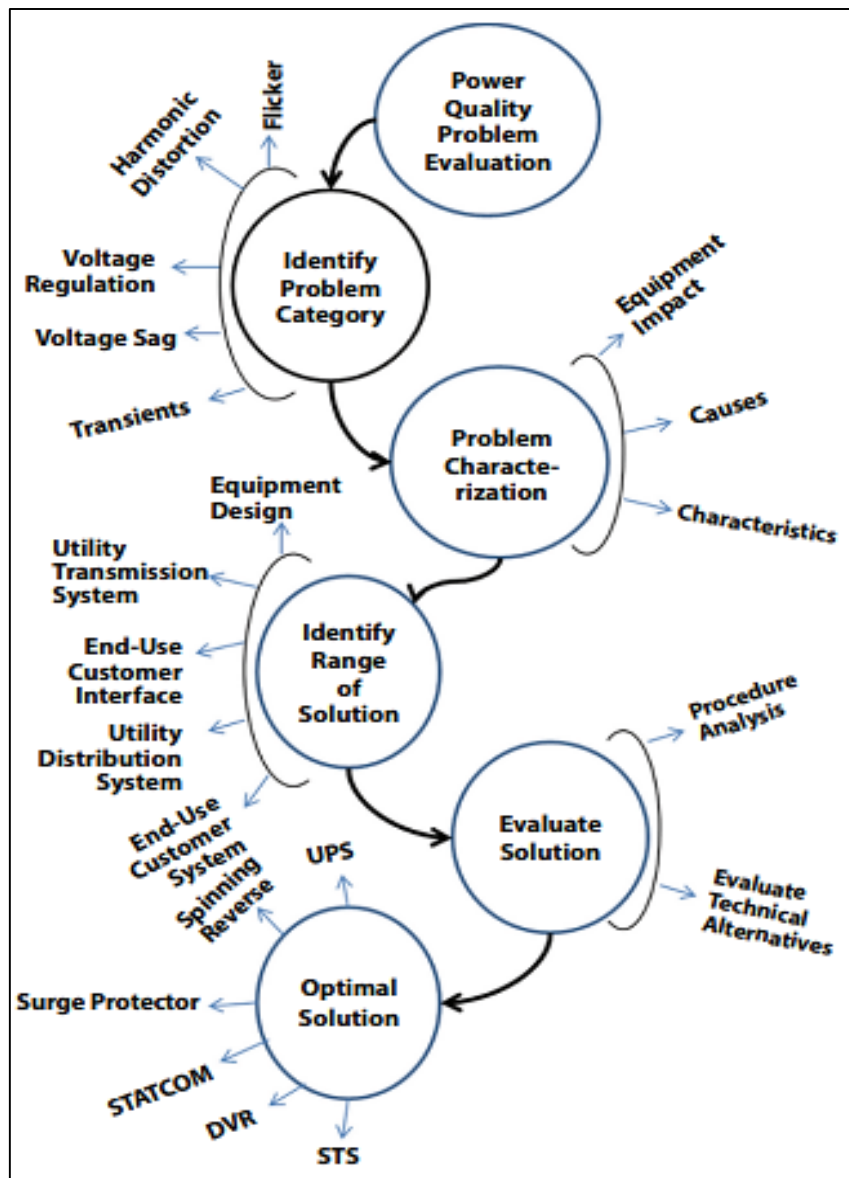


Figure 2.10: Flow diagram of PQ issues (Hepsiba et al., 2021)

Several international technical and standardization bodies handle and define PQ. Well-known examples of these organizations are the IEC (International Electrotechnical Commission) and IEEE (Institute of Electrical and Electronics Engineers) (Misak & Prokop, 2017).

Based on the former, measures can be developed to limit the consequences of power quality deterioration on the electrical grid. Solutions can come in grid codes like the IEC 61400-21.

2.7 Power quality characteristic in WECS based on IEC 61400-21

The grid code is the technical requirement for the reliable, secure, and safe functioning of the electrical grid. Those in charge of the operation, integrity, and monitoring of the electrical system establish various grid codes. All wind energy power suppliers must comply with the grid regulations, including those for power frequency and voltage variations, wind farm fault ride-through capabilities, reactive power control, and power factor management capabilities (Ahmed et al., 2020). PQ issues are often caused by non-linear loads, variable speed drives, switching of large electrical motor loads, electrical transients, arc furnaces, lightning, and grid faults (Mikkili & Panda, 2016).

The IEC standard 61400-21 specifies the power quality characteristics for grid-connected wind turbines (Jerin A et al., 2018).

The wind farm's power quality characteristics must comply with the IEC 61400-21 standard, which is based on the following criteria (Kannan & Ali, 2017; Mikkili & Panda, 2016; Fang, 2021b):

- Harmonic distortion.
- Flicker and voltage fluctuations.
- Voltage unbalance.
- Voltage sags.
- Voltage swells.
- Undervoltage.
- Overvoltage.

This dissertation will concentrate on resolving the voltage-related power quality concerns described above to improve WECS in the electrical grid in accordance with IEC 61400-21.

2.7.1 Harmonics distortion

Power system harmonics comprise sinusoidal voltage and current waveforms having multiple integers of 50 Hertz (Hz) or 60 Hz as the fundamental frequency (Kannan & Ali, 2017). The multiple integer frequency leads to the distorted waveform, as seen in Figure 2.11. The most common harmonic order injected from WECS into the power system is the 5th, 7th, 11th, 13th, and 17th (Ahmed et al., 2020).

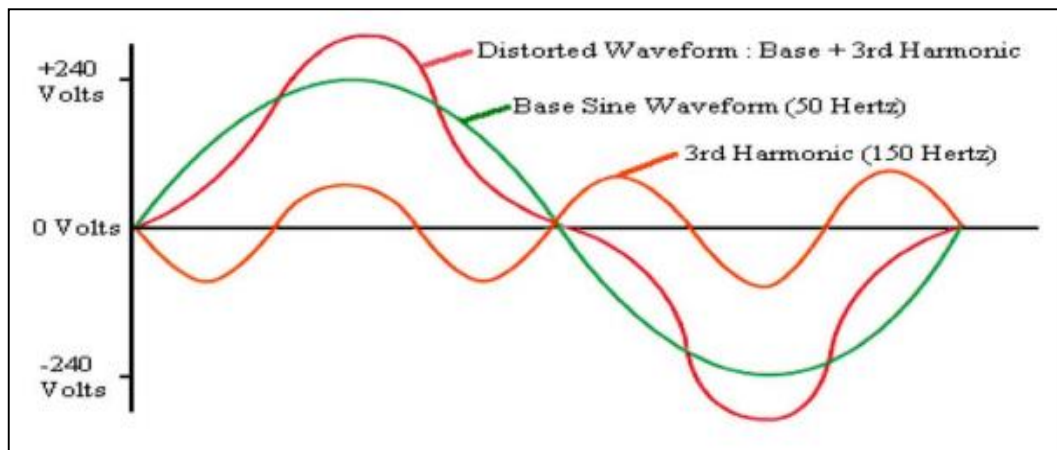


Figure 2.11: Harmonic waveforms (Gupta, 2018)

Harmonic disturbance in wind turbines is related to the distorted voltage and current fundamental sine waveforms created by external controllers connected to the network to which wind turbines are connected, such as non-linear electronic or electrical equipment. These controllers can be electrical machines operating above their magnetic saturation point, arc furnaces, fluorescent lights, power electronic equipment, switch-mode power supplies, or variable frequency drives (Mikkili & Panda, 2016).

In WECS, insulated-gate bipolar transistor (IGBT) switching controllers in the power electronic converters are crucial in controlling active and reactive power. Adverse effects from these switching controllers are the voltage and current harmonics created in converting variable frequency to constant frequency. Harmonic emissions need to be eliminated because they can lead to high current levels in the neutral conductor if the system is a three-phase star-connected system (Nobela et al., 2019).

Voltage harmonics do not originate from non-linear loads. Instead, current harmonics are generated from these loads. With the current harmonics flowing through the system impedances, a harmonic voltage drop is caused that distorts the voltage waveform that creates voltage harmonics. The impact of these harmonics causes an increase in current that will lead to more power losses and overheating of equipment that can be highly destructive (Kannan & Ali, 2017).

The ratio of total harmonic distortion (THD) is the root-sum-square of the harmonics in the power system divided by the fundamental component. THD is measured as (Fang, 2021a),

$$THD_v = \frac{\sqrt{V_{s,rms}^2 - V_{0,rms}^2}}{V_{0,rms}} \quad (2.5)$$

Where, V_{0_rms} is the root-mean-squared (RMS) value of the fundamental voltage component and $V_{s_rms}^2$ is the RMS of the voltage signal.

The quantity of voltage THD is dependent on the number of harmonics. Therefore, higher THD translates to more harmonics, which should be less than 5% to maintain a sinusoidal waveform and be allowed to be connected to the grid.

The standard of IEC 61000-3-6 for harmonic control provides a guideline to assess the harmonic emission to ensure the emission is within the required, acceptable limit at all times. Mitigating harmonics, filters are widely used in electrical and electronic systems to suppress unwanted voltage and current magnitudes. Combining inductors (L) with capacitors (C) creates passive filters. Previous research has shown that LC filters are an efficient method for mitigating undesired current harmonics in WECS. Active filters are gaining popularity in WECS by using the filters in the converter controller to decrease THD. To decrease THD, it will be necessary to configure the generator side converter (GSC) for active filtering. For the switching equipment, STATCOM-based control methods and hysteresis current regulation have also been suggested to limit harmonic injection into the electrical grid (Nobela et al., 2019).

2.7.2 Flicker and voltage fluctuation

Voltage flickering refers to the variation in the visual intensity of electric light sources caused by changes in the supply voltage (Fang, 2021a; Ameer et al., 2019).

Network operators generally have a voltage range in that they set their acceptable voltage fluctuation percentage. In some cases, the asymmetrical range may be preferred. The IEC 60038 and the European EN 50160 standard have a $\pm 10\%$ voltage limit on the allowable voltage fluctuation on voltage levels of 230 V line-to-neutral and 400 V line-to-line. The American national standard ANSI C84.1 standard allows a 5% voltage fluctuations limit between voltage levels of 120 V and 600 V operating at 60 Hz. The Australian AS 61000.3.100 standard allows a voltage fluctuation of +10% and -6% of the nominal voltage (Perera & Elphick, 2023).

Figure 2.12 illustrates the voltage fluctuations that cause a fluctuated voltage waveform with voltage envelopes that cause flickering.

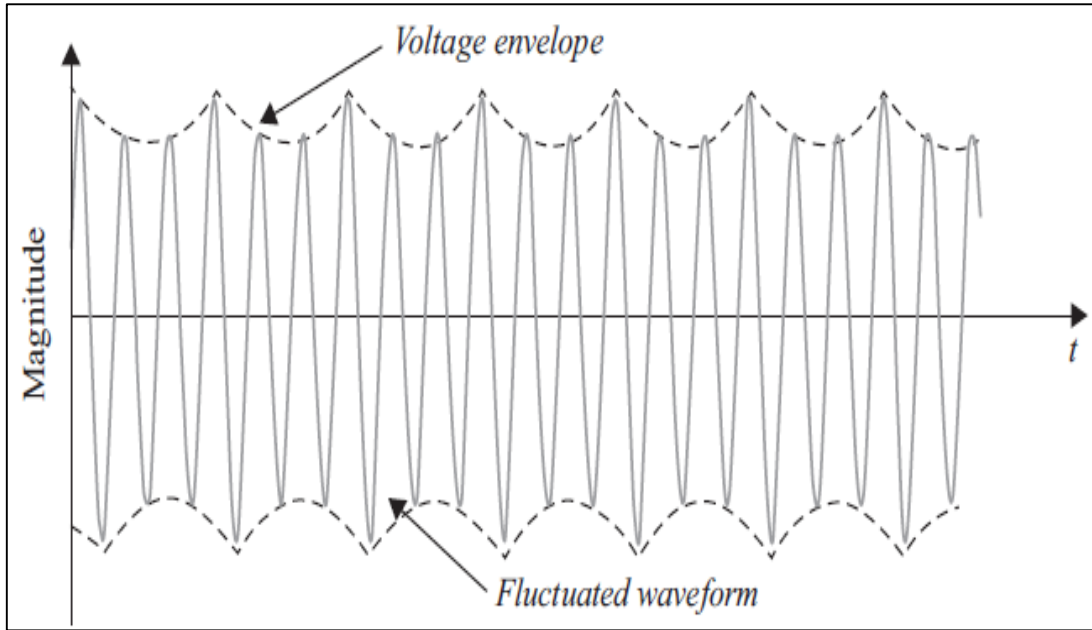


Figure 2.12: Voltage fluctuations at the load (Kannan & Ali, 2017)

P_{st} is the short-term flicker severity factor assessed over a period of 10 minutes while P_{lt} is known as the long-term flicker severity factor recorded across 2 hours. Flickering is divided into short-term and long-term categories. IEC 61000-3-3 states that the limit for P_{st} and P_{lt} shall not be more than 1.0 and 0.65, respectively. The expressions for P_{st} and P_{lt} can be determined by (Sivaraman & Sharmeela, 2021),

$$P_{st} = \left(\frac{S_L}{S_{TR}}\right)^{\frac{1}{3}} \quad (2.6)$$

$$P_{lt} = 0.65 \left(\frac{S_L}{S_{TR}}\right)^{\frac{1}{3}} \quad (2.7)$$

Where, S_{TR} represents the rated apparent power of the transformer supplying the load and S_L represents the rated power of the load.

A wind turbine's flicker emissions also rely on its short-circuit power capacity. The short-circuit power capacity of the wind turbine describes the network's ability to deliver electricity to varying loads without excessive flickering. Due to the low short-circuit power capacity of the distribution networks to which wind turbines are connected, their short-circuit power capacity is often low and more prone to flicker emissions. Therefore, raising the grid's impedance angle from 0 to 90 degrees may strengthen the grid and reduce flicker emissions (Nobela et al., 2019).

Causes for voltage fluctuations are usually found in non-linear power electronic converters in WECS, arc furnaces, starting and stopping electric motors, load fluctuation in the power system, and wind speed fluctuation that causes power output variations (Misak & Prokop, 2017; Mikkili & Panda, 2016; Kannan & Ali, 2017).

2.7.3 Voltage unbalance

Voltage unbalance arises in a three-phase system when the phase angles and voltage magnitude are unequal (Mikkili & Panda, 2016). Figure 2.13 illustrates the unbalanced voltage waveforms in a three-phase system.

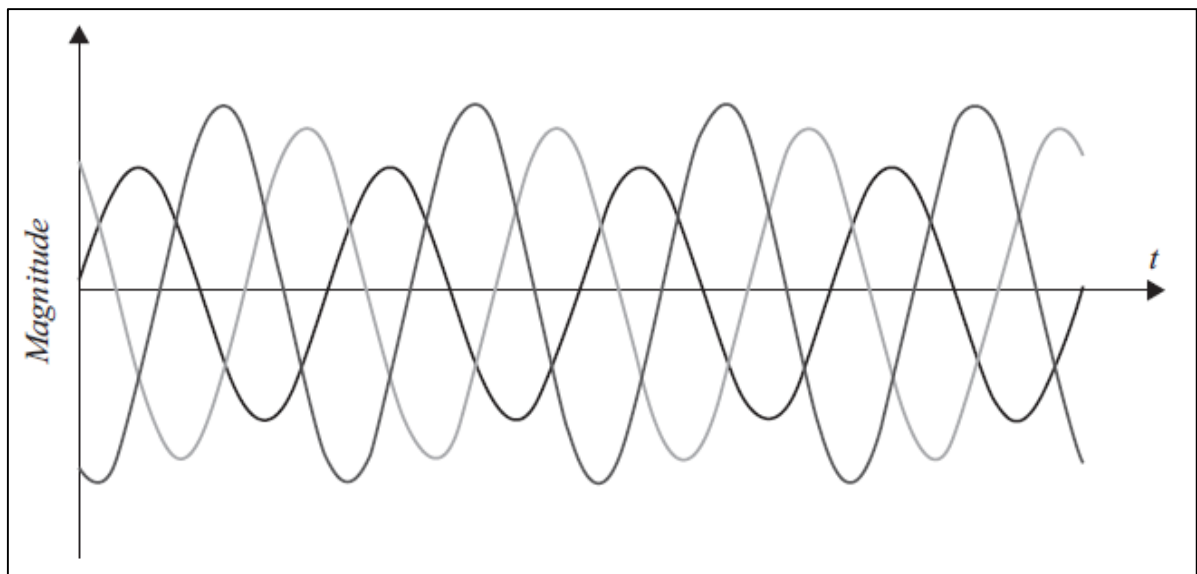


Figure 2.13: Voltage unbalance in a three-phase system (Kannan & Ali, 2017)

Voltage unbalance is the ratio, expressed as a percentage, of the positive and negative sequence components (Sivaraman & Sharmeela, 2021). The voltage unbalance factor (VUF) is expressed as follows: (Mahela et al., 2019),

$$VUF (\%) = \frac{V_2}{V_1} \times 100 \quad (2.8)$$

Where, V_1 is the positive sequence voltage and V_2 is the negative sequence voltage.

Unbalanced voltages are the result of asymmetrical loads among the three phases and incorrect sizing of individual cables (Fang, 2021a). Effects of voltage unbalance can lead to more reactive power and unbalanced currents, heating in electrical motors' windings, reduced performance in electrical motors and transformers, and oscillating torque in electrical motors (Kannan & Ali, 2017; Sivaraman & Sharmeela, 2021).

2.7.4 Voltage sag

Voltage sags are short episodes of undervoltage supply followed by rapid recovery (Musoni, 2018). Voltage sags in power networks are quite troublesome in terms of interruptions. The RMS of a voltage drop from 0.9 per unit (p.u) to 0.1 p.u for a duration of one minute, or half a frequency cycle, is used to determine the magnitude of voltage sags (Kaushal & Basak, 2020). Some of the principal causes of voltage sags include short circuits and large motor drives' start-up, which drastically diminish voltage magnitude (Morshed, 2018). Figure 2.14 depicts a voltage sag that generally has a rectangular shape.

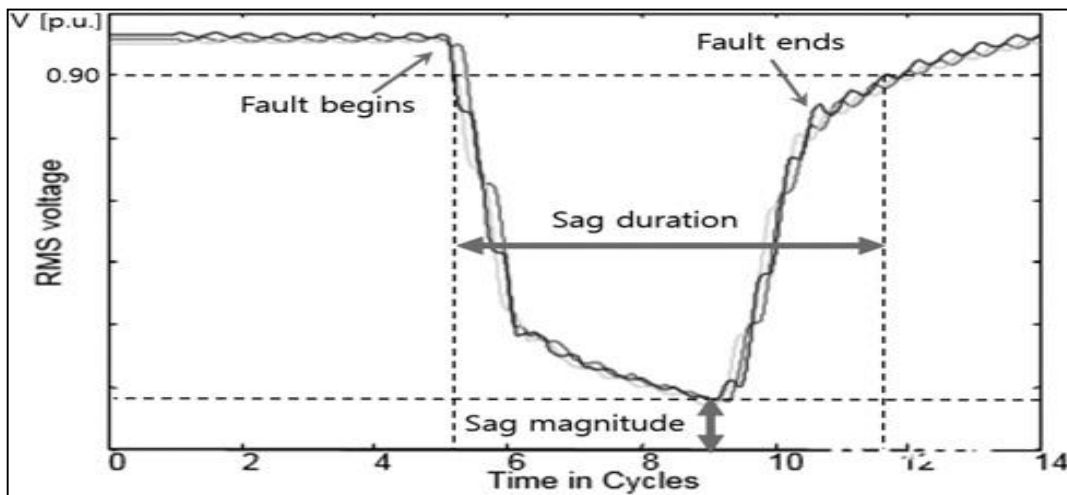


Figure 2.14: Voltage sag caused by a fault (Park & Jang, 2016)

As seen in Figure 2.14, when a problem develops in the grid, the voltage drops significantly; it then rises once the protection system fixes the fault. The fault location, fault type, grid voltage prior to the fault, transformer connection type, and fault impedance significantly impact the voltage sag's amplitude. In addition, the system protection coordination and equipment employed, such as circuit breakers, fuses, and overcurrent relays, determine how long the voltage sag lasts. An extremely problematic issue near a wind turbine may result in significant voltage sags and maybe sags that might lead the voltage at the PCC to drop to 0 p.u (Park & Jang, 2016).

Reactive power fluctuation and voltage variation in induction generators are proportional. Due to the torque imbalance between the generator and the wind turbine, the short-circuit current in the case of a malfunction may result in a voltage dip and the generator's voltage terminal. The induction generator needs reactive power to recover the voltage at its terminals once the fault has been fixed and the system voltage has been restored. The generator's inrush current and reactive power absorption might cause a voltage drop. The voltage dip causes the terminal voltage to recover slowly, speeding up the generator and raising reactive power consumption.

If the generator cannot recover, the wind turbine is removed from the grid, which greatly affects system stability (Aluko, 2018). When a wind turbine with a large megawatt rating to be removed from the grid owing to severe voltage sag, a significant blackout may result (Park & Jang, 2016). Customers may see the voltage sag's effects in various ways, including annoying light flickering, tripping sensitive loads, and electrical motor stalling (Musoni, 2018).

Voltage sag is represented as a relative percentage change in the linked wind turbine's system voltage. The relative variation is represented as (Aluko, 2018),

$$d = k_u \frac{S_n}{S_k} \quad (2.9)$$

S_n is defined as the rated apparent power, S_k is defined as the short-circuit apparent power, d represents the relative change in voltage, whereas k_u denotes the voltage reduction factor.

2.7.5 Voltage swell

Voltage swells happen when the nominal RMS voltage increases from 1.1 p.u. to 1.8 p.u. within 0.5 to 1 minute (Sivaraman & Sharmeela, 2021). Less often than voltage sags, voltage swell is typically brought on by a fault condition, the starting, and stopping of large loads on the power grid, or the switching of capacitor banks. However, this phenomenon has the potential to disrupt current flow, creating a high voltage that might harm delicate machinery or even disconnect wind turbine engines (Almohaimed & Abdel-Akher, 2020). A situation with a voltage swell is shown in Figure 2.15.

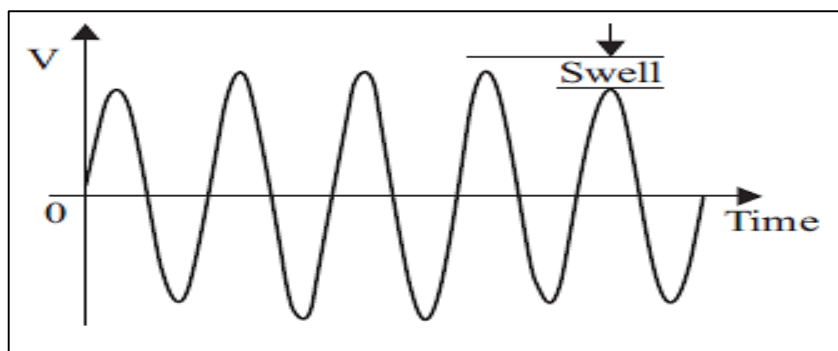


Figure 2.15: Voltage swell (Kannan & Ali, 2017)

2.7.6 Undervoltage

Undervoltage occurs when the nominal RMS voltage decreases within 0.8 p.u. and 0.9 p.u. for more than one minute (Kannan & Ali, 2017). As per the definition of undervoltage, a total system blackout can also be classified as an undervoltage scenario (Fang, 2021b). Figure 2.16 illustrates an undervoltage trend.

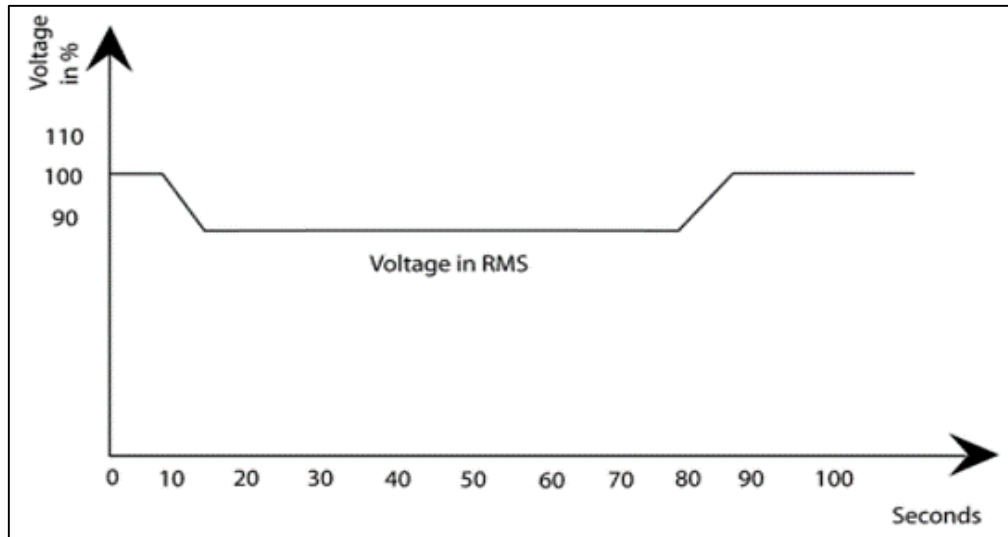


Figure 2.16: Undervoltage trend (Sivaraman & Sharmeela, 2021)

Causes of undervoltage events occur when starting heavy loads or switching off large capacitor banks that supply reactive power (Mikkili & Panda, 2016). Effects of undervoltage events come in the form of overloading due to the low voltage amplitude that leads to overheating of electrical motor windings consuming more power and voltage instability, leading to high reactive power demand (Sivaraman & Sharmeela, 2021; Kannan & Ali, 2017).

2.7.7 Overvoltage

Overvoltage occurs when the nominal RMS voltage rises from 1.1 p.u. to 1.2 p.u. for longer than one minute (Kannan & Ali, 2017). When heavy loads are turned off, huge capacitor banks that generate reactive power are turned on, and incorrect transformer tap settings, overvoltage events can occur (Mikkili & Panda, 2016). Overvoltages are also caused by improper reactive power regulation and excessive reactive power production (Fang, 2021a). Figure 2.17 depicts a trend in overvoltage.

Effects of overvoltage events come in the form of dielectric failure that causes tripping of protection equipment, reduced performance on equipment, and risk of data loss in computer and healthcare centers (Sivaraman & Sharmeela, 2021; Kannan & Ali, 2017).

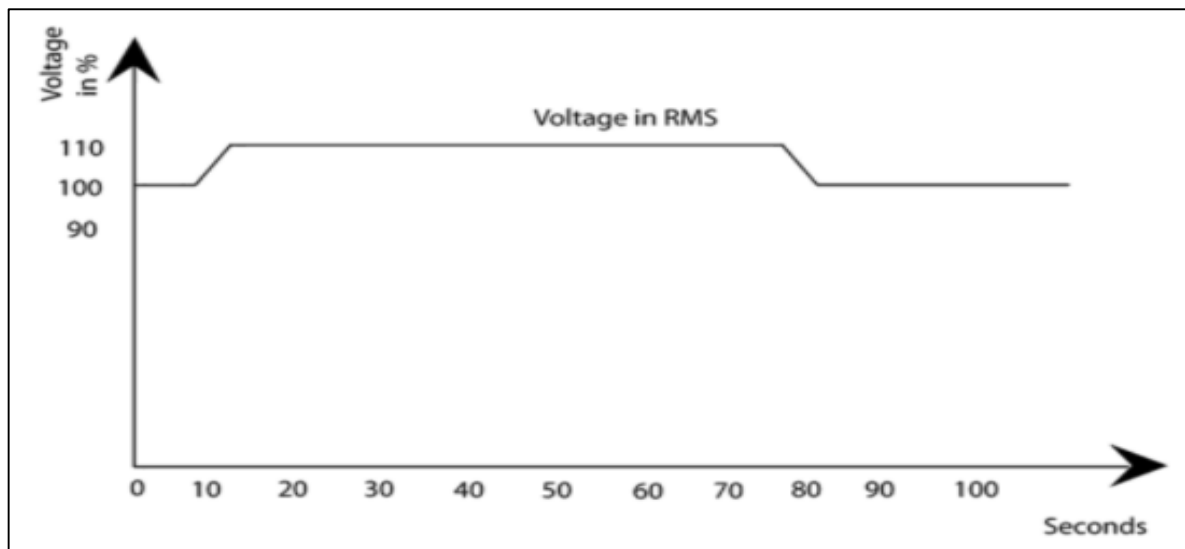


Figure 2.17: Overvoltage trend (Sivaraman & Sharmeela, 2021)

2.8 Grid strength

Integrating a wind turbine plant into the grid affects power system quality parameters at the PCC. The severity of this effect depends on the ratio of the short-circuit power of the electrical grid (Misak & Prokop, 2017).

On the basis of their short-circuit ratio (SCR), electrical grids may be classified as weak or strong. The electrical grid contains power lines that introduce line impedances. Strong grids have small line impedances with close to zero effects and can be considered an ideal voltage source. On the other hand, weak grids have varying line impedances based on the changes in grid configurations and operating conditions (Fang, 2021c).

Improper use of inverter-based resources with RES can severely affect weak electrical grids. The typical protective relay system, which was first created for synchronous generators, is predicted to behave differently as a result of the inverter-based resources' unique short-circuit characteristics (Haddadi et al., 2021). Grid operators face transmission line overloading, deviation of voltage levels, and a low short-circuit ratio. The strength level should be determined on each bus to analyze the grid performance with the presence of RES by the sensitivity of the voltage terminal at the PCC to its current injection variations. The SCR index is a tool to determine the relative strength of the electrical network (Zare Oskouei & Mohammadi-Ivatloo, 2020).

SCR index refers to the ratio of short-circuit power at the PCC where the RES is linked. The RES's nominal capacity is given as,

$$SCR_i = \frac{SK_i^n}{Pn_i} \quad (2.10)$$

Where, i is the selected busbar, SK_i^n is the short-circuit power level at busbar i^{th} and Pn_i is the RES's ability to inject power. According to the IEC 60909 standard, the busbar shall have an adequate strength level with an SCR index of less than 3. The short-circuit power is defined by,

$$SK_i^n = \sqrt{3}x IK_i^n x U_i^n \quad (2.11)$$

Where IK_i^n is the short-circuit current at the i^{th} busbar and U_i^n is the line-to-line voltage at the i^{th} busbar (Zare Oskouei & Mohammadi-Ivatloo, 2020).

To investigate how the grid's strength influences the supply's voltage quality, system operators should compute the short-circuit power levels at the PCC where RES is present (Rosin et al., 2017).

2.9 Voltage quality enhancement in WECS

Some basic voltage quality mitigation techniques are discussed in this section to enhance voltage quality in WECS.

Renewable energy systems use two strategies to address power quality difficulties. The first approach is load conditioning, in which equipment is put on the utility side. As a result, they are less sensitive to power disturbances up to a particular level, even under severe voltage distortion. The second method is line conditioning, where equipment is installed at the consumer end to suppress or counteract power system disturbances (Mikkili & Panda, 2016; Hepsiba et al., 2021).

Various voltage quality enhancement approaches are discussed, such as,

- Reactive power and voltage control.
- Power filters.
- Low-voltage ride-through capabilities.
- Flexible AC transmission controllers.

2.9.1 Reactive power/voltage control

Voltage is required for the movement of electricity via any electrical grid. Changing the reactive power reference of power stations and their active and passive sources controls the power flow. Voltage control entails the supply of reactive power from either static or dynamic sources, including capacitor banks, voltage controllers, and flexible AC transmission controllers. Synchronous compensators, generators, and voltage regulators are examples of dynamic sources. Voltage control, according to (Molina-Garcia et al., 2017), serves two purposes:

1. Steady-state reactive power and voltage control:

The objective of steady-state reactive power and voltage regulation is to retain the magnitude and profile of the voltage as close to the intended magnitude and profile within the tolerance band margins and over the course of hours. At a voltage-controlled node, reactive power and voltage control may be achieved by injecting or absorbing reactive power.

2. Dynamic voltage stability:

Dynamic voltage stability strives to preserve the grid voltage within a dynamic time frame of seconds to minutes by avoiding a gradual voltage collapse event and the degree of system damage during an occurrence such as a generator unit loss.

Grid regulations like the IEC 61400-21 mandate that renewable generating units contribute to managing reactive power and power system voltage as RES increases.

The machines used in the wind turbines are usually induction generators that absorb reactive power for the excitation to create magnetic flux. However, these induction generators do not have reactive power support to the electrical grid like synchronous generators. Therefore, a suitable design of the control systems in wind turbines is vital for optimal operation by replacing conventional induction generators with generators that can absorb and supply reactive power. The replaced generators may contribute to the voltage profile of the power grid by providing reactive power assistance. Maintaining the grid's voltage within the acceptable operational limit is a critical issue because of the nature of wind that fluctuates, which leads to changes in the power production and may cause voltage fluctuations and flickering that depends on the generating system use for the mitigation of this issue. Supporting the grid to maintain a healthy voltage profile is challenging for some wind turbines. However, it can meet the grid code requirement as it does not have power electronic controllers to depend on for the supply of reactive power for reactive power support (Ahmed et al., 2020).

The employment of switched capacitor banks, Static VAR compensators (SVC), and Static Synchronous Compensators (STATCOM), which may perform voltage regulation, is required by international grid regulations for WECS (Mahela & Shaik, 2016).

Reactive power control is needed in electrical grids to reduce the voltage fluctuations caused by varying loads in the system and reduce power transmission losses. Traditionally reactive power compensations were provided by capacitor banks or on-tap load changers. Still, as newer technology has been developed in power electronic controllers, reactive power compensation is supplied by FACTS controllers, which have much better performance and response time (Aluko, 2018).

2.9.2 Power filters

Current harmonics affect the voltage quality. Power filters can be introduced to reduce current harmonics in an electrical grid to mitigate the harmonics. These power filters come in the form of passive and active filters (Mikkili & Panda, 2016). Figure 2.18 illustrates the classifications of power filters.

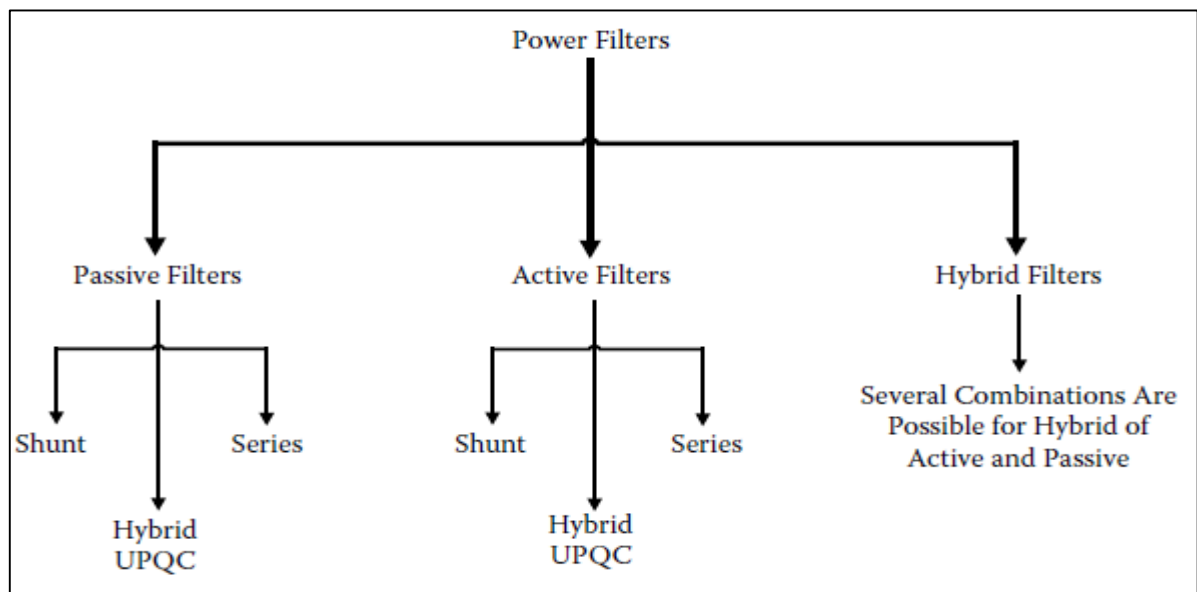


Figure 2.18: Power filters classification (Mikkili & Panda, 2016)

Passive filter:

Passive power filters are designed using a combination of passive electronic components like inductors and capacitors. The passive filter intends to block harmonic frequencies and provide reactive power support (Bajaj & Singh, 2020).

Series, shunt, or mixed series-and-shunt passive power filters are the several types of passive power filters (Mikkili & Panda, 2016). To create a detour for harmonics, shunt filters are put in parallel with the loads, and their inductance and capacitance are tuned to a value that makes their impedance high, causing the harmonic current frequencies that have a low impedance to be absorbed. However, to prevent harmonic currents from entering the load, series filters are put in series with the load (Naderi et al., 2018).

The benefits of passive power filters are their simplicity, low cost, and dependability as well as their ability to reduce harmonics and compensate for reactive power. However, the drawback of passive power filters is that they are often custom-designed for application and might cause electrical grid resonance (Mikkili & Panda, 2016; Naderi et al., 2018).

Active filter:

To circumvent the limitations of passive power filters, active power filters were developed. Active power filters may also be characterized as series or shunt, or as a combination of series and shunt.

Shunt active power filters compensate for the existing harmonic by injecting a current with the same amplitude and a 180-degree phase shift. Consequently, the grid current is close to sinusoidal, and the harmonic current is canceled. Furthermore, by introducing a series of harmonic voltages with a reverse phase, series active power filters operate as a regulated voltage source while reducing voltage harmonics (Naderi et al., 2018).

The active power filter has multiple advantages: they cancel out harmonics, have reactive power capability, and are small in size. However, some disadvantages are that they are costly and can introduce inherent harmonics due to power electronic equipment.

Hybrid filter:

Active and passive power filters are both used in hybrid power filters. In addition, hybrid power filters circumvent the physical limitations and application-specific design of passive power filters and are less expensive than high-capacity active power filters (Naderi et al., 2018).

Figure 2.19 illustrates the active power filter configurations.

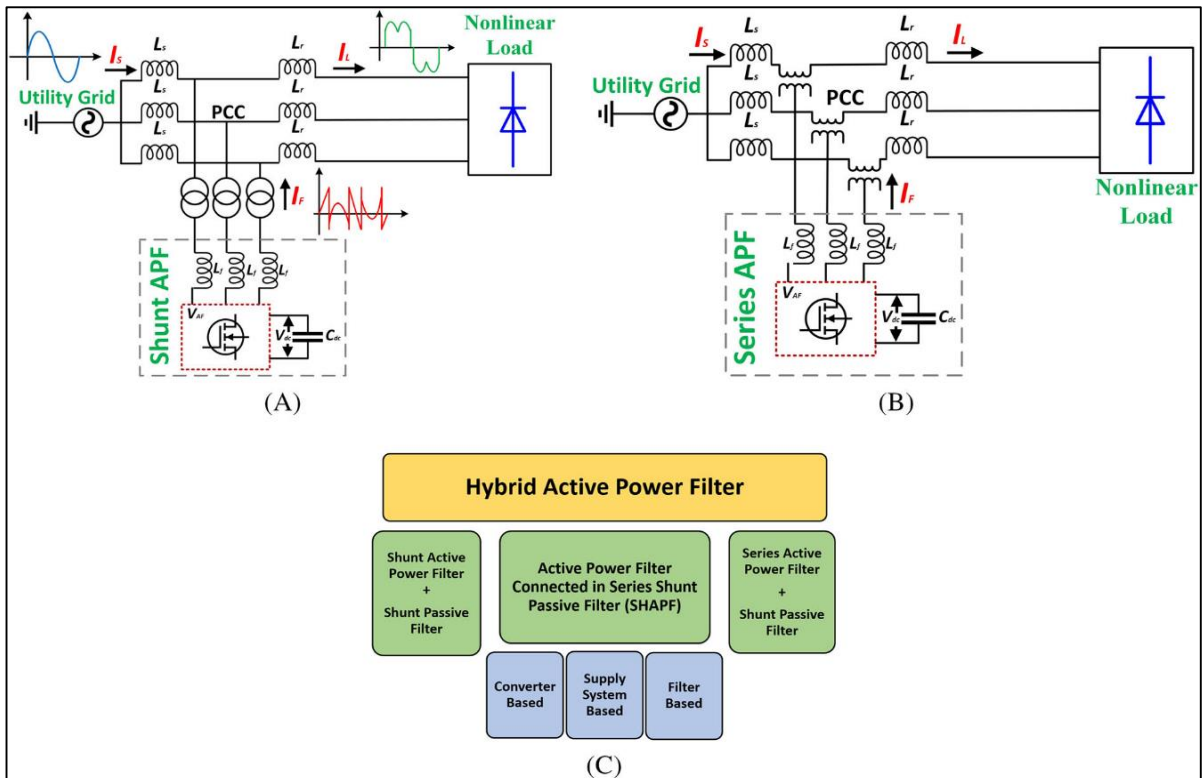


Figure 2.19: (A) Shunt active power filter, (B) Series active power filter, and (C) Hybrid active power filter (Bajaj & Singh, 2020)

Active power filters can contribute towards (Mikkili & Panda, 2016):

Shunt:

- Reactive power compensations.
- Voltage regulation.
- Compensation in unbalanced currents.

Series:

- Reactive power compensations.
- Voltage regulation.
- Compensation in voltage sags and swells.
- Unbalance voltage compensation.

Hybrid:

- Reactive power compensations
- Voltage regulation.
- Compensation in voltage sags and swells.
- Compensation in unbalanced voltages and currents.

2.9.3 Low-voltage ride-through capability

For a stable electrical system, several nations have adopted grid standards with low-voltage ride-through (LVRT) requirements. One of the primary criteria of the LVRT is that the wind turbine must remain connected to the electrical grid and produce reactive current during voltage sags (Popavath & Kaliannan, 2018). However, due to the unpredictability of any network fault that can cause voltage sag, the occurrence of the fault is treated as a random incident. Because of this unexpected phenomenon, it is crucial to establish efficient countermeasures and corrective mitigation plans for the fault that causes voltage sag and assess the effectiveness of the voltage sag performance (Shakeri et al., 2020).

During a fault situation experienced by a wind turbine, the electrical grid of the wind turbine encounters a voltage sag. If the wind turbine trips due to the fault state, the electrical grid voltage continues to decrease even more. The frequency of the grid will be impacted by the power imbalance caused by the loss of a generating unit. With the loss of the generator, a cascade effect may result from the overloading of generators remaining linked to the grid, which may also trip and cause a blackout. In order to maintain the generator's connection to the grid during faults, wind turbines must be provided with LVRT capabilities. Figure 2.20 illustrates the requirements for the LVRT capabilities.

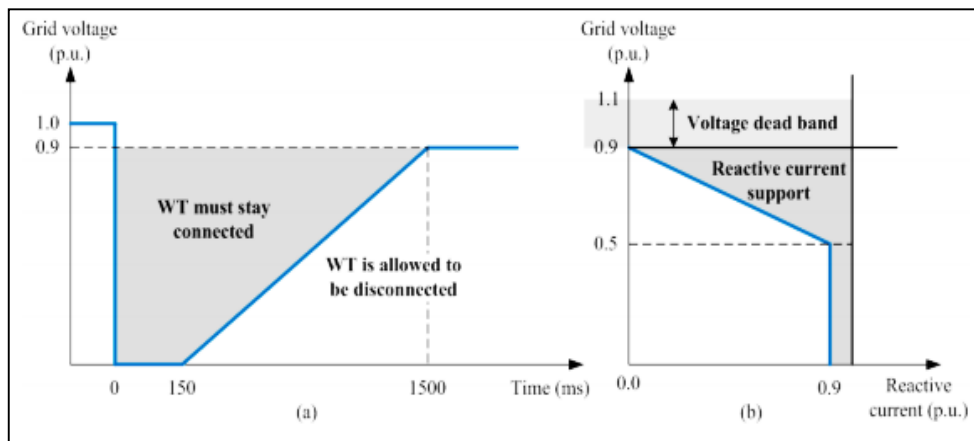


Figure 2.20: Grid code requirement during fault consists of (a) Ride-through curve and (b) Reactive power support curve (Hu et al., 2017)

Figure 2.20 (a) demonstrates that the wind turbine should stay connected to the grid so long as the grid voltage and duration of the fault remain within the shaded region. The decrease in grid voltage will result in an overcurrent in the generator windings and an increase in DC-link voltage. In order to limit the consequences of the malfunction on the generator and its control systems, protective equipment must be added. Figure 2.20 (b) demonstrates that in order to maintain operable grid voltage, the wind turbine must assist the grid by producing reactive current during the fault when the voltage sags. When a fault occurs, the voltage corrective

control should be initiated within 20 milliseconds (ms). The wind turbine should supply reactive current according to the magnitude of the voltage sag and inside the shaded region. After the fault has been rectified, the wind turbine should continue to provide active power at a gradient of 20% of the wind turbine generator's rated active power (Hu et al., 2017).

Figure 2.21 depicts the grid code requirements for wind turbines connected to the grid at or above 110 kV in several European countries. The turbines must be transiently stable and linked to the electrical grid even if the RMS voltage exceeds the minimum voltage limit. In addition, the turbine must not be isolated from the electrical grid owing to a three-phase or unbalanced short-circuit failure during the transient event (Molina-Garcia et al., 2017).

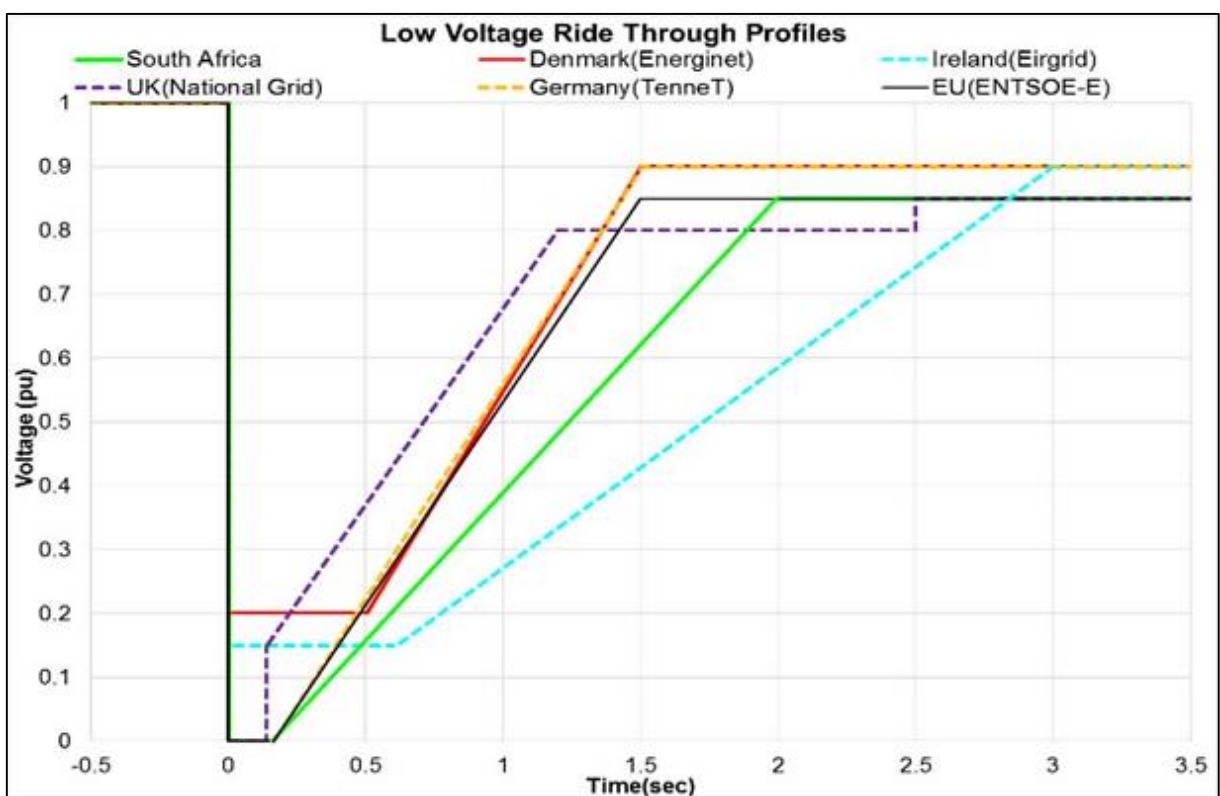


Figure 2.21: European grid code requirements of grid-connected wind power plant (Nhlapo & Awodele, 2020)

Table 2.1 indicates the extent to which the wind turbine needs to remain grid-connected. For each country, there are regulations that the wind turbines must adhere to for grid support during a fault. First, the voltage magnitude can decrease to the listed p.u value, but only for a certain duration. After that, the voltage magnitude should increase again above the listed p.u value within the time limit after the initial fault occurred. The wind turbine should be disconnected from the electrical grid for any condition outside the listed voltage magnitudes and time limits.

Table 2.1: Voltage magnitude and duration for LVRT international grid codes (Mahela et al., 2019; Aluko & Akindeji, 2018)

| Country | Voltage sag magnitude and duration | Voltage recovery within a time limit |
|----------------|------------------------------------|--------------------------------------|
| Australia | 0.00 p.u. for 100 milliseconds | 0.70 p.u. within 2000 milliseconds |
| Canada | 0.00 p.u. for 150 milliseconds | 0.85 p.u. within 1000 milliseconds |
| Denmark | 0.20 p.u. for 500 milliseconds | 0.90 p.u. within 1500 milliseconds |
| Germany | 0.00 p.u. for 150 milliseconds | 0.90 p.u. within 1500 milliseconds |
| India | 0.15 p.u. for 300 milliseconds | 0.85 p.u. within 3000 milliseconds |
| Ireland | 0.15 p.u. for 625 milliseconds | 0.90 p.u. within 3000 milliseconds |
| New Zealand | 0.00 p.u. for 200 milliseconds | 0.60 p.u. within 1000 milliseconds |
| Spain | 0.00 p.u. for 150 milliseconds | 0.85 p.u. within 1000 milliseconds |
| United Kingdom | 0.15 p.u. for 140 milliseconds | 0.80 p.u. within 1210 milliseconds |
| USA (FERC) | 0.15 p.u. for 625 milliseconds | 0.90 p.u. within 3000 milliseconds |
| USA (WECC) | 0.00 p.u. for 150 milliseconds | 0.90 p.u. within 1750 milliseconds |
| South Africa | 0.00 p.u. for 150 milliseconds | 0.85 p.u. within 2000 milliseconds |

The reactive power compensating controllers provide the reactive power source for the LVRT (Lee et al., 2017).

2.9.4 Flexible AC transmission controllers

Flexible AC transmission system (FACTS) controllers may assist electrical grids by managing the associated factors that affect transmission system performance. These controllers may manage oscillation damping, current and voltage, phase angle, series and shunt impedance, and phase angle. In addition, FACTS controllers provide control for steady-state power flows, dynamic stability controls, transient stability enhancements, voltage management, and voltage stability controls (Mishra et al., 2020).

FACTS controllers can be integrated into the electrical grid in different configurations and are categorized into four categories. FACTS controllers have series, shunt, shunt-series, or series-series configurations (Vishnupriyan & Dhanasekaran, 2021).

The four categories with the type of controllers are known as (Singh & Agrawal, 2018):

1. Series controllers:
 - Static Synchronous Series Compensators (SSSC).
 - Thyristor Controlled Series Capacitor (TCSC).

2. Shunt controllers:
 - Static VAR Compensators (SVC).
 - Static Synchronous Compensators (STATCOM).

3. Series-series controllers:

- Interline Power Flow Controllers (IPFC).
- Thyristor-Controlled Voltage Regulators (TCVR).
- Thyristor-Controlled Voltage Limiters (TCVL).

4. Shunt-series controllers:

- Thyristor-Controlled Phase Shifting Transformers (TCPST).
- Unified Power Flow Controllers (UPFC).

Frequent applications of the FACTS controllers SVC and STATCOM enhance power transmission efficiency in power systems. For example, FACTS controllers have been used in wind energy conversion systems (WECS) to enhance their transient stabilities, voltage qualities, and regulations (Morshed, 2018; Ezhiljenekha & MarsalineBeno, 2020).

As WECS chose SVC and STATCOM as its FACTS controllers, the focus will continue solely on SVC and STATCOM for voltage quality improvement.

2.9.4.1 Static VAR Compensator (SVC)

SVC is one of the shunt-connected FACTS controllers, a crucial device for enhancing electrical grid stability and voltage management. The SVC can manage the voltage profile by absorbing and injecting adequate reactive power. Figure 2.22 depicts the different kinds of reactive power control components that make up an SVC device, including a thyristor-controlled reactor (TCR) for absorbing reactive power and a thyristor-switched capacitor (TSC) for injecting reactive power (Rezaie & Kazemi-Rahbar, 2019).

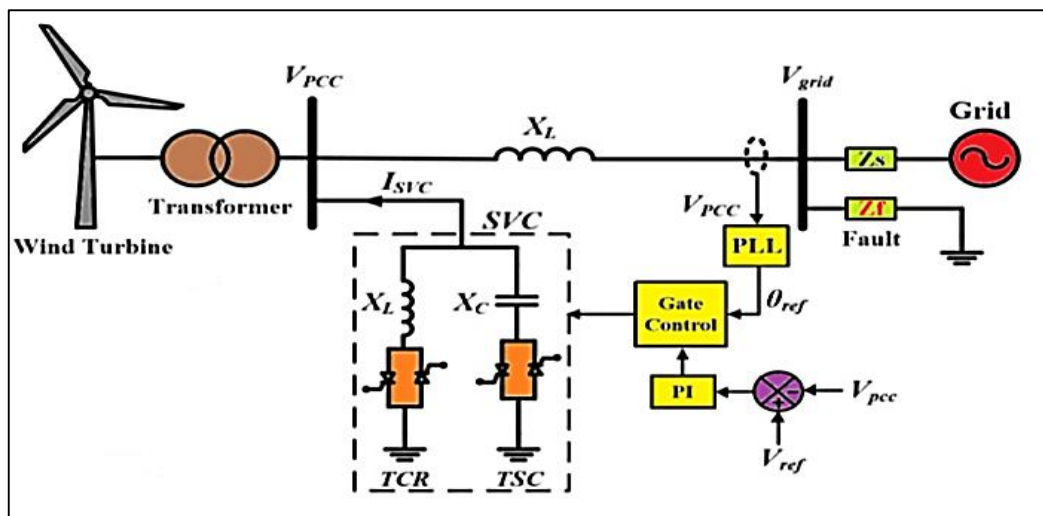


Figure 2.22: SVC in WECS (Ganthia et al., 2020)

Due to its TCR and TSC components, the SVC is capable of inductive or capacitive operation and is linked in parallel to the electrical grid. The SVC employs its TCR to absorb reactive power from a capacitive system load, whilst its TSC creates reactive power from an inductive system load in order to enhance voltage conditions (Ćalasan et al., 2021).

The reactance value of the inductor is continuously altered by modifying the firing angle of the thyristor. In order to avoid inrush currents, the capacitor is cycled on and off at intervals corresponding to zero-crossings of the current. Within a certain range, the SVC may continuously generate reactive power (Hossain et al., 2018).

Two modes of operation for SVCs are voltage regulation and volt-ampere reactive (VAR) regulation mode. Figure 2.23 depicts the SVC's typical voltage-current (V-I) and voltage-reactive power (V-Q) curves.

As demonstrated in Figure 2.23 (a), the SVC's maximum capacitive or inductive compensating current decreases linearly with system voltage. Figure 2.23 (b) shows that the maximum capacitive or reactive compensating reactive power reduces according to the square of the system voltage (Barrios-Martínez & Ángeles-Camacho, 2017).

The voltage reference V is maintained by droop control, as seen by the slope in Figure 2.23 (Bajaj & Singh, 2020; Omran et al., 2018). Therefore, based on the voltage droop, the maximum reactive currents and power the SVC can operate between are dependent on the voltage terminals of the SVC (Paredes et al., 2021).

SVC does have some disadvantages as it provides delayed responses due to its thyristor switching delay, voltage overshoots, and occasional causes cascading trips of wind turbines. Therefore, the installation of SVCs is limited. In addition, because of the large capacitive current consumption controlled by the capacitance bank size and system voltage, SVCs cannot enhance their VAR production during transient occurrences. Therefore, using SVC for large-scale wind farms for reactive power compensation is difficult (Ouyang et al., 2019; Barrios-Martínez & Ángeles-Camacho, 2017).

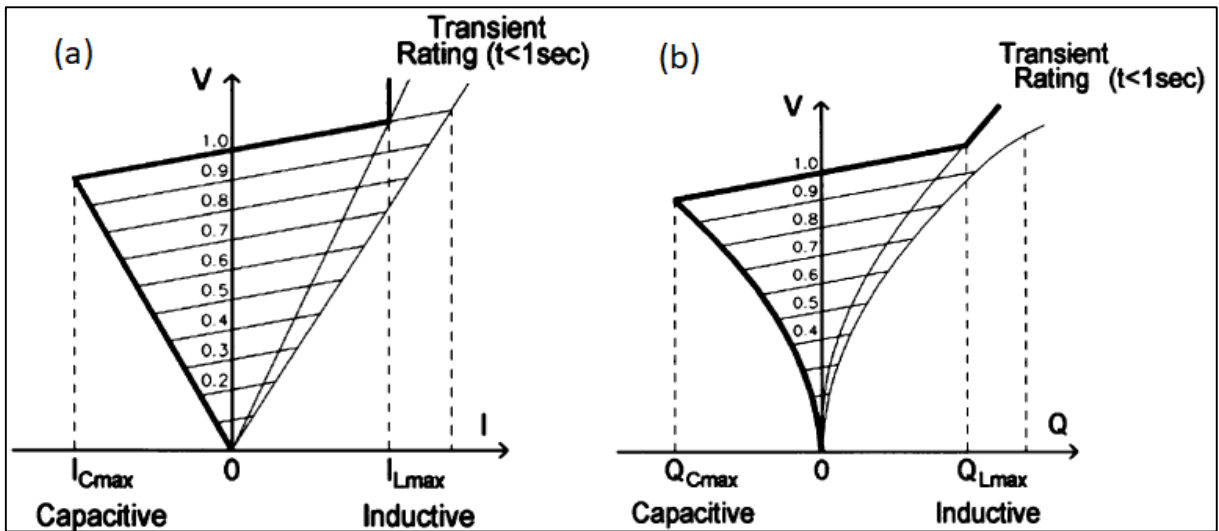


Figure 2.23: (a) SVC V-I characteristics curve, (b) SVC V-Q characteristics curve (Davidson & de Oliveira, 2020)

2.9.4.2 Static Synchronous Compensator (STATCOM)

STATCOM was introduced for electrical induction machines used in wind turbines to help stabilize and recover faults in the grid the wind turbines connected to. STATCOM will inject or absorb reactive power during steady-state to maintain a constant bus voltage and suppress voltage fluctuations. In addition, during any transient-state activity, the STATCOM will inject maximum reactive power to maintain the grid and restore the system voltage. Compared to SVC, the STATCOM allows higher transient margins with overloading capability (Rini Ann Jerin et al., 2018).

STATCOM has gained ground in the last decade. STATCOM is a voltage source converter (VSC) technology using insulated-gate bipolar transistor technology, which is more effective in voltage quality enhancement but, compared to the SVC technology, proposes a higher investment cost (Čerňan et al., 2021).

Figure 2.24 depicts the shunt connection of STATCOM to the electricity grid. The electronic STATCOM device is shunt-connected to the power grid and may absorb or provide reactive power to the grid in order to adjust for fluctuations. VSCs serves as the power electronic controllers for the STATCOM. There is an interaction between the power grid and the STATCOM in order to manage the flow of reactive power. Consider the example when the STATCOM terminal voltage is greater than the grid voltage. When this happens, the STATCOM acts as a capacitor to provide reactive power to the grid. Conversely, when the grid voltage is larger than the voltage at the STATCOM terminals, the STATCOM acts as an inductor, absorbing reactive power to reduce the grid voltage (Hossain et al., 2018).

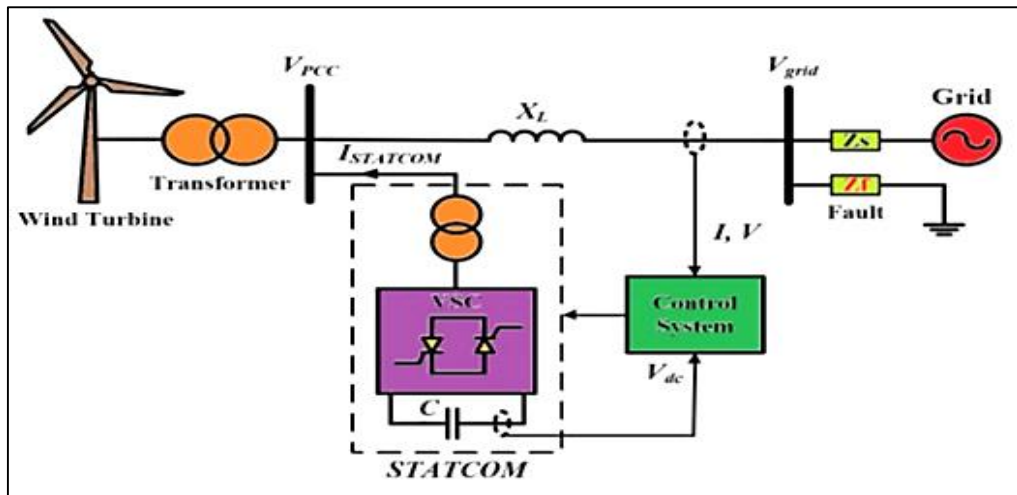


Figure 2.24: STATCOM in WECS (Ganthia et al., 2020)

In addition, STATCOM offers modes for voltage control and VAR regulation. Figure 2.25 shows the STATCOM V-I and V-Q characteristic curves. As demonstrated in Figure 2.25, the maximum capacitive or inductive compensating current from the STATCOM is greater than the SVC (a). Consequently, the maximum compensating current may be supplied at drastically reduced system voltage levels, as low as 0.2 p.u. Figure 2.25 (b) demonstrates that the maximum capacitive or reactive corrective reactive power from the STATCOM controller decreases linearly with the system voltage (Barrios-Martínez & Ángeles-Camacho, 2017).

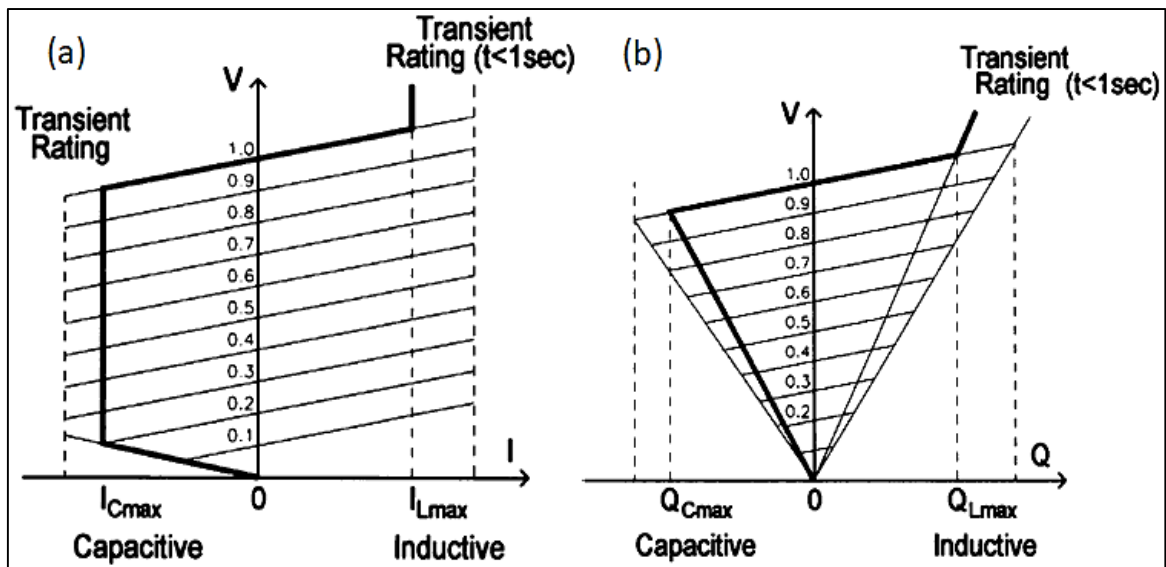


Figure 2.25: (a) STATCOM V-I characteristics curve, (b) STATCOM V-Q characteristics curve (Davidson & de Oliveira, 2020)

The system voltage will be controlled to be maintained at V as long as the reactive currents and powers stay between the limits. (Cherkaoui et al., 2018). Compared to the SVC V-I

characteristics curve, it is evident that the STATCOM is capable of exchanging maximal reactive current regardless of system voltage. (Vetoshkin et al., 2019).

The STATCOM regulates the terminal voltage to simulate a sinusoidal waveform. In order to mimic the waveform, the IGBTs are turned on and off in a specified sequence. As illustrated in Figure 2.26, the simulated waveform is generated utilizing two switch methods—square-wave modulation and pulse-width modulation—and four full bridges.

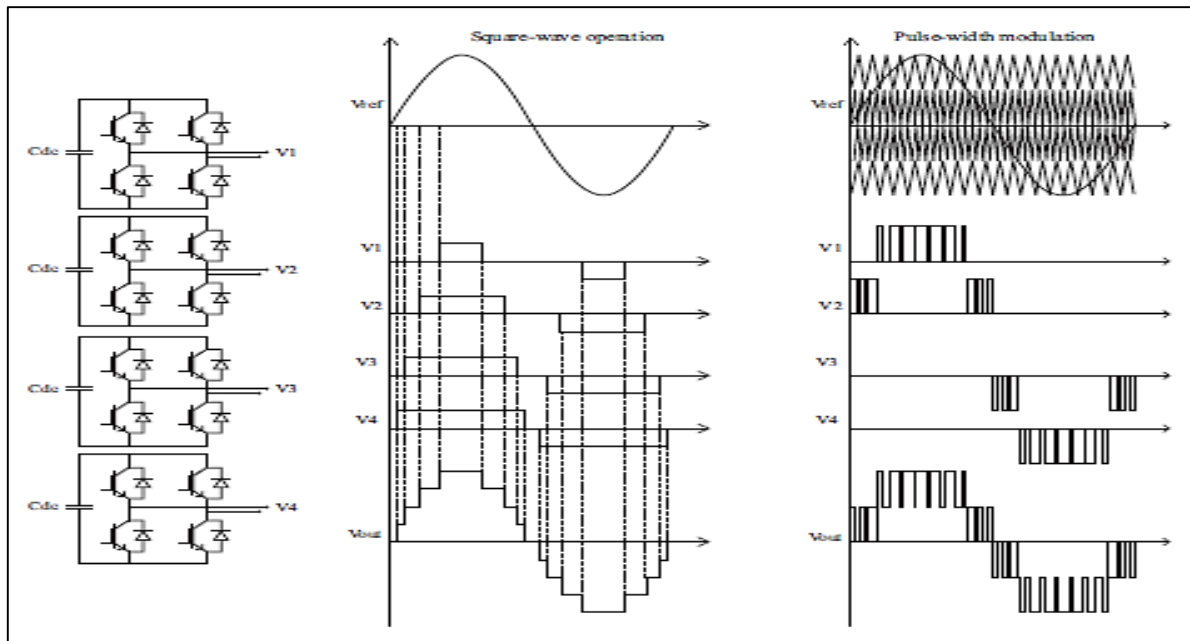


Figure 2.26: Output waveforms for square-wave modulation and pulse-width modulation (Todeschini, 2017)

2.10 Summary and Conclusion

This chapter provided a study on existing literature for voltage quality enhancement in WECS. The chapter started with an introduction to renewable energy, with brief discussions of common types of renewable energy. The objective of this chapter was to give the reader an idea of what an electrical grid is and what the technical requirement is to integrate renewable energy systems into the grid. The chapter then shifted its emphasis to wind energy conversion systems, presenting the various wind turbine components and designs. It has been explained how the power output of a wind turbine is determined by discussing the power characteristics.

On the basis of the IEC 61400-21 standard, voltage-related power quality concerns were explored, including harmonic distortions, voltage flickering and fluctuations, voltage unbalance, voltage sags, voltage swells, under and overvoltage. Mitigation techniques must be applied to the grid to enhance the voltage quality within the IEC 61400-21 standard limits. Most of the

research determined that FACTS controllers are the most effective method of enhancing voltage quality with reactive power control.

For this reason, the focus will be on FACTS controllers for the rest of this dissertation by focusing on SVC and STATCOM. Chapter 3 will be the mathematical modeling for individual system components in the MATLAB/Simulink model in chapter 4.

CHAPTER THREE: MATHEMATICAL MODELING

3.1 Introduction

This chapter discusses the mathematical modeling of all the individual system components in a wind energy conversion system (WECS) virtual simulated grid. The mathematical modeling contains mathematical equations and equivalent circuits for the components.

The block diagram of the virtual model is seen in Figure 3.1. The first component is a variable-pitch wind turbine, whose turbine blades transform wind energy into mechanical energy. The mechanical energy is fed into the second component, the induction generator, which produces the electrical power. The third component is the step-up transformer to raise the wind turbine's voltage to the required grid voltage level. The fourth component is the transmission line that carries the generated power and feeds it into the electrical grid. Finally, the FACTS controllers, which consist of the SVC and STATCOM controllers, are presented that connect to the wind turbine in a shunt configuration as the reactive power compensating device for the voltage quality enhancement.

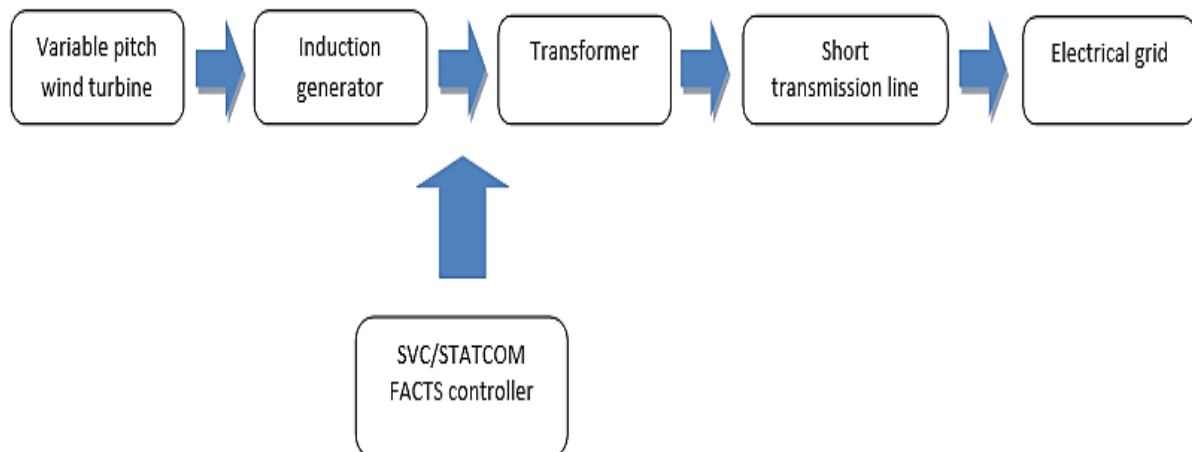


Figure 3.1: Block diagram for the proposed virtual simulation model

3.2 Variable pitch wind turbine

Wind turbines collect kinetic energy from the wind and transform it into mechanical energy for the generator. The mechanical power that a turbine is able to generate is dependent on the power coefficient C_p . Please refer back to Chapter 2 section 2.5.3 for the wind turbine power characteristics.

A proportional-integral (PI) controller controls the blades of the wind turbine. Figure 3.2 depicts the operation of the PI controller. The blade pitch angle is maintained constant at 0 degrees to get the maximum power coefficient. When the power output surpasses the reference power, the PI controller increases the pitch angle to reduce the power output to the nominal amount (Solanki & Mittal, 2017).

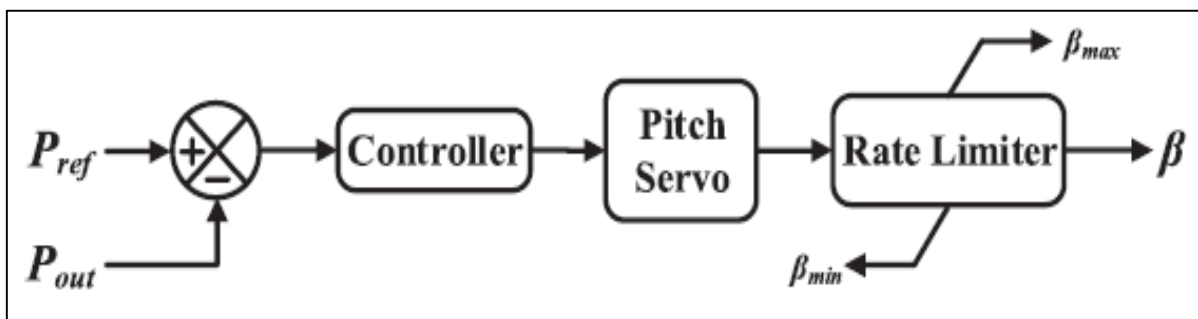


Figure 3.2: Control system for pitch angle control (Moghadasi et al., 2016)

3.3 Induction generator

An induction generator, also known as an asynchronous generator, is an AC generator with the same construction as an AC induction motor. The induction generator has a quicker rotor speed than the synchronous speed. When it is linked to an electrical grid, an induction generator begins as an induction motor utilizing grid power. The prime mover raises the rotor speed above synchronous speed once the induction generator is almost at its rated speed to produce a negative slip. The induction generator provides active power to the electrical grid because of the negative slip. The induction generator uses grid magnetization current to keep the magnetic field in the stator windings (Abdin et al., 2021).

A back-to-back VSC, a fixed capacitor bank, or FACTS controllers can all be used to link an induction generator to a wind turbine. When the induction generator is combined with the FACTS controller and capacitor bank, the WECS works at a constant speed and cannot provide its maximum output power at fluctuating wind speeds. Through its maximum power point tracking, the WECS functions at varying speeds when the induction generator and back-to-back VSC are combined (Satpathy et al., 2021).

For this study, the induction generator is a fixed-speed squirrel cage induction generator (SCIG) operating with the FACTS controller and fixed capacitor bank.

Figure 3.3 (a) illustrates a fixed-speed SCIG linked to bus k of an electrical grid. S_g is the generator output power and P_m wind turbine mechanical input power. Figure 3.3 (b) and (c) illustrate the steady-state equivalent circuits of the SCIG. Figure 3.3 (b) illustrates the steady-state equivalent circuit of the SCIG in terms of resistances and reactances. R_s is the stator winding resistance and X_s is the stator winding reactance, R_r is the rotor resistance and X_r is the rotor reactance, R_c is the core resistance and X_M is the core reactance, V_s is the stator voltage and I_s is the stator current, V_r is the rotor voltage and I_r is the rotor current, and s is the slip of the induction generator. Figure 3.3 (c) illustrates the steady-state equivalent circuit of the SCIG in terms of impedances.

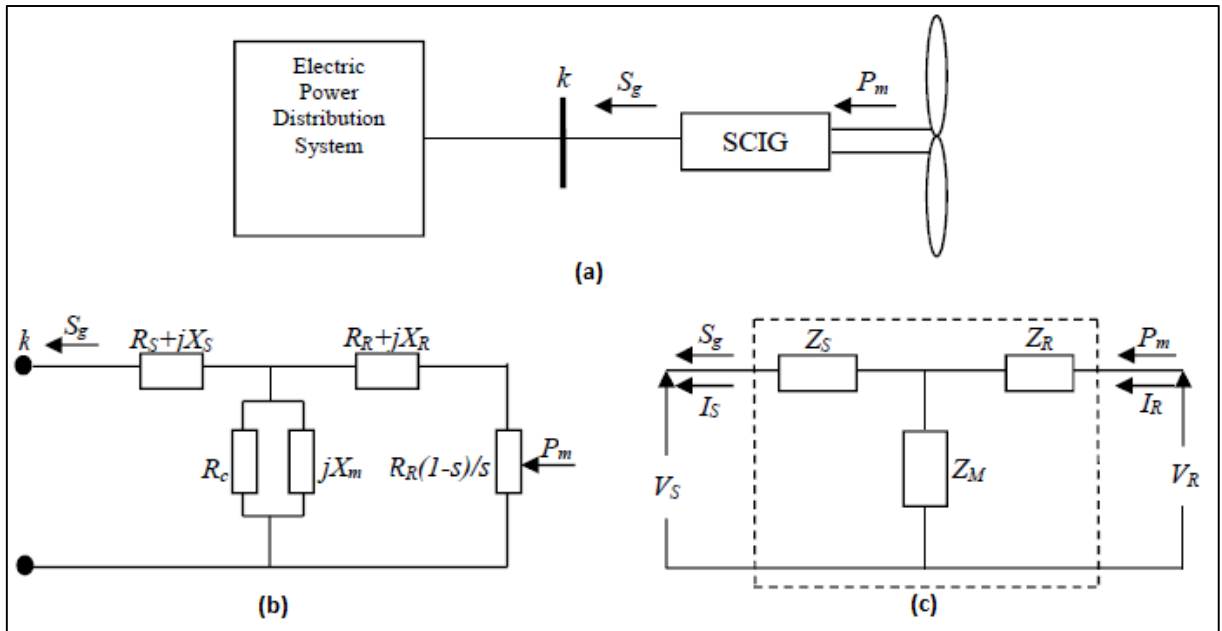


Figure 3.3: (a) Squirrel cage induction generator connected to an electrical, (b) Steady-state equivalent circuit in terms of resistances and reactances, and (c) Steady-state equivalent circuit in terms of impedances (Gianto & Purwoharjono, 2022)

The impedances of Z_s , Z_r , and Z_M can be calculated by (Gianto & Purwoharjono, 2022),

$$Z_s = R_s + jX_s \quad (3.1)$$

$$Z_r = R_r + jX_r \quad (3.2)$$

$$Z_M = \frac{jR_c X_M}{R_c + jX_M} \quad (3.3)$$

Using Figure 3.3 (c) and basic Kirchoff and Ohm laws, equations can be derived for stator and rotor currents (Gianto, 2020),

$$I_S = \frac{1}{Z_S}(V_R - V_S - Z_R I_R) \quad (3.4)$$

$$I_R = \frac{Z_M}{Z_R + Z_M} I_S + \frac{1}{Z_R + Z_M} V_R \quad (3.5)$$

The generator output power and mechanical input power are derived by,

$$S_g = P_g + jQ_g = V_S I_S^* \quad (3.6)$$

$$S_m = P_m + j0 = V_R I_R^* \quad (3.7)$$

Using Equation 3.6 and Equation 3.7, the stator and rotor currents are formulated by,

$$I_S = \frac{S_g^*}{V_S^*} \quad (3.8)$$

$$I_R = \frac{P_m}{V_R^*} \quad (3.9)$$

The following formulae are generated by replacing Equations 3.8 and 3.9 into Equations 3.4 and 3.5,

$$\frac{S_g^*}{V_S^*} - \frac{1}{Z_S}(V_R - V_S) + \frac{Z_R P_m}{Z_S V_R^*} = 0 \quad (3.10)$$

$$\frac{P_m}{V_R^*} - \frac{Z_M}{Z_R + Z_M} \frac{S_g^*}{V_S^*} - \frac{1}{Z_R + Z_M} V_R = 0 \quad (3.11)$$

Equation 3.10 and Equation 3.11 are the mathematical modeling for a wind turbine linked to an electrical network and can be used for any load flow analysis.

In order to supply reactive magnetization for the stator winding, a capacitor bank is employed with a SCIG that is directly linked to the electrical grid. The magnetizing reactance of the SCIG, which can be found in the nameplate data, is taken into consideration to estimate the value of the capacitor bank. The capacitor's value is determined using (Silva et al., 2020),

$$C_{minimum} = \frac{3}{\omega X_m} \quad (3.12)$$

The induction generator's magnetizing reactance must be supplied with a minimum amount of three-phase reactive power, which is defined by,

$$Q = 3 \left(\frac{V_1^{phase}}{\omega C_{minimum}} \right) \quad (3.13)$$

3.4 Transformer

Transformers are used to achieve the increase and decrease of voltage levels. The simplest transformer is a single-phase transformer that consists of an iron core with two windings known as the primary and secondary winding (Melkebeek, 2018).

Figure 3.4 illustrates the steady-state per-phase equivalent circuit, which consists of ohmic losses, primary and secondary winding leakage flux, series resistances, and reactances. The primary side for the transformer's equivalent circuit is shown, with the apostrophe (') symbol representing the secondary side value that is referred to the primary side.

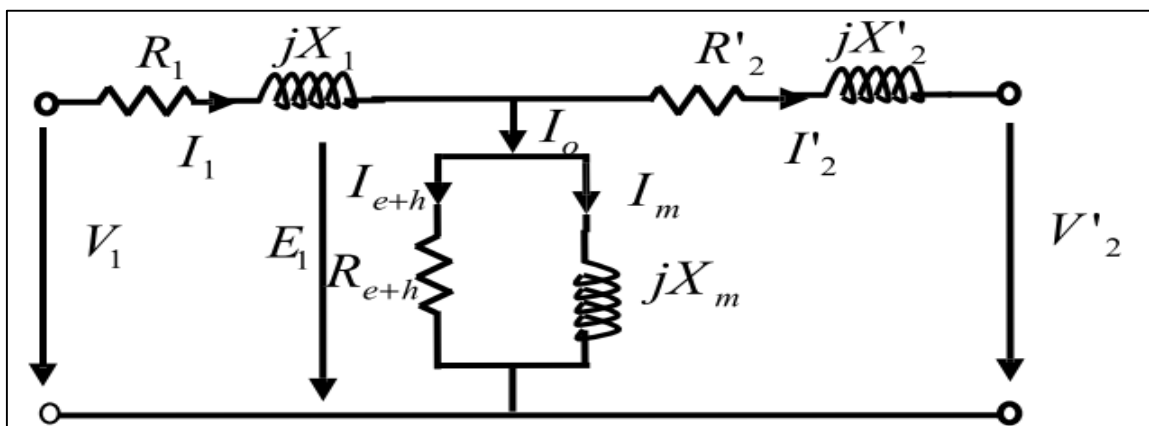


Figure 3.4: Per-phase transformer equivalent circuit (Abdelwanis et al., 2020)

The following equations may be determined by using the Kirchoff voltage law on the equivalent circuit in Figure 3.4 (Abdelwanis et al., 2020; Calasan et al., 2020),

The primary side impedance is,

$$Z_1 = R_1 + jX_1 \quad (3.14)$$

The secondary side impedance is,

$$Z'_2 = R'_2 + jX'_2 \quad (3.15)$$

The primary voltage is,

$$V_1 = E_1 + I_1 Z_1 \quad (3.16)$$

The primary induced EMF is,

$$E_1 = V'_2 + I'_2 Z'_2 \quad (3.17)$$

$$E_1 = I_0 Z_m \quad (3.18)$$

The primary current is,

$$I_1 = I_0 + I'_2 \quad (3.19)$$

Using Equation 3.14 to Equation 3.19, the primary current and primary induced EMF is formulated by,

$$I_1 = \frac{V_1 + I'_2 Z'_2}{Z_1 + Z_m} \quad (3.20)$$

$$E_1 = V_1 - I_1 Z_1 \quad (3.21)$$

The secondary voltage is,

$$V'_2 = E_1 - I'_2 Z'_2 \quad (3.22)$$

The core current is determined by considering the core magnetizing and core loss current components,

$$I_0 = \frac{E_1}{Z_m} = \frac{E_1}{R_{e+h}} - j \frac{E_1}{X_m} = I_{e+h} - jI_m \quad (3.23)$$

The transformer voltage regulation is defined by,

$$VR = \frac{V_1 - V_2'}{V_1} \quad (3.24)$$

The input power is,

$$P_{in} = \text{real}(V_1 - I_1^*) \quad (3.25)$$

The output power is,

$$P_{out} = \text{real}(V_2' - I_2'^*) \quad (3.26)$$

The efficiency of the transformer is calculated by,

$$n = \frac{P_{out}}{P_{in}} \quad (3.27)$$

3.5 Transmission line

Transmission lines in the electrical grid transport electricity from a power source to the substation. Electrical characteristics like series resistances, series inductances, shunt capacitances, and shunt conductances are present in transmission lines. Transmission lines only exhibit resistance based on the conductor material's physical structure at a specific temperature. Transmission lines experience inductance and capacitance because of the electric and magnetic fields around the conductor. Long transmission lines, the actual earth, and conductor lines all generate capacitance. Leakage current that crosses insulators and air cause conductance to appear, although it is often negligible in comparison to the nominal current in the transmission lines and is typically disregarded. Transmission line modeling requires understanding the impacts of transmission lines' resistance, inductance, and capacitance (Salam, 2020; Hernández, 2012).

Transmission lines have consistently distributed resistance, inductance, and capacitance along their whole length. Resistance, inductance, and capacitance all make up the line's series impedance, whereas capacitance creates the shunt path. The length of a transmission line can be categorized as short, medium, or long depending on the impact of capacitance. The effect of capacitance is negligible and is thus ignored on short transmission lines, which have voltages of less than 69 kV and lengths of up to 80 km. Medium transmission lines have a length greater than 80 km but less than 250 km, voltage levels greater than 20 kV but less than 100 kV, and capacitance as a factor. When all line parameters are considered, large transmission lines have a length of more than 250 km and a voltage of more than 100 kV (Salam, 2020; Ponce et al., 2017; Ashida Salim et al., 2019).

Equivalent ABCD models are presented, which relate to the voltage and current at one side of the transmission line and on the other side of the line. The model helps explain to the exact transmission line model because the ABCD matrix can relate non-linear relations between inputs and outputs (Ponce et al., 2017).

The ABCD matrix defines four variables relating to the total voltage and current in each port (Weber, 2018),

$$V_1 = AV_2 + BI_2 \quad (3.28)$$

$$I_1 = C_{ABCD}V_2 + DI_2 \quad (3.29)$$

Where, V_1 represents the entire voltage at port 1 of the ABCD model, V_2 represents the entire voltage at port 2 of the model, I_1 represents the entire current at port 1 of the model, and I_2 represents the entire current at port 2 of the model.

From Equation 3.28 and Equation 3.29, it can be determined that parameter A is the ratio between the voltage at the transmitting end and the open-circuit voltage at the receiving end. B is the ratio between the transmitting end voltage and the short-circuit current at the receiving end. C is the ratio between the transmitting end current and the receiving end voltage in open circuit. Finally, D represents the relationship between the transmitting end current and the short-circuit receiving end current (Salam, 2020).

Rewriting the variables in matrix form leads to,

$$\begin{bmatrix} V_1 \\ I_1 \end{bmatrix} = \begin{bmatrix} A & B \\ C_{ABCD} & D \end{bmatrix} \begin{bmatrix} V_2 \\ I_2 \end{bmatrix} \quad (3.30)$$

Figure 3.5 illustrates the diagram of the ABCD matrix representation of a two-port grid.

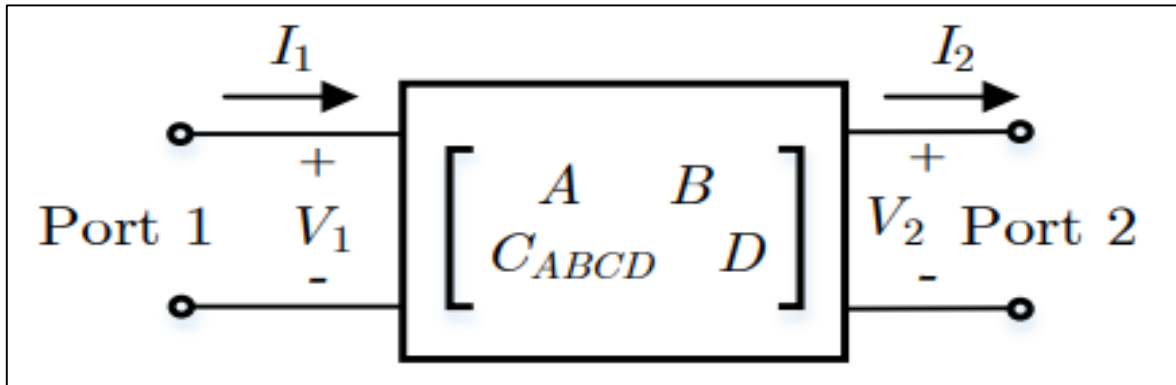


Figure 3.5: ABCD matrix representation (Weber, 2018)

A short transmission line is considered for this study.

3.5.1 Short transmission line

Capacitance is not considered in short transmission lines, but resistance and inductance effects are. Figure 3.6 shows a short transmission line single-phase equivalent circuit.

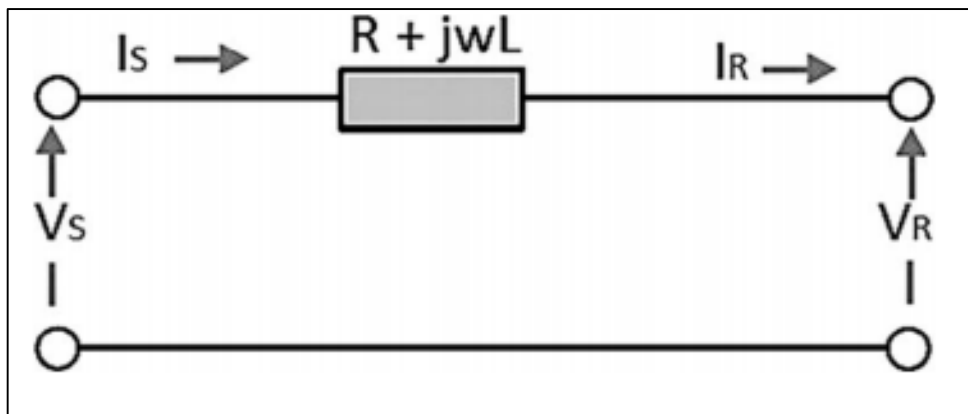


Figure 3.6: Short-length line equivalent circuit (de Moura et al., 2020)

The impedance of the transmission line is determined by (Salam, 2020),

$$Z = R + jX_L \quad (3.31)$$

The voltage per phase at the sending end is,

$$V_s = V_r + I_r Z \quad (3.32)$$

The sending and receiving end current is the same and expressed as,

$$I_s = I_r \quad (3.33)$$

Where, R is the resistive element, jX_L is the inductive element, V_s is the sending end line to neutral voltage, I_r is the receiving end current and I_s is the sending end current.

The A, B, C, and D parameters are determined by the voltage and current equations for the short transmission line and are defined by (de Moura et al., 2020),

A=1, B=Z, C=0, and D=1.

3.6 Static VAR compensator (SVC)

As demonstrated in Figure 3.7, an SVC consists of reactive power shunt components. (a). Components include a thyristor-controlled reactor (TCR) and a thyristor-switched capacitor (TSC). These components function as a controlled shunt susceptance to provide the required reactive current to the system to which the SVC is connected. The TCR is a variable susceptibility, whereas the TSCs are distinct sets of susceptibility. The TCR susceptance value is dependent on the firing angle of the thyristors. Figure 3.7 (b) provides a clear example of the idea of varied susceptibility (Belati et al., 2019).

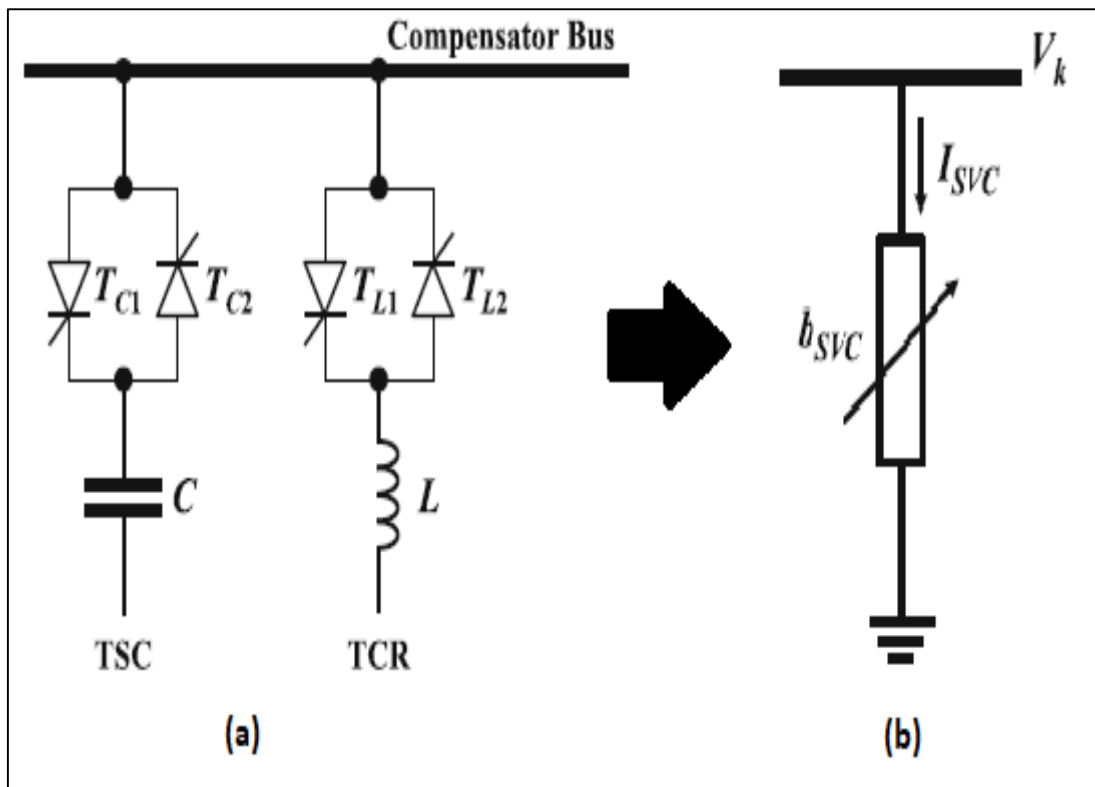


Figure 3.7: (a) Basic layout of SVC, where T_{C1} , T_{C2} , and C are the switching thyristors and capacitor of the TSC; and T_{L1} , T_{L2} , and L are the switching thyristors and inductor of the TCR. (b) Variable susceptance SVC model (Belati et al., 2019)

The TSC branch is composed of a capacitor and a bidirectional thyristor valve linked in series. On the TCR branch, a bidirectional thyristor valve is linked in series with an inductor (Jena et al., 2021). Figure 3.8 depicts the block diagram for the TSC-TCR SVC's control algorithm.

The control system monitors the required positive sequence voltage for control. The computed difference between the measured voltage ΔU_m and the reference voltage U_{ref} is transmitted to the voltage regulator to determine the SVC susceptance value B_{SVC} required to maintain a constant system voltage. B_{SVC} is sent to the allocation unit, the distribution unit, which calculates the needed firing angle for the TCR and determines the number of TSC branches to switch in and out. The pulse generator then transmits the correct pulses to the thyristors (Xu et al., 2014).

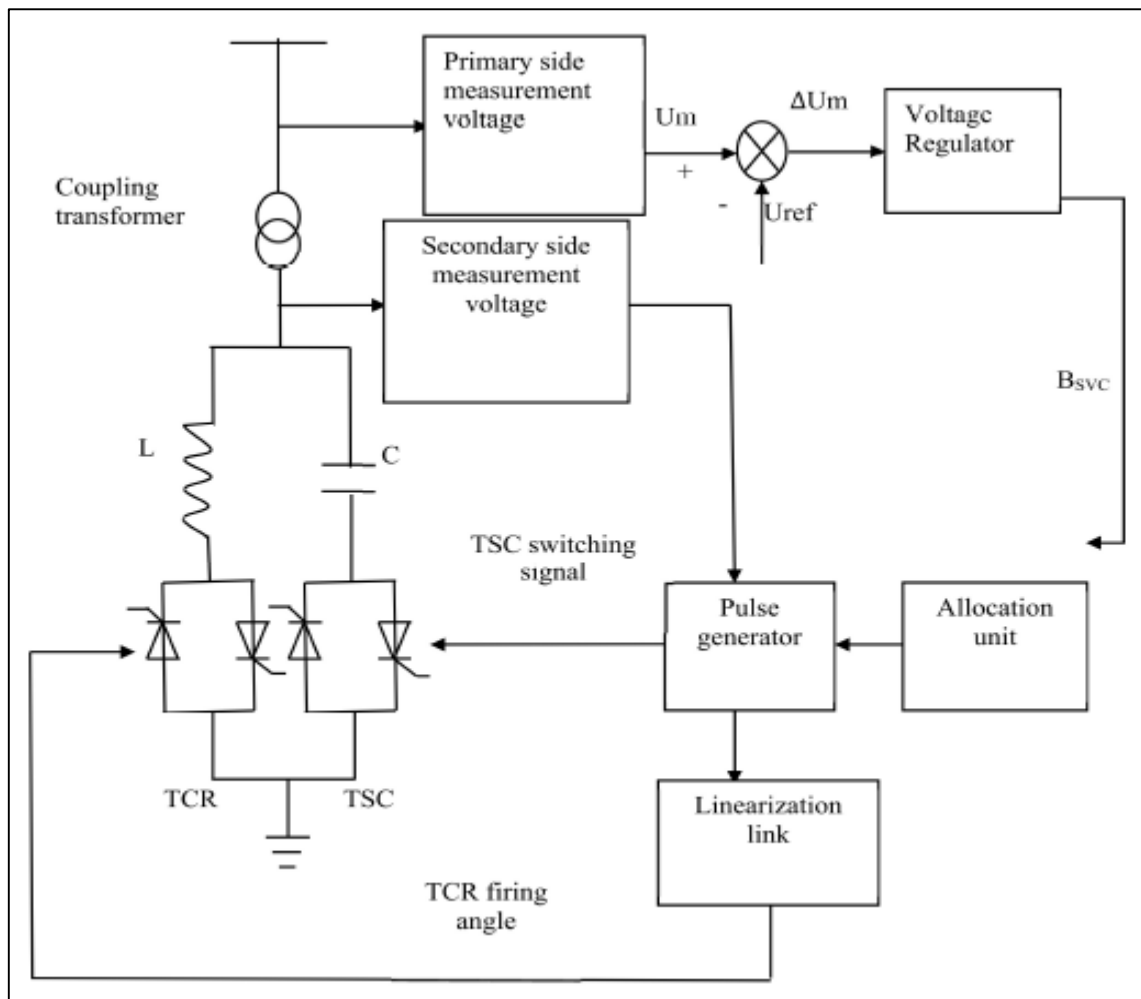


Figure 3.8: Control principle of SVC operation (Chen & Hu, 2021)

When the system voltage is low, switching TSC branches to the grid compensates the capacitive reactive power. When the capacitive reactive power that the TSC supplies are too high, the TCR branch is switched to absorb excess capacitive reactive power (Chen & Hu, 2021).

The SVC reactive power is controlled by the trigger angle α , which varies from 90° to 180° . The SVC injects reactive power specified by (Ćalasan et al., 2021),

$$Q_{SVC} = \frac{U^2}{X_c} - U^2 * B_{SVC}(\alpha) \quad (3.34)$$

Where, U is defined as the terminal voltage of the SVC, X_c is defined as the capacitor reactance and B_{SVC} is defined as the variable susceptance, which can be determined by,

$$B_{SVC} = \left(\frac{2 * (\pi - \alpha) + \sin 2\alpha}{\pi * X_L} \right) \quad (3.35)$$

Where, X_L is the total inductive reactance.

Using X_L and X_C , the minimum and maximum reactive power that the SVC can inject is determined by,

$$\frac{U^2}{X_C} - \frac{U^2}{X_L} \leq Q_{SVC} \quad (3.36)$$

The firing angle α of the TCR varies between 90° and 180° . Figure 3.9 illustrates that the susceptance decreases between its maximum value and zero as the firing angle is varied between 90° and 180° . For the value $\alpha = 90^\circ$, the susceptance B_{TCR} is at its maximum, and as the value of α increases, B_{TCR} decreases to its minimum value to zero (Rahmouni, 2020).

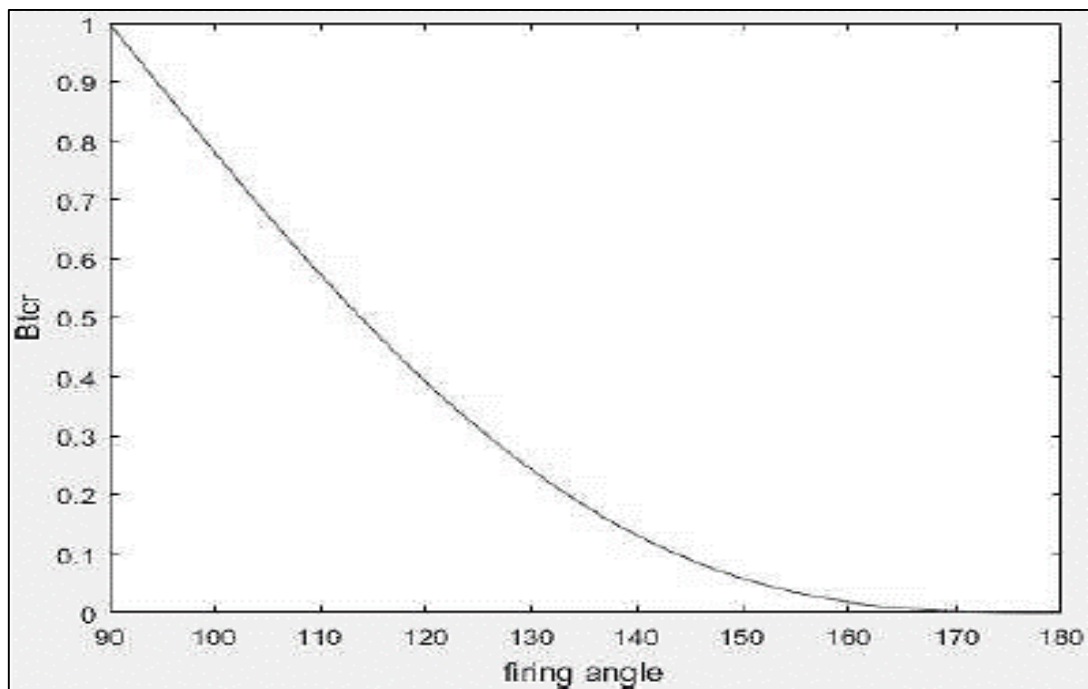


Figure 3.9: TCR susceptance versus firing angle (Pekdemir & Yildiz, 2018)

3.7 Static Synchronous Compensator (STATCOM)

STATCOM, a shunt-connected reactive power compensation device, may create or absorb reactive power from its linked system, and its output can be modified to govern certain parameters. In contrast to the SVC controller, which is a system-voltage-dependent voltage-controlled shunt susceptance, STATCOM is equivalent to a voltage source wherein the voltage magnitude may be rapidly modified by a reactance. Figure 3.10 depicts the STATCOM components, including a VSC with power electronic switching devices and converter controls that regulate the terminal voltage of the STATCOM (Davidson & de Oliveira, 2020).

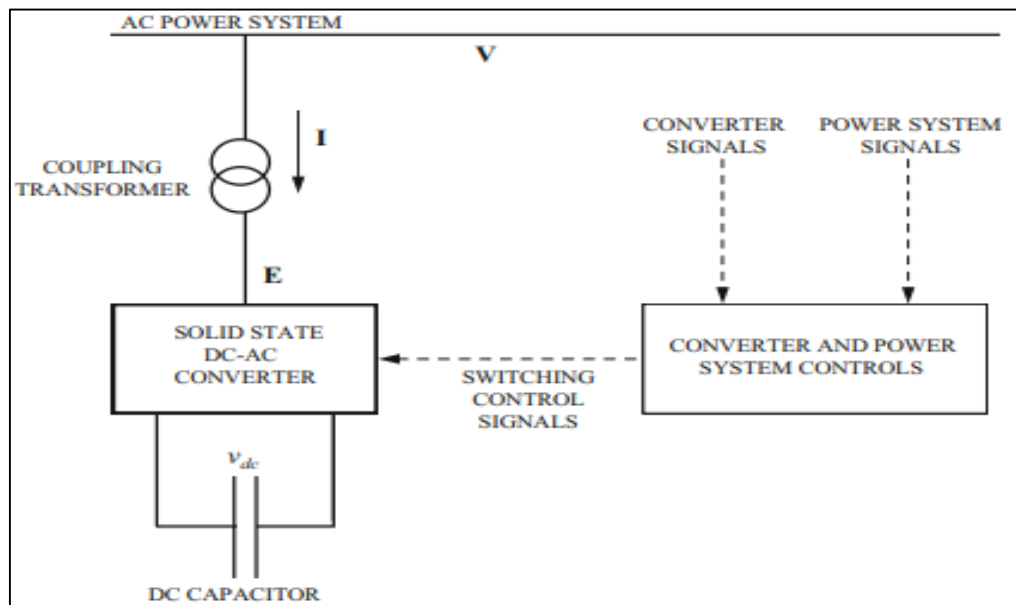


Figure 3.10: STATCOM system overview (Davidson & de Oliveira, 2020)

A coupling transformer connects the VSC to the electrical grid to reduce the voltage on the VSC's power electronic components. The reactive power flow between the grid and the STATCOM is determined by the magnitude and phase angle of the voltage at the STATCOM output terminals. When the amplitude and phase angle of the voltage between the grid and the STATCOM are identical, there will be no reactive power. As shown in Figure 3.11, when the voltage magnitude of the STATCOM is increased (V_{inv}), reactive power will flow from the VSC to the network, and the STATCOM will inject reactive power and increase the grid voltage (V_M) (a). As shown in Figure 3.11, when the magnitude of the STATCOM voltage is decreased, reactive power will flow from the network to the VSC, and the STATCOM will absorb reactive power and reduce the grid voltage (b). The DC capacitor voltage can be controlled by altering the active power flow between the VSC and the network. To create active power flow, the phase angle between the VSC output and the grid is moved out of phase (Mikwar, 2017; Wang et al., 2020).

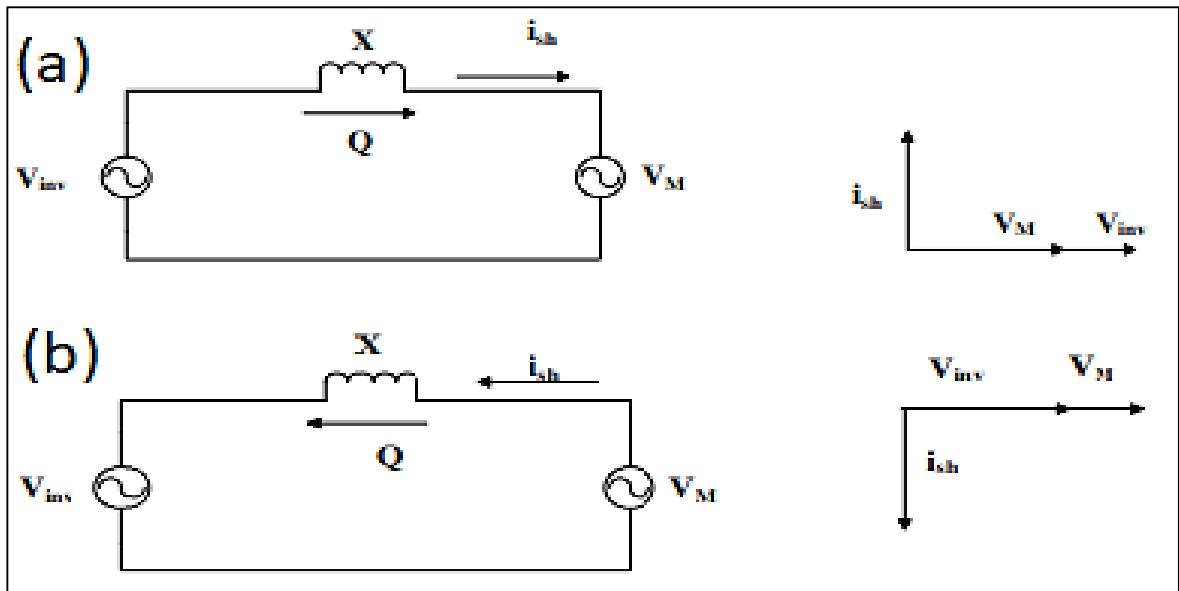


Figure 3.11: (a) Phasor diagram of capacitive operation, and (b) Phasor diagram of inductive operation (Murali et al., 2016)

The control goals of STATCOM are to maintain a constant voltage on the DC capacitor and to regulate the reactive output power. To regulate its reactive power, the STATCOM employs a dual closed-loop management of the reactive outer side loop and inner current loop. Figure 3.12 is a block diagram of reactive power control.

The actual measured value of reactive power Q is compared to the reference value of reactive power Q_{ref} . The reference reactive current i_{qref} that the STATCOM must transmit while leaving the inner current loop is calculated by comparing the reference and actual values, which generates an error value that is provided to the PI controller (Wang et al., 2020).

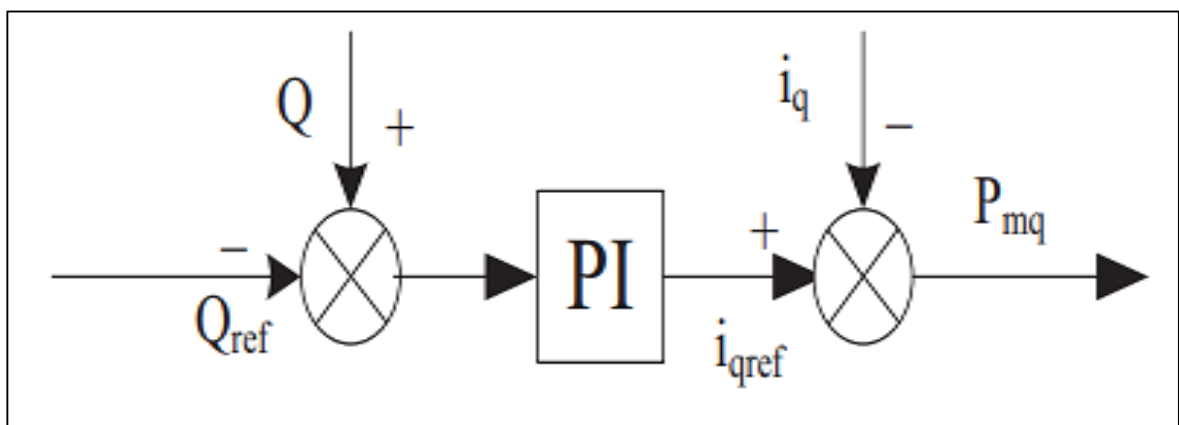


Figure 3.12: STATCOM reactive power control model (Wang et al., 2020)

A block diagram of the STATCOM controller control system is seen in Figure 3.13. The phase-locked loop (PLL) utilized by the STATCOM control system is synced to the positive sequence component of the three-phase primary voltage V_1 . Using the PLL output (angle = $\theta = \omega t$), the direct- and quadrature-axis components of the three-phase AC voltages and currents (I_q , I_d , V_q and V_d) are determined. In addition to the DC voltage V_{dc} , measurement equipment is used to monitor the d and q components of the required positive sequence three-phase AC voltages and currents. In the control system, two regulation loops are used. A voltage regulator for both AC and DC is a component of the outer regulation loop.

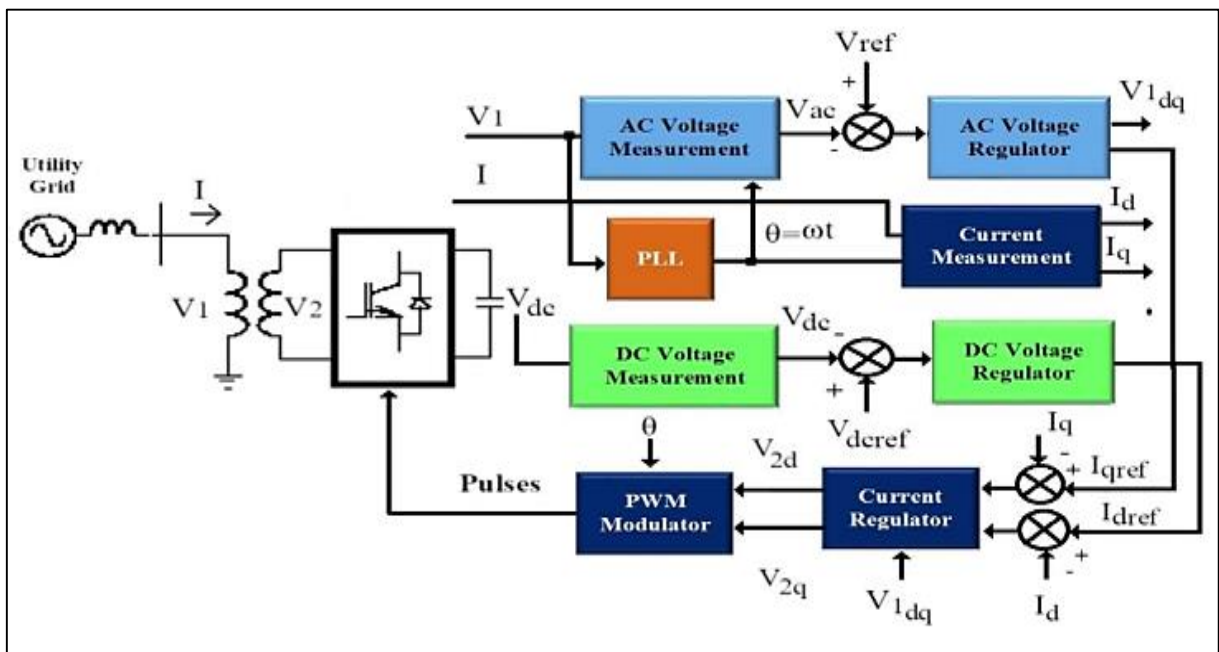


Figure 3.13: STATCOM control block diagram (Gandoman et al., 2018)

Since I_q represents the quadrature current and voltage controlling reactive power flow, the output of the AC voltage regulator acts as the reference current I_{qref} of the current regulator. The output of the DC voltage regulator is the current regulator reference current I_{dref} , where I_d represents the in-phase current and voltage that governs active power flow. On the inner regulation loop, the current regulator is located. The current regulator is used to regulate the magnitude and phase of the voltage generated by the pulse width modulation (PWM) converter V_{2d} and V_{2q} , which receives reference currents I_{dref} and I_{qref} from the AC and DC voltage regulators in voltage control mode. Additionally, there is a feedforward regulator that is used for the prediction of the V_2 output voltage V_{2d} and V_{2q} from the V_1 measurement V_{1d} and V_{1q} with the transformer leakage reactance (Gandoman et al., 2018).

Based on the STATCOM equivalent circuit in Figure 3.14, mathematical equations can be derived for load flow calculations.

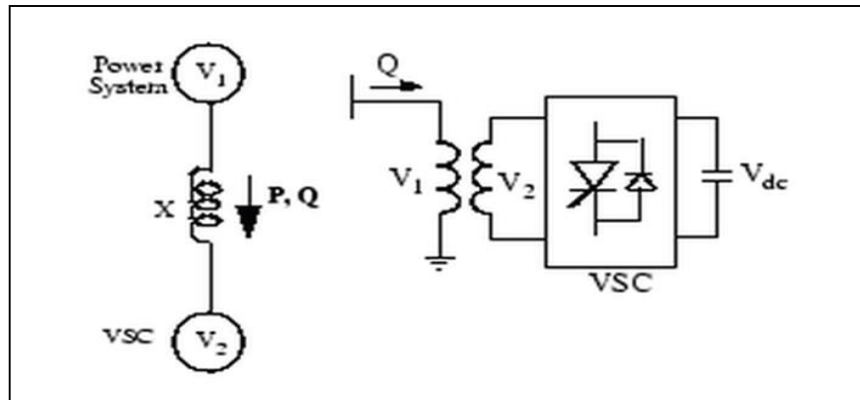


Figure 3.14: STATCOM equivalent circuit (Kamel et al., 2021)

The STATCOM model's power injection mathematical equations are defined by (Abdelsattar et al., 2022; Kamel et al., 2021),

$$V_1 = V_2 + jXI \quad (3.37)$$

$$I = \frac{V_1 - V_2}{jX} \quad (3.38)$$

It is possible to determine the complex apparent power S with,

$$S = V_1^* I^* = \frac{V_1^* - V_2^*}{-jX} \quad (3.39)$$

Where V_1 is defined as the grid voltage, V_2 is defined as the VSC terminal voltage, X is defined as the coupling transformer reactance, I is defined as the STATCOM current, and V_1^* , I^* and V_2^* are the conjugate of V_1 , I and V_2 .

The apparent power is given by S that is defined by,

$$S = P + jQ \quad (3.40)$$

Where, P is the active power and jQ is the reactive power.

Utilizing Equation 3.39 and Equation 3.40, P and Q can be determined by,

$$P = \frac{V_1 V_2 \sin \delta}{X} \quad (3.41)$$

$$Q = \frac{V_1(V_1 - V_2 \cos \delta)}{X} \quad (3.42)$$

Where, δ is the power angle that denotes the difference in phase angle between the voltages V_1 and V_2 .

To identify which mode the STATCOM is functioning in, it is possible to draw the following conclusions,

- When $V_2 > V_1$ then reactive power $Q < 0$: STATCOM functions in the capacitive mode.
- When $V_2 < V_1$ then reactive power $Q > 0$: STATCOM functions in the inductive mode.
- When $V_2 = V_1$ then reactive power $Q = 0$: STATCOM is not operational.

3.8 Summary and Conclusion

Chapter 3 provided the mathematical modeling for power system components of a WECS virtual simulated grid. The mathematical modeling contained mathematical equations and equivalent circuits for the components.

The first component of the modeled WECS system was the variable pitch wind turbine that receives the wind energy and converts it to mechanical energy through its turbine blades. Next, the mechanical energy is fed into the second component, the induction generator, which produces the electrical power. The third component is the step-up transformer to raise the wind turbine's voltage to the required grid voltage level. The fourth component is the transmission line that carries the generated power and feeds it into the electrical grid. Finally, the FACTS controllers, consisting of the SVC and STATCOM controllers, were presented that connect to the wind turbine in a shunt configuration as the reactive power compensating device for the voltage quality enhancement.

It can be observed that the STATCOM is equivalent to a voltage source wherein the voltage magnitude may be rapidly modified by a reactance. The SVC, in contrast, is comparable to a system-voltage-dependent voltage-controlled shunt susceptance. Therefore, mathematical formulae were presented to estimate the shunt susceptance for the SVC to manage the reactive power exchange and the STATCOM to identify the load flow at the bus where the STATCOM is connected.

Chapter 4 will describe and model the virtual simulation models for both FACTS controllers based on the mathematical modeling.

CHAPTER FOUR: COMPUTER MODELING

4.1 Introduction

In this chapter, the computer modeling in MATLAB/Simulink will be expressed as individual system components for a wind energy conversion system (WECS) electrical network. Component blocks are used in the MATLAB/Simulink software package to perform computer modeling.

The individual system components used for the simulation model can be found in Appendix A.

The components in Appendix A consist of a:

Control block for a three-phase programmable voltage source.

Control block for a three-phase mutual inductance.

Control block for a three-phase transformer.

Control block for a grounding transformer.

Control block for a three-phase pi section.

Control block for a three-phase parallel RLC load.

Control block for a three-phase V-I measurement.

Control block for a three-phase fault.

Control block for a three-phase series RLC load.

This chapter will discuss the computer modeling for the wind turbine induction generator, SVC, STATCOM, and the monitoring signals for the FACTS controllers.

4.2 Wind turbine induction generator

As shown in Figure 4.2, the wind turbine generator used in the computer modeling is a squirrel cage induction generator (SCIG). Each setup block is equipped with two 1.5 MW induction generator sets that are linked to a 575 V bus and run at 60 Hz with the generator's maximum output power at a wind speed of 9 m/s. The wind speeds for the wind turbine are fed into the block by the "wind" terminal input. Figure 4.1 to Figure 4.4 illustrate the icon of the component used in the computer modeling and the setup of these blocks.

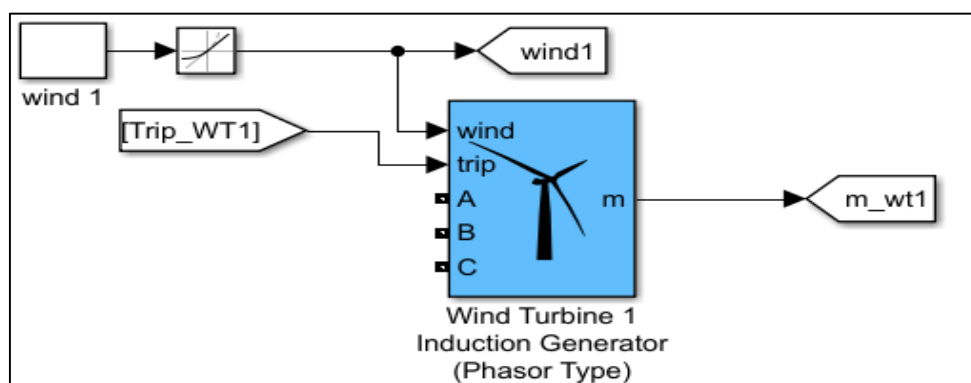


Figure 4.1: Wind turbine generator block icon

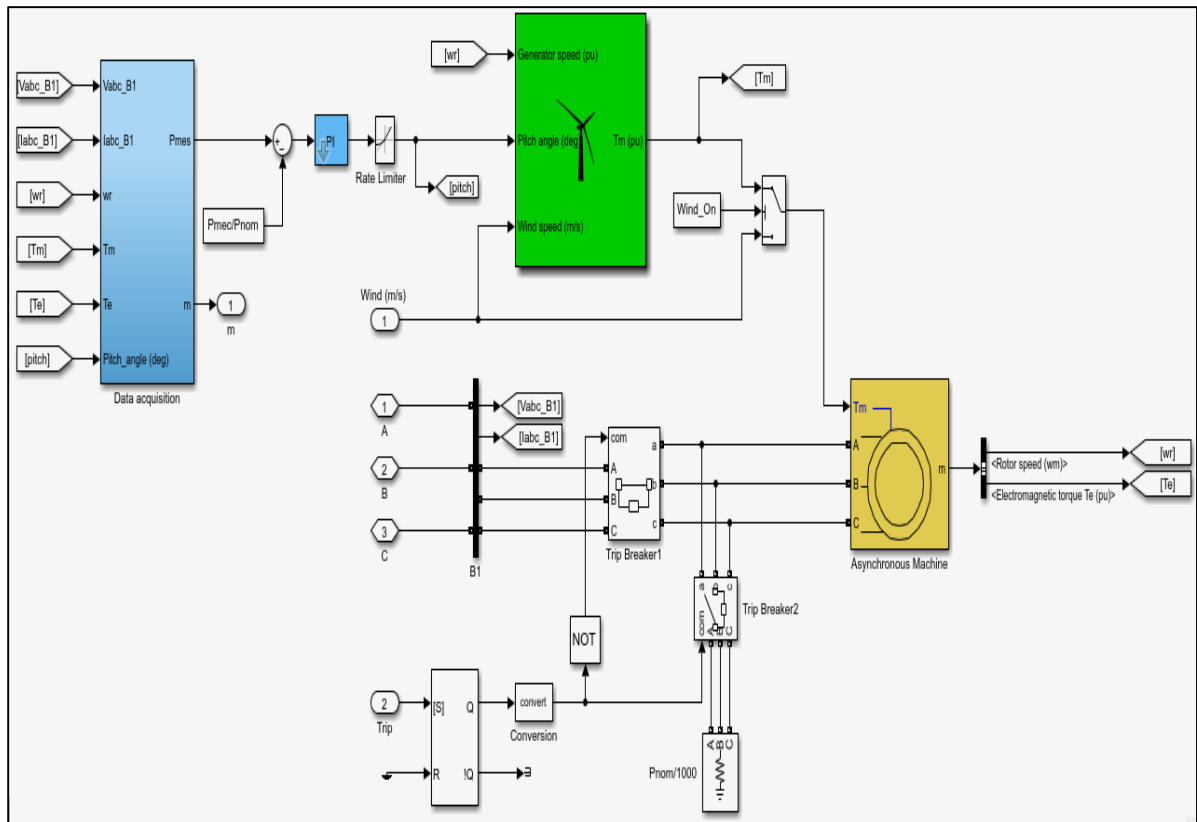


Figure 4.2: Wind turbine induction generator detailed model

Block Parameters: Wind Turbine 1 Induction Generator (Phasor Type)

Wind Turbine Induction Generator (Phasor Type) (mask) (link)

Implements a phasor model of a squirrel-cage induction generator driven by a wind turbine.

Generator **Turbine**

External turbine (Tm mechanical torque input)

Nominal power, line-to-line voltage, frequency [Pn(VA), Vn(Vrms), fn(Hz)]: [2*1.5e6/0.9 575 60]

Stator [Rs, Lls] (pu): [0.004843 0.1248]

Rotor [Rr', Llr'] (pu): [0.004377 0.1791]

Magnetizing inductance Lm (pu): 6.77

Inertia constant, friction factor, and pairs of poles: [H(s), F(pu), p] [5.04 0.01 3]

Initial conditions [s, th(deg), ias, ibs, ics (pu), ph_as, ph_bs, ph_cs (pu)]: [-0.01,0 0,0,0 0,0,0]

Figure 4.3: Wind turbine generator setup block

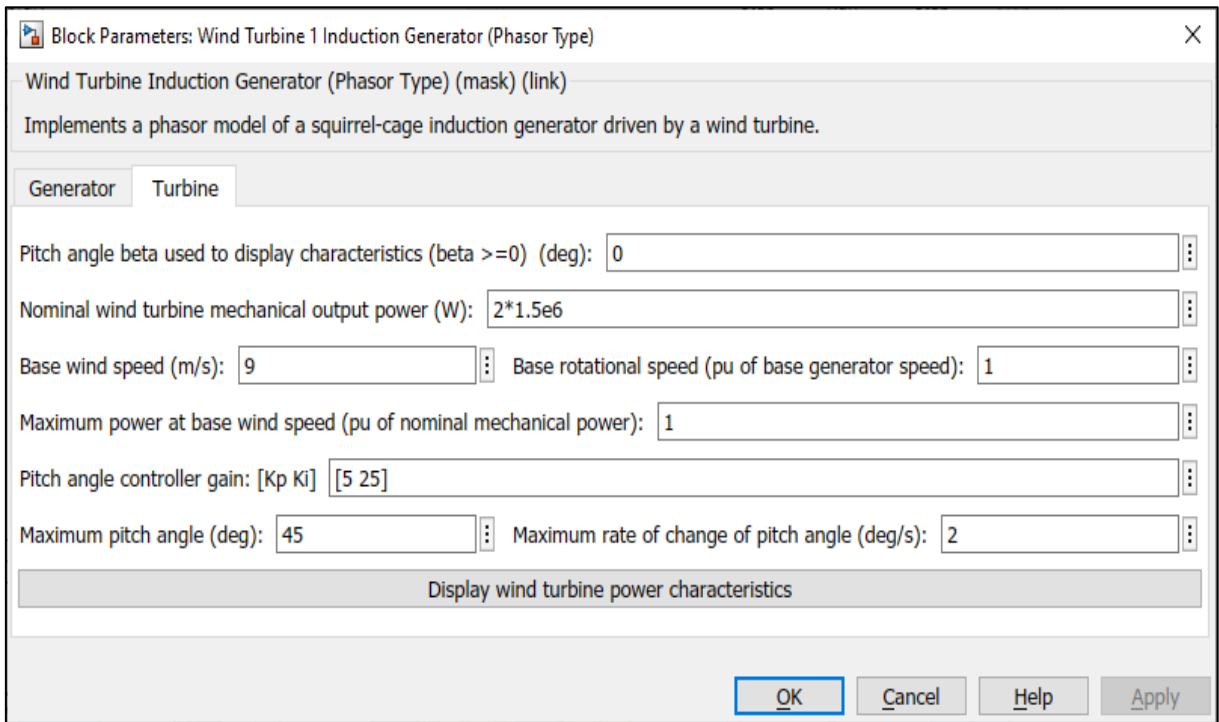


Figure 4.4: Wind turbine setup block

4.3 Static VAR Compensator (SVC)

The inductive and capacitive components of the SVC controller are thought to have a combined base power of 3 MVA and a maximum reactive power of 3 MVar. The SVC is used in voltage regulation mode in this model. In voltage regulation mode, the proportional gain is defined as K_p , the integral gain is defined as K_i , the droop reactance is defined as X_s , and the network short-circuit level dictates the controller's response time to changes in system voltage. The icon of the component used in the computer modeling and the setting of this block are shown in Figures 4.5 and 4.6.

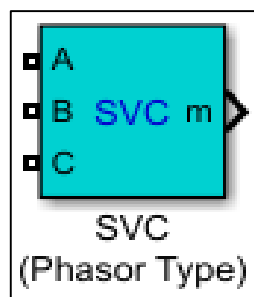


Figure 4.5: SVC block icon

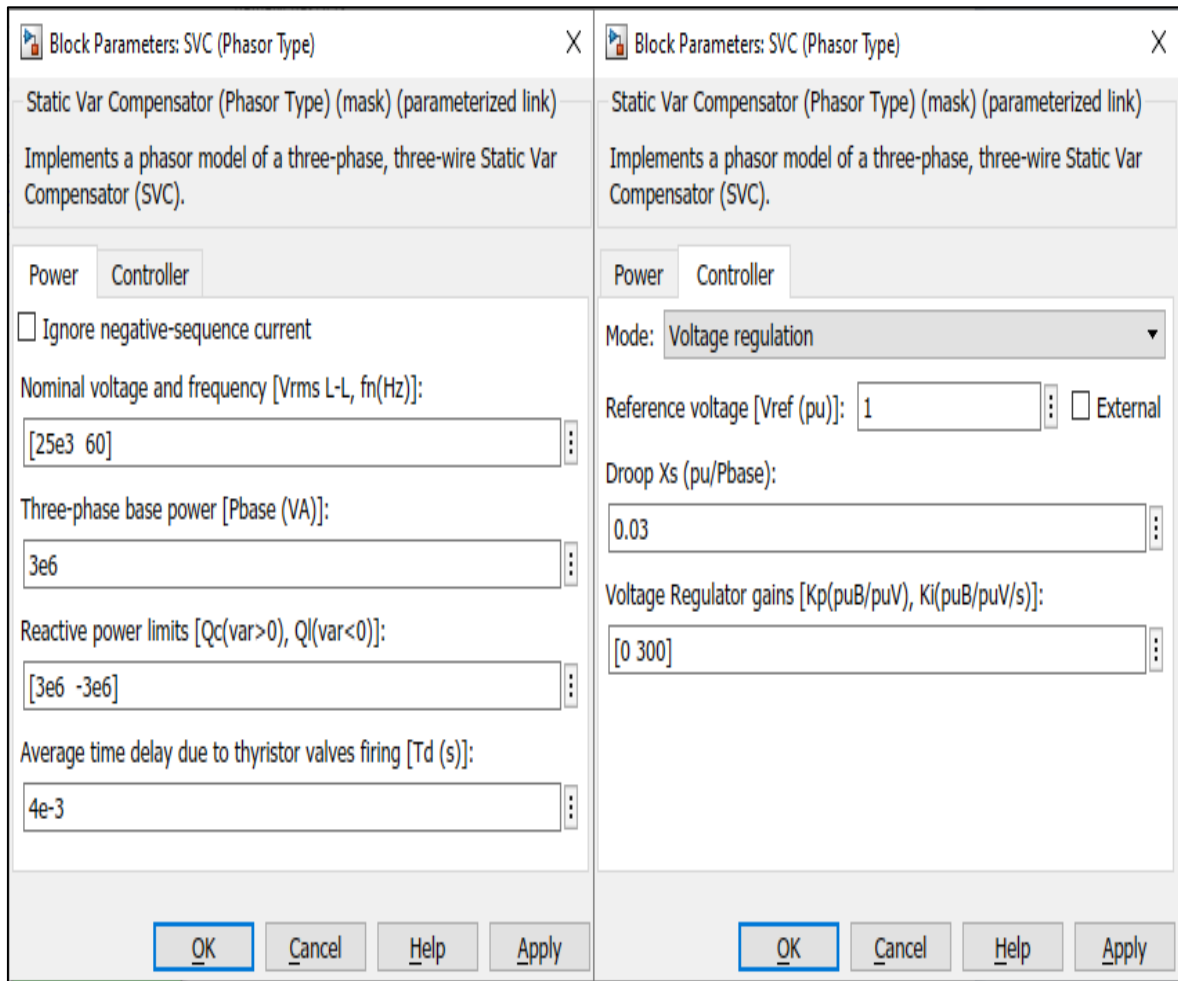


Figure 4.6: SVC block setup

Figure 4.7 is the control model of the SVC block. This model can be compared to the SVC control principle of the operational model in Figure 3.8, where the blocks are discussed.

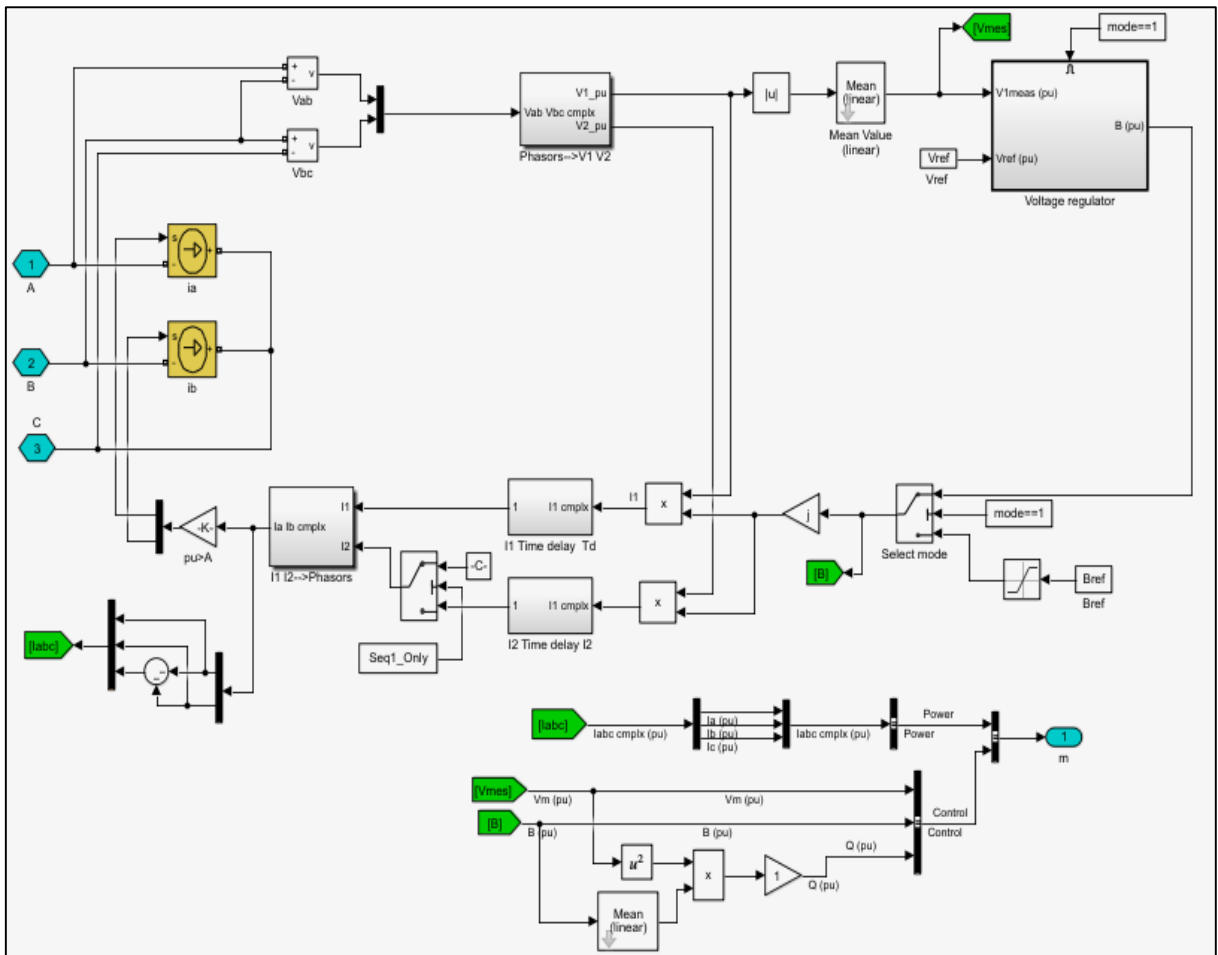


Figure 4.7: SVC block control model

Figure 4.8 is the measuring block used to measure per-unit values and actual voltages received from the SVC block. The signals received from the SVC are fed into a scope block for waveform representation.

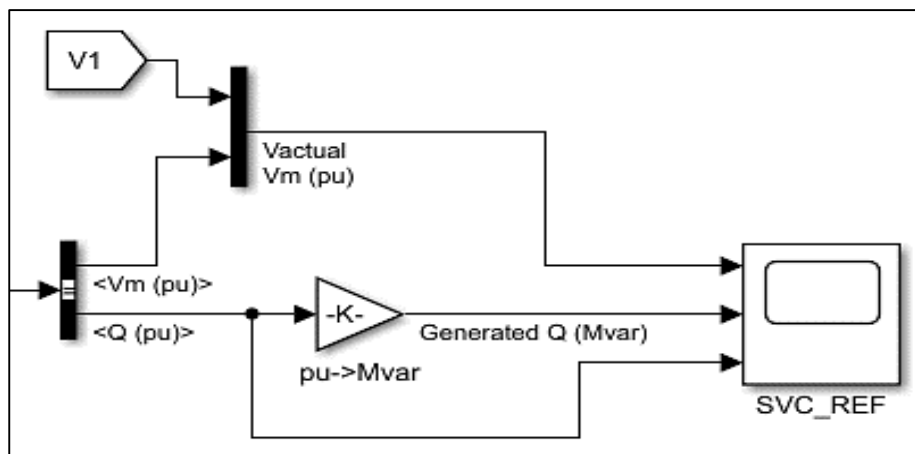


Figure 4.8: SVC signal monitoring blocks

4.4 Static Synchronous Compensator (STATCOM)

The STATCOM controller has a rated capacity of 3 MVA and is linked to the 25 kV grid. The STATCOM controller is operating in voltage regulation mode. Figures 4.9 and 4.10 depict the icon of the component used in computer modeling and the configuration of this block, respectively.

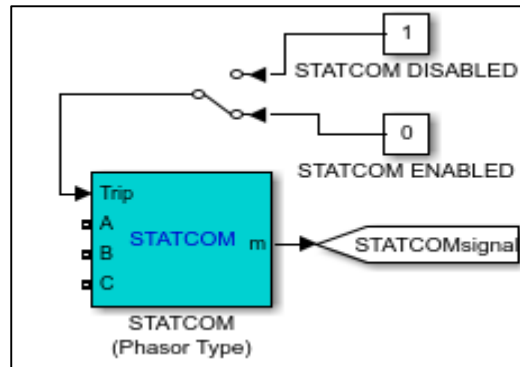


Figure 4.9: STATCOM block icon

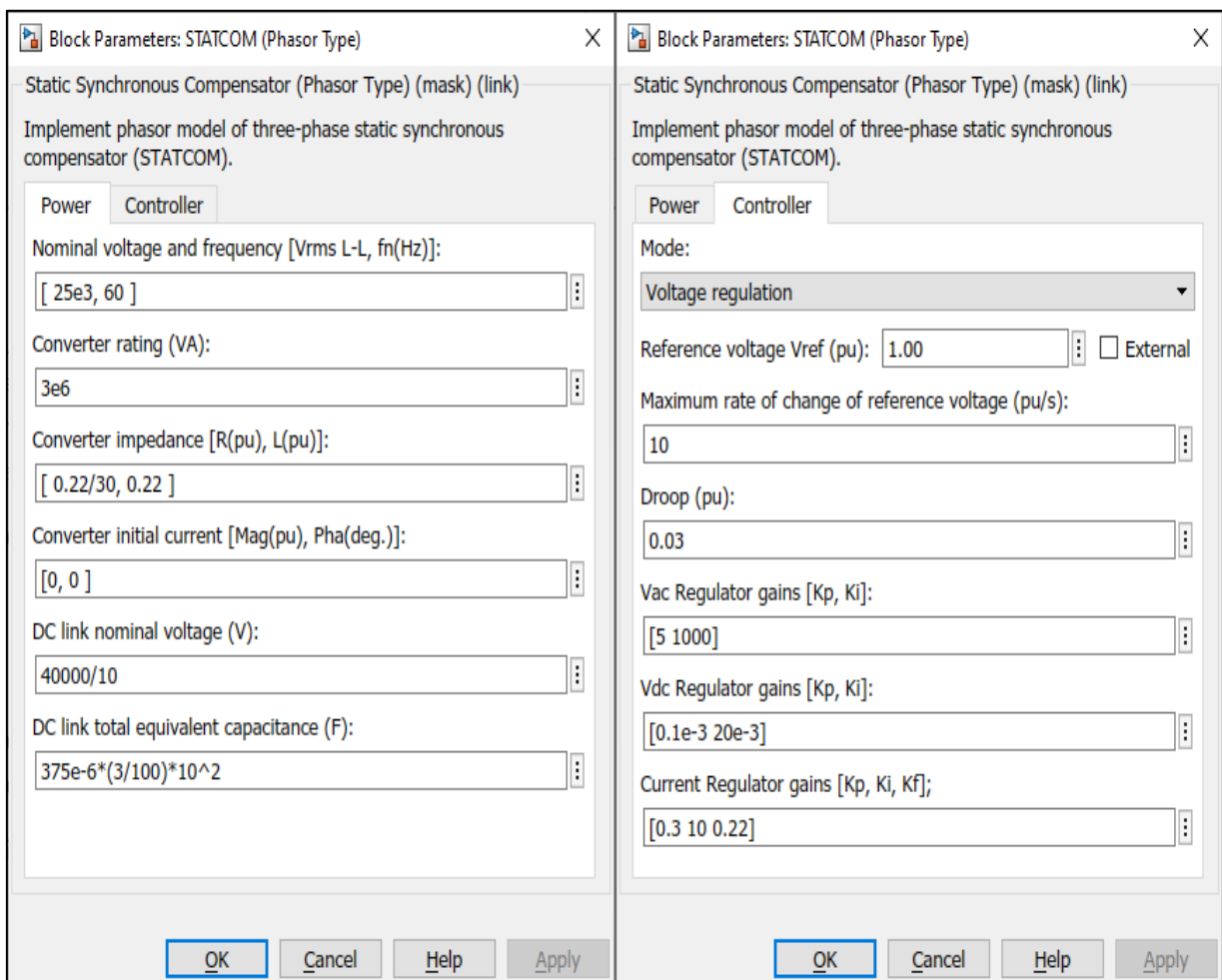


Figure 4.10: STATCOM block setup

Figure 4.11 is the control model of the STATCOM block, with Figure 4.12 illustrating the control model for the STATCOM controller alone. The STATCOM controller model can be compared to the STATCOM control principle of the operational model in Figure 3.13, where the blocks are discussed.

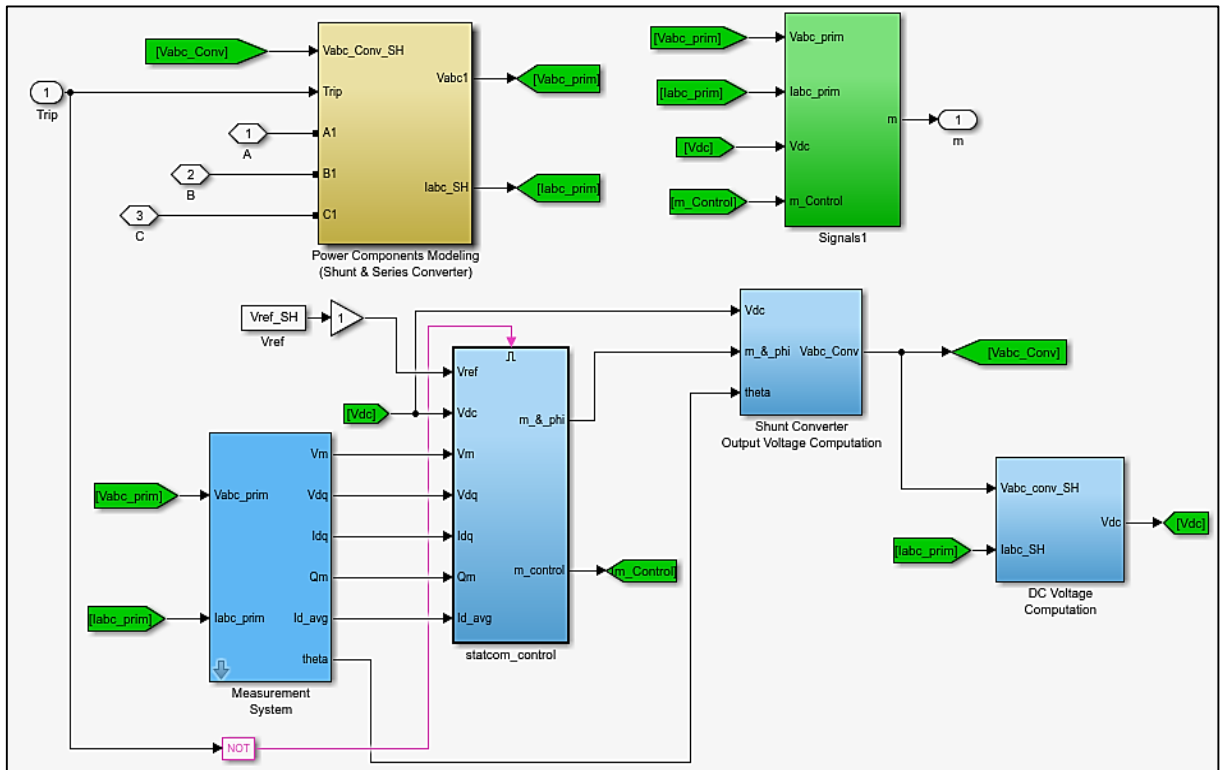


Figure 4.11: STATCOM block control model

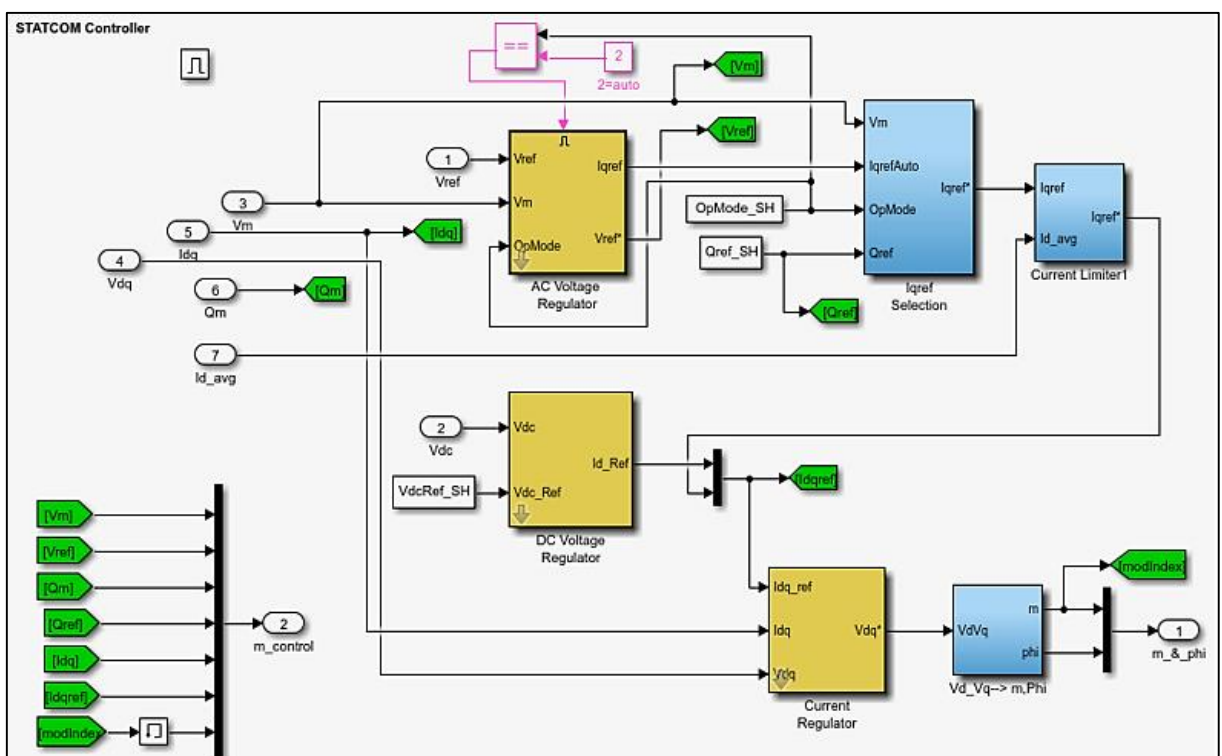


Figure 4.12: STATCOM controller model

Figure 4.13 is the measuring block used to measure per-unit values and actual values of voltages received from the STATCOM block. The signals received from the STATCOM are fed into a scope block for waveform representation.

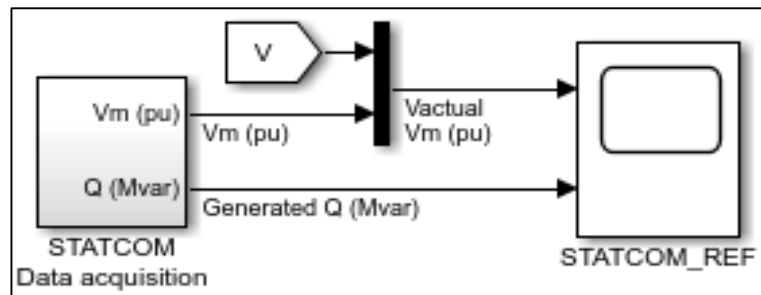


Figure 4.13: STATCOM signal monitoring blocks

4.5 STATCOM and SVC monitoring signals

Figure 4.14 displays all the monitoring blocks used within the STATCOM and SVC to measure signals like the voltage, current, active power, reactive power, wind speeds, trip times, etc.

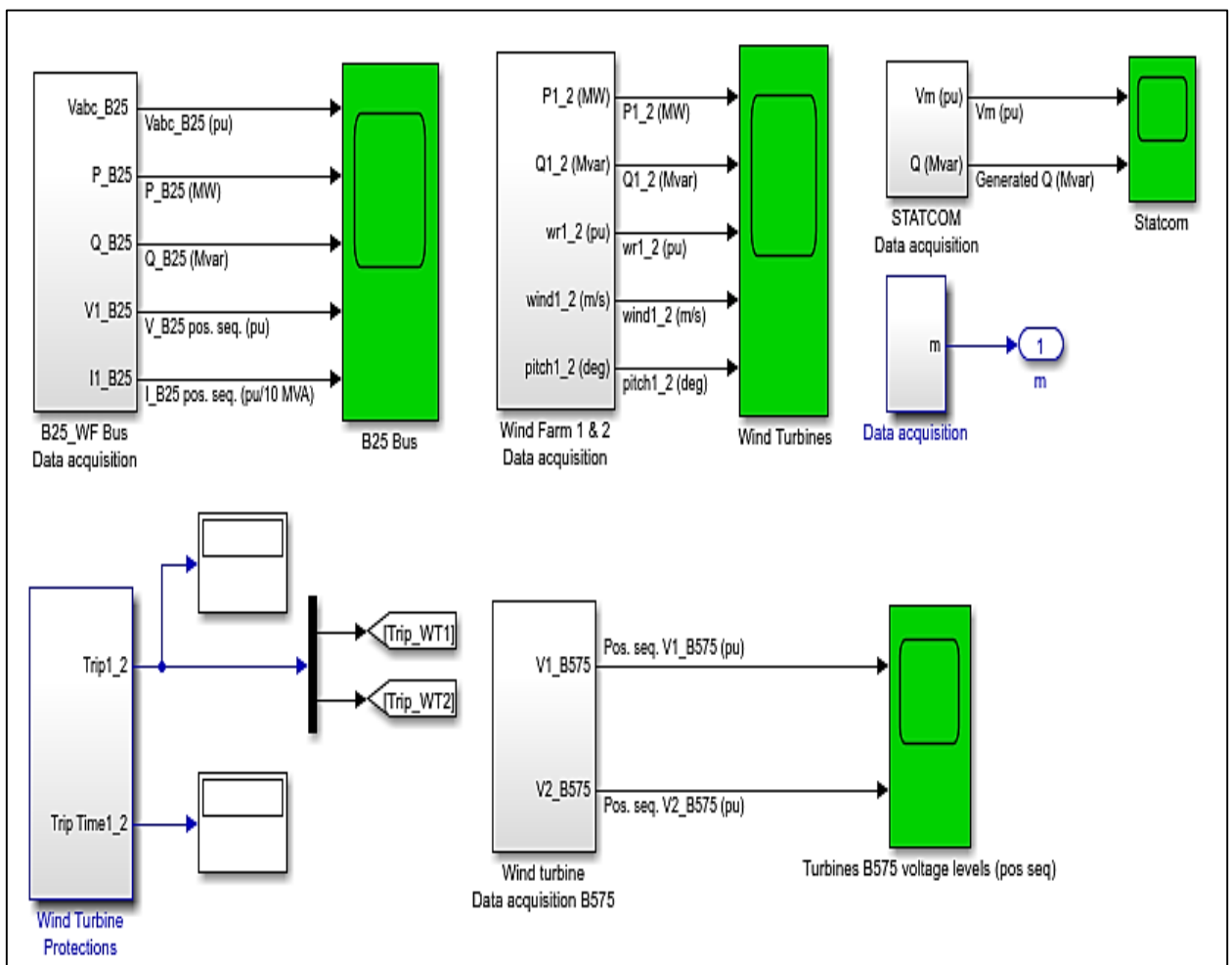


Figure 4.14: STATCOM and SVC monitoring signal blocks

4.6 Complete simulation models

The final complete model is built to do the simulations with all the individual components.

4.6.1 SVC model

Figure 4.15 is the complete simulation model that uses the SVC to improve voltage quality during momentary fault conditions. This model will be used in chapter 5 with different case studies.

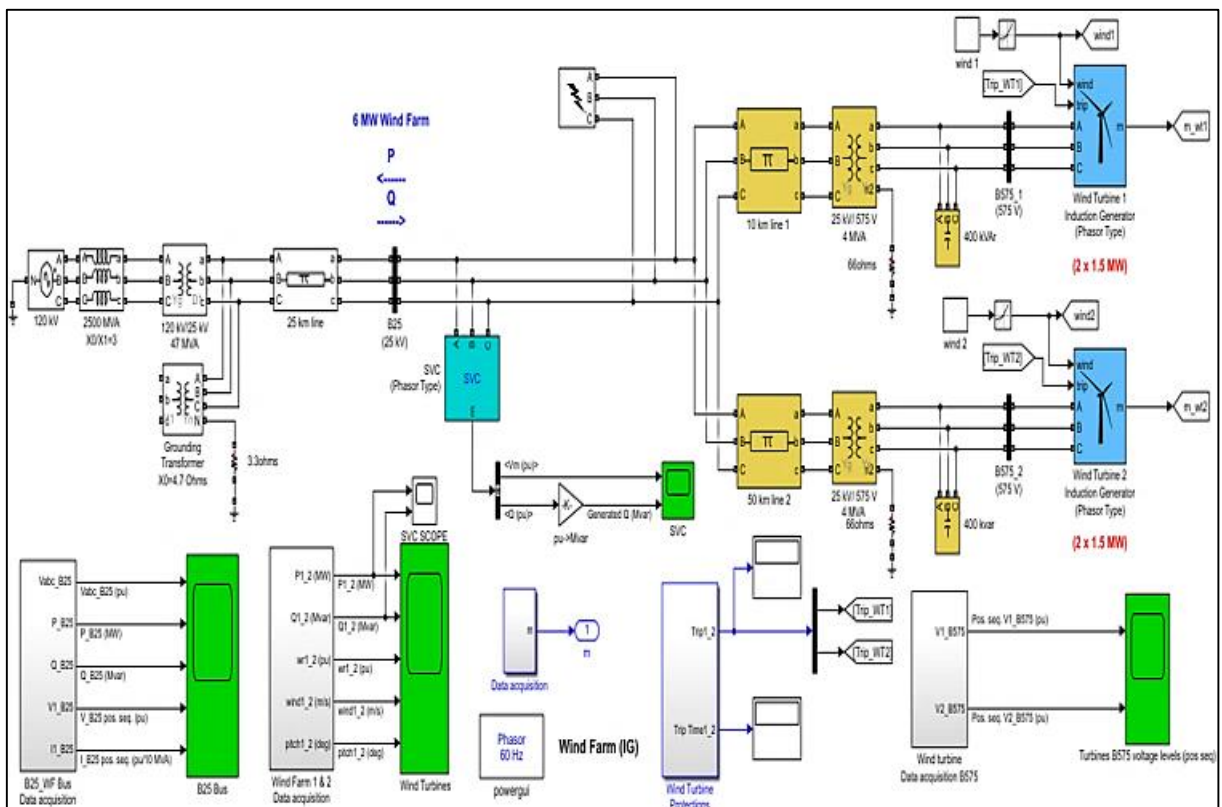


Figure 4.15: Complete SVC simulation model

4.6.2 STATCOM model

Figure 4.16 is the complete simulation model that uses STATCOM to improve voltage quality during momentary fault conditions. This model will be used in chapter 5 with different case studies.

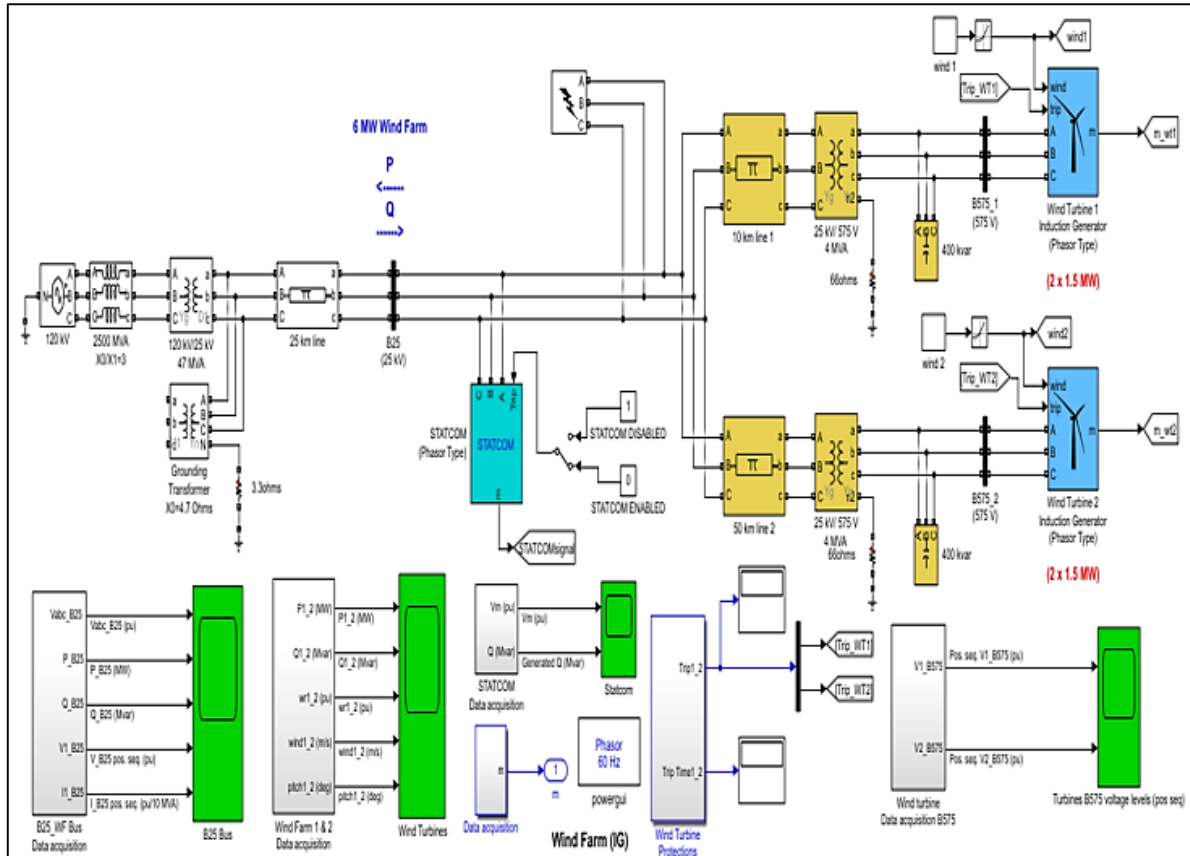


Figure 4.16: Complete STATCOM simulation model

4.7 Summary and Conclusion

In this chapter, the computer modeling in MATLAB/Simulink was expressed in terms of individual system components for a WECS electrical grid. Component blocks have been chosen in MATLAB/Simulink to perform computer modeling to build the models.

Section 4.1 described various three-phase system components that were modeled, which can be found in Appendix A.

This chapter provided the computer modeling for the wind turbine induction generator, SVC, STATCOM, and the monitoring signals for the FACTS controllers.

Using all the individual system components, a complete WECS simulation model was built. Two models were built, one WECS model that included the SVC FACTS controller and the second WECS model that included the STATCOM FACTS controller.

Chapter 5 will cover the simulations of the complete models with results and a discussion of how FACTS controllers impact voltage quality enhancement.

CHAPTER FIVE: SIMULATION RESULTS AND DISCUSSIONS

5.1 Introduction

This chapter uses a reference model of a WECS network without FACTS controllers and with FACTS controllers. First, simulations are performed by applying a momentary fault condition and monitoring how the voltage profile is affected by this fault. SVC and STATCOM are then introduced to the reference model to see how the voltage profile is enhanced. The results include a comparative analysis to identify which voltage profile is the least affected by the fault condition.

After acquiring the results of the simulations on how the FACTS controllers improve the voltage profile in the reference model, the same FACTS controllers are included in a newly designed WECS model and are expected to achieve similar results.

Finally, simulations of momentary fault conditions with faults of different natures are performed. The results are then observed on how the FACTS controllers perform and their effect on the system voltage quality.

5.2 Reference WECS modeling with a momentary fault condition

Researching existing literature from a similar research area that used the MATLAB/Simulink software environment with models integrating FACTS controllers with WECS is vital to get a baseline reference on what simulation results to expect.

FACTS controllers like SVC and STATCOM can be integrated into the power system to improve the momentary fault conditions where WECS are present. The FACTS controllers can also support the power system with voltage stability and reactive power support by meeting grid code requirements.

The literature serves as the basis for reference modeling (Sharma et al., 2021). The WECS doubly-fed induction generator serves as the model's foundation. The wind farm consists of three 1.5 MW wind turbines and is rated at 4.5 MW. The output line voltage of the wind turbine is increased from 575 V to 13.8 kV. At the PCC, which is also where the load block is mounted, FACTS devices such as SVC and STATCOM are shown. The internal transformer of the load block decreases the 13.8 kV voltage to 2300 V and 480 V. The load block consists of a 1.68 MW electrical motor with a nominal voltage of 2300 V, a 570 kW load with a nominal voltage of 480 V, a 470 kW inductive reactance, and a 470 kW inductive reactance.

The complete reference model, system parameters for the electrical grid, transformers, transmission lines, capacitor bank, wind farm, SVC, STATCOM, and protection system parameters are listed in Appendix B, Figure 9.1, and Table 9.1 to Table 9.2.

The complete reference models for the 13.8 kV bus B13.8, where the SVC and STATCOM are coupled, are shown in Figures 5.1 and 5.2. The SVC and STATCOM are both connected to a 13.8 kV feeder that operates at 60 Hz and has a combined rated capacity of 3 MVar. A step-up transformer is linked to the 13.8 kV with a 2.05 km three-phase PI section line. Then, through an additional 3.05 km three-phase PI section line, the voltage of the 13.8 kV is increased to 69 kV, the voltage of the electrical grid.

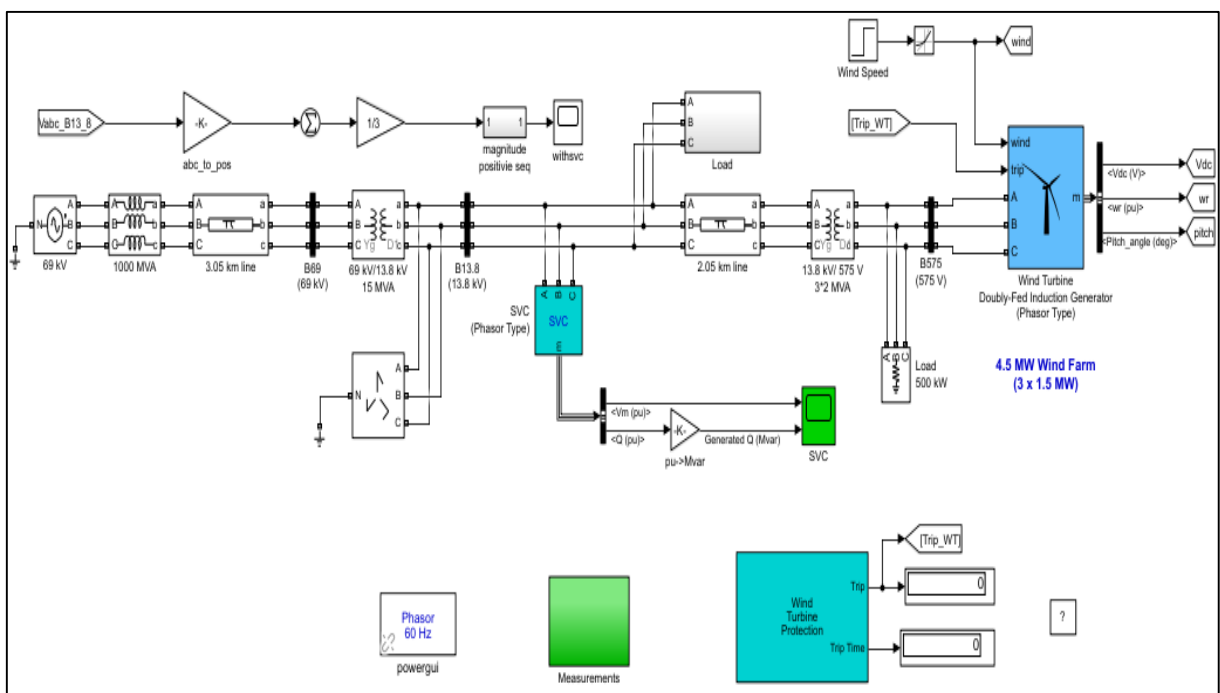


Figure 5.1: Complete reference model with SVC controller

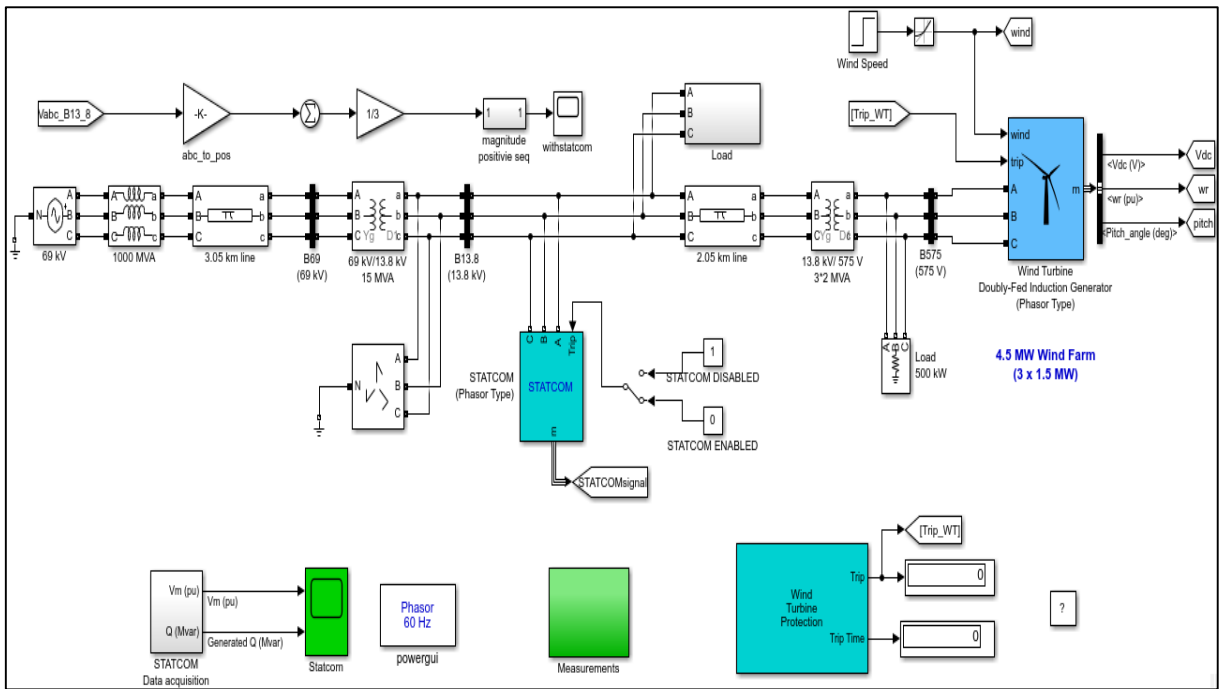


Figure 5.2: Complete reference model with STATCOM controller

Figure 5.3 illustrates the load block where a momentary line-to-line fault is created, connected to the 2300 V feeder starting at $t = 5$ s and lasting 150 ms to $t = 5.15$ s.

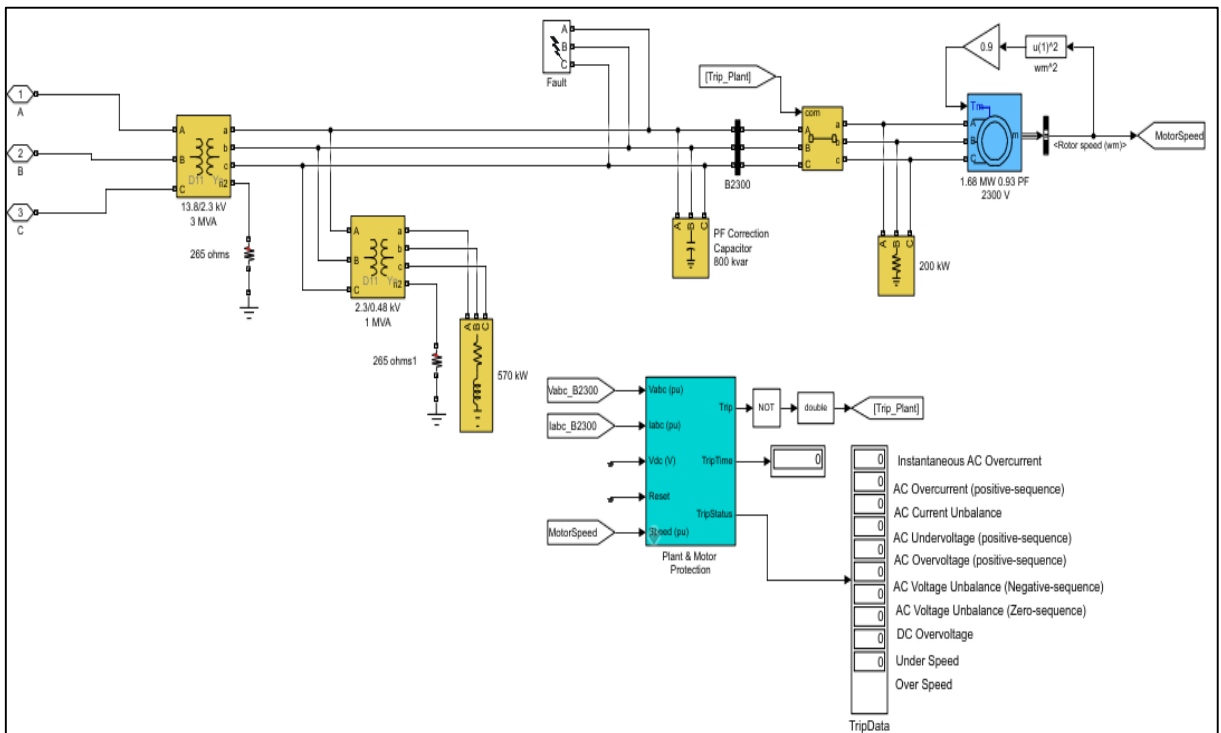


Figure 5.3: Fault location for the reference model

When applying the line-to-line fault at $t = 5$ s, the voltage profile at B13.8 is monitored to see what effect the fault has on the voltage profile. The results illustrated in Figure 5.4 illustrate three voltage profiles. In these results figures, a comparative analysis is made between voltage

profiles between a network without any FACTS controllers connected and a network to where FACTS controllers are connected.

The voltage profile in black represents the network without any FACTS controllers connected, the blue for the network where SVC is included, and the red for the network where STATCOM is included.

Figure 5.4 demonstrates that the network without FACTS controllers experiences a more severe dip in voltage than the system with FACTS controllers. The STATCOM performs better than the SVC, with a less severe voltage dip between the FACTS controllers.



Figure 5.4: Reference model - Voltage profile at B13.8 - Line-to-line fault

Figure 5.5 illustrate the reactive power that SVC and STATCOM supplied at B13.8 to help lower the voltage dip at B13.8 during the fault at $t = 5$ s. Figure 5.5 shows that STATCOM performs more quickly than the SVC for the first injection of reactive power and injects more reactive power overall. As seen in Figure 5.4, a voltage overshoot occurs after the fault is rectified. The STATCOM also performs faster to reduce reactive power injection to reduce the voltage overshoot back to the nominal 1 p.u.

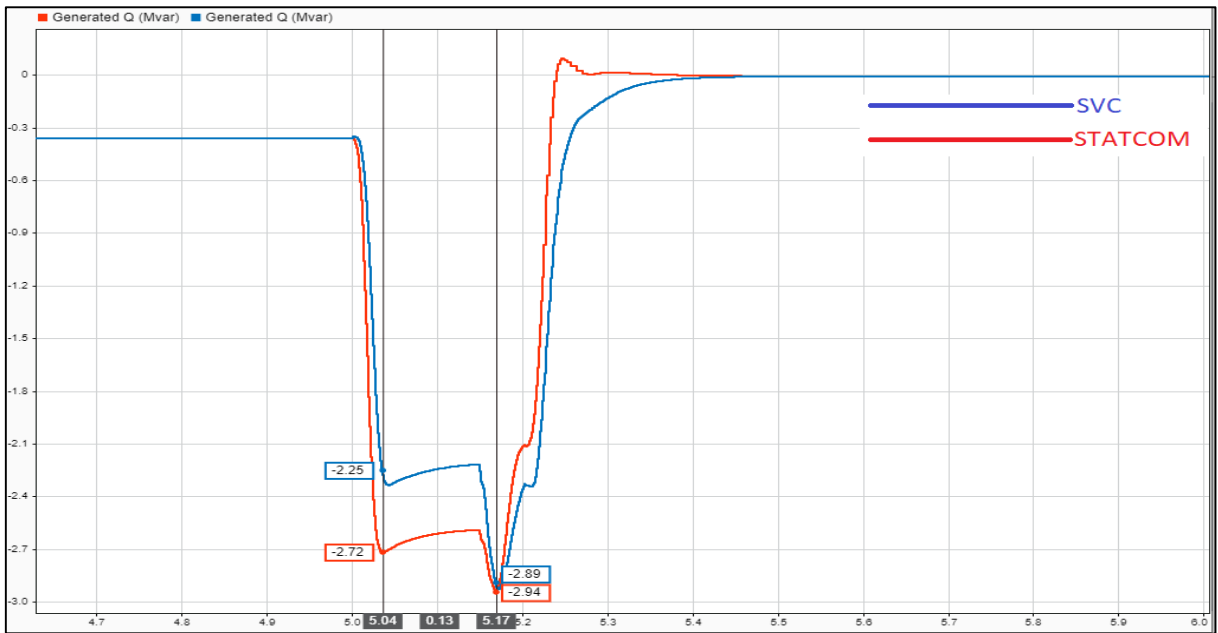


Figure 5.5: Reference model - Reactive power supplied at B13.8 from the FACTS controllers

The reference model also considers the settling time to determine what system recovers back to the nominal 1 p.u voltage level after the fault has been cleared. Figure 5.6 is a closer view of all three systems. The settling time is taken from the start of the fault at $t = 5$ s to the initial recovery of the voltage to 1 p.u.

Figure 5.6 illustrates that STATCOM again performed the fastest to recover the system to 1 p.u, followed by SVC and the system without any FACTS controllers.

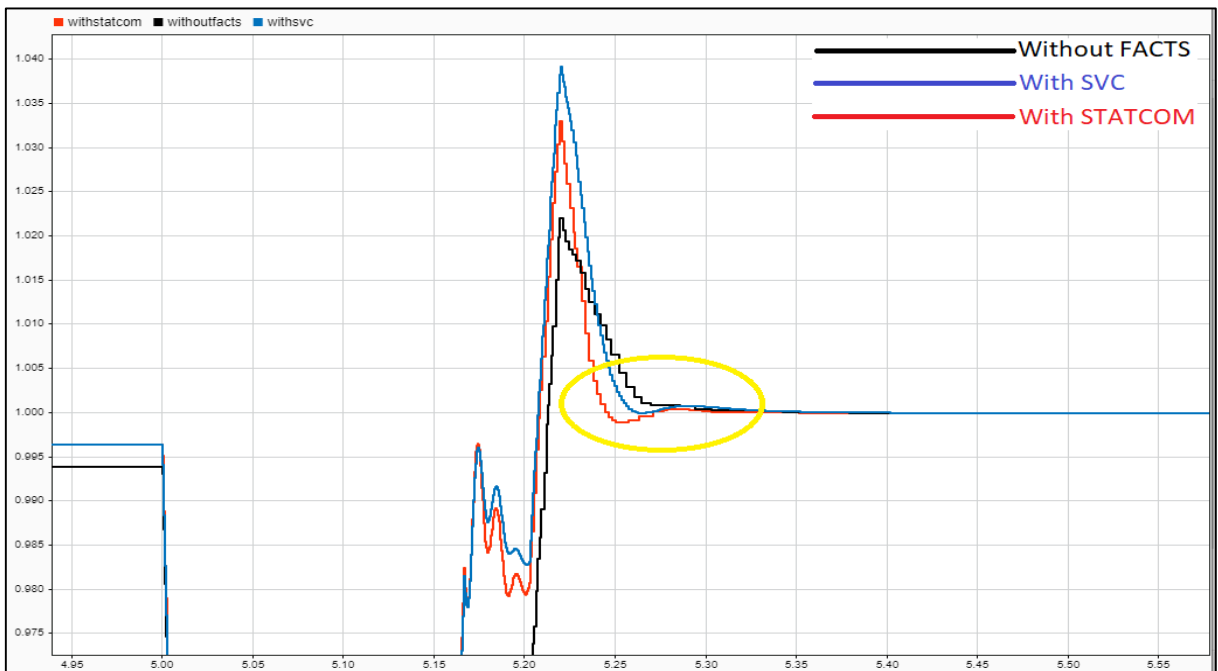


Figure 5.6: Reference model settling time

Table 5.1 illustrates all the results discussed above in tabular form. It was seen that the network without FACTS controllers had the most severe voltage dip compared to the networks with FACTS controllers. STATCOM responded quicker than SVC by supplying more reactive power, resulting in the least severe voltage dip between FACTS controllers. The reactive power compensation of STATCOM also proved that it is vital for settling time. The settling time to recover the network back to its 1 p.u reference voltage level was the fastest for STATCOM, followed by the SVC, and the longest for the network without any FACTS.

Table 5.1: Reference model results

| Reference model | PCC Voltage | Reactive power provided during a fault by the FACTS controllers | Settling time to recover to 1 p.u |
|-----------------|-------------|---|-----------------------------------|
| Without FACTS | 0.834 p.u | - | 0.363 s |
| With SVC | 0.859 p.u | -2.25 MVar | 0.266 s |
| With STATCOM | 0.863 p.u | -2.72 MVar | 0.245 s |

All the reference simulation model results correspond to the reference literature and confirm that the FACTS controllers used in the model improve voltage stability during momentary fault conditions. In addition, STATCOM performs faster than SVC with a higher amount of injected reactive power and a shorter settling time.

The SVC and STATCOM assisted in reducing the voltage dip, enabling the LVRT functioning of the wind turbines to maintain grid connectivity throughout the fault and afterward for all wind turbines.

According to findings in the literature, the network with linked FACTS has greater voltage stability than the network without linked FACTS. In addition, STATCOM outperformed SVC with the same rating, and it outperformed both SVC and the network without FACTS in terms of the time it took the network to settle after the fault.

5.3 Newly designed WECS modeling with momentary fault conditions

Section 5.3 introduces a newly designed WECS model with a different layout and components. This new model aims to observe the performances of the SVC and STATCOM and how they enhance the voltage profile. The voltage profile is expected to be enhanced as the reference modeling in Section 5.2 proved that SVC and STATCOM do enhance the voltage profile during momentary fault conditions.

The overall system model shown in Figures 5.7 and 5.8 includes a 6 MW wind farm consisting of four 1.5 MW wind turbines or two sets of 1.5 MW wind turbines. The wind farm is linked to

a 25 kV distribution system, and its power is exported to the 120 kV grid through a 25 km 25 kV feeder line.

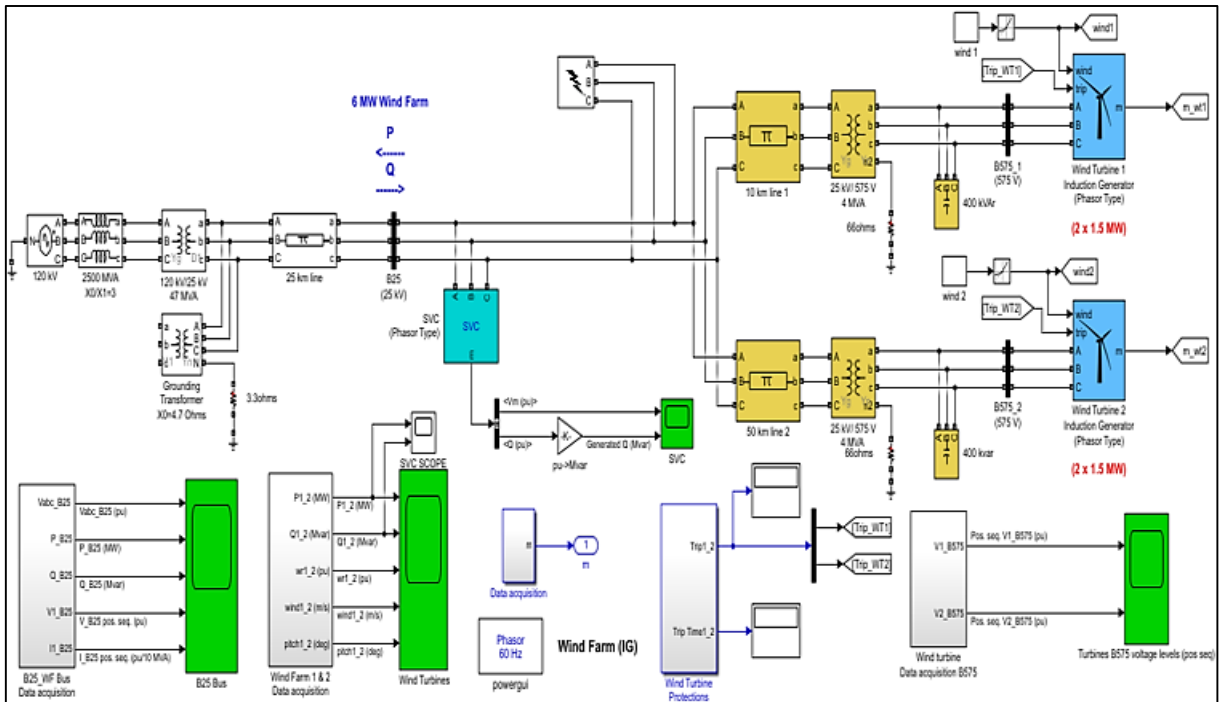


Figure 5.7: Complete SVC simulation model

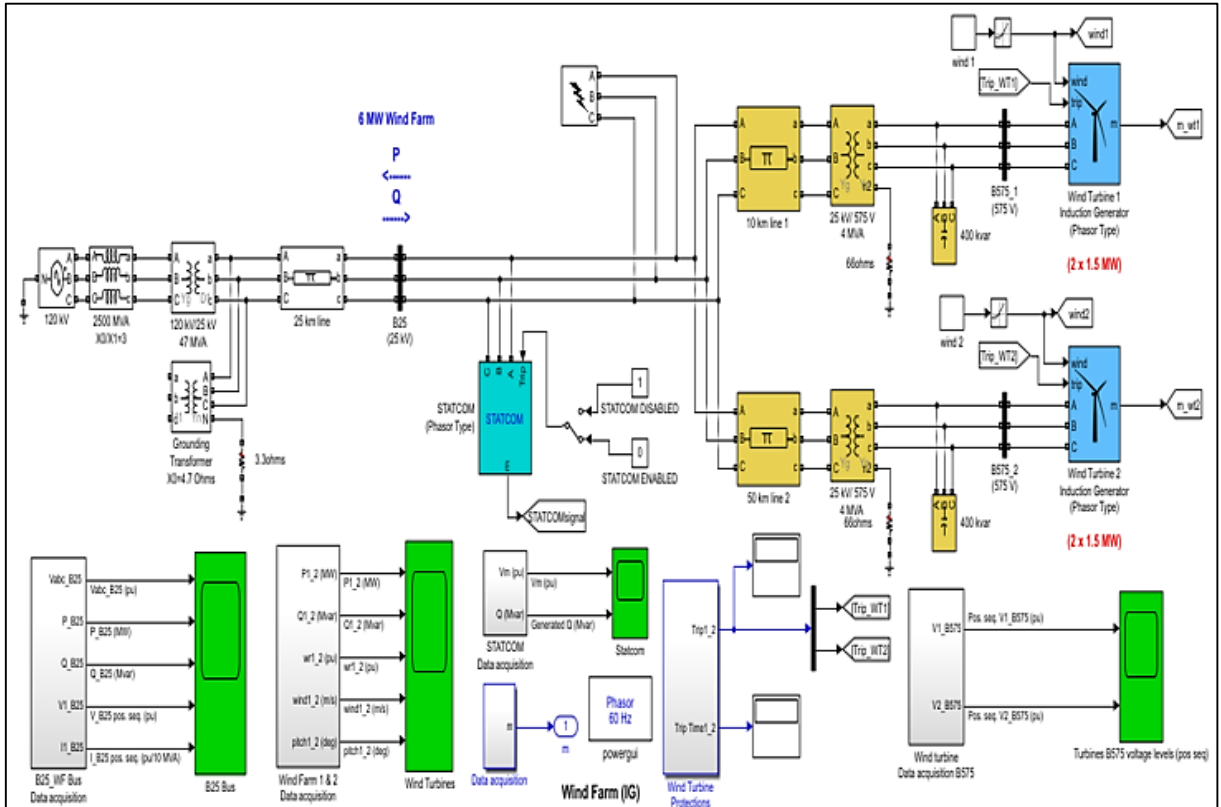


Figure 5.8: Complete STATCOM simulation model

As was said before, the wind turbine is made up of a fixed speed SCIG that has variable pitch angle blade control for speed control to keep the generator's rotor running at rated speed to keep the generator output to a maximum. Each wind turbine furthermore includes a 400 kVAR capacitor bank linked to its terminals to compensate for the reactive power absorbed by the SCIG. The SVC and STATCOM controllers supply the remaining reactive power, which helps keep the bus voltage at B25 near 1 p.u.

The synchronous speed is the difference between the speed of the rotor of the induction generator and the spinning magnetic field necessary for the induction generator to generate electricity. The rotor's speed varies from around 1 p.u. with no load to 1.005 p.u. in situations of heavy load.

The wind farm network is modeled with faults introduced to the grid under momentary fault situations with and without FACTS controllers. When the FACTS controllers are disconnected and connected, the effects on the grid are explained. Each wind turbine is equipped with a protection system that monitors the generator's voltage, current, and rotor speed.

The characteristics of the investigated system for the electrical grid, transformers, transmission lines, loads, capacitor bank, wind farm, SVC, and STATCOM are presented in Tables 5.2 through Table 5.4. The doubly-fed induction generator's controller portion won't be taken into consideration because the FACTS controllers that supply reactive power are the main concern.

Table 5.2: Parameters of the WECS

| The parameters of the electrical grid | | | | | |
|--|--|-----------|--------------------|-------|------|
| Parameter | | Value | Unit | | |
| Rated voltage | | 120 | kV | | |
| Frequency | | 60 | Hz | | |
| The parameters of transformers | | | | | |
| Parameter | | Value | Unit | Value | Unit |
| Transformer | | 120/25 | kV | 47 | MVA |
| Transformer (x2) | | 25/0.575 | kV | 4 | MVA |
| The parameters of the transmission line | | | | | |
| Parameter | | Value | Unit | | |
| The positive - sequence resistance | | 0.1153 | Ω/km | | |
| The positive - sequence inductance | | 1.05 e-3 | H/km | | |
| The positive - sequence capacitance | | 11.33 e-9 | F/km | | |
| The length of the transmission line | | 25 | km | | |
| The length of the transmission line | | 10 | km | | |
| The length of the transmission line | | 50 | km | | |
| The parameters of the capacitor | | | | | |
| Parameter | | Value | Unit | | |
| Rated voltage | | 575 | V | | |
| Capacitive reactive power | | 400 | kVar | | |
| The parameters of the wind farm | | | | | |
| Parameter | | Value | Unit | | |
| Power rating of the wind farm | | 6 | MW | | |
| Base wind speed | | 9 | m/s | | |
| Power rating of the wind turbine | | 1.5 | MW | | |
| Number of wind turbines | | 4 | - | | |
| Generator type | | SCIG | - | | |
| The generator rated voltage | | 575 | V | | |
| The generator stator resistance | | 0.004843 | pu | | |
| The generator stator inductance | | 0.1248 | pu | | |
| The generator rotor resistance | | 0.004377 | pu | | |
| The generator rotor inductance | | 0.1791 | pu | | |
| The generator magnetizing inductance | | 6.77 | pu | | |
| The generator pole pairs | | 6 | - | | |
| The inertia constant | | 5.04 | s | | |

Table 5.3: Parameters of the FACTS controllers

Table 5.4: Parameters of the wind turbine protection system

| The parameters of the SVC | | |
|--|--------------------|------|
| Parameter | Value | Unit |
| The SVC rated voltage | 25 | kV |
| Frequency | 60 | Hz |
| Rated power | 3 | MVar |
| Thyristor switching delay time | 4 e-3 | s |
| Mode | Voltage regulation | - |
| Voltage reference | 1 | p.u |
| Droop reactance | 0.03 | p.u |
| The SVC voltage regulator gains Kp | 0 | - |
| The SVC voltage regulator gains Ki | 300 | - |
| The parameters of the STATCOM | | |
| Parameter | Value | Unit |
| The STATCOM rated voltage | 25 | kV |
| Frequency | 60 | Hz |
| Rated power | 3 | MVar |
| The STATCOM DC link voltage | 4000 | V |
| The STATCOM DC link equivalent capacitance | 1125 | uF |
| Mode | Voltage regulation | - |
| Voltage reference | 1 | p.u |
| Droop reactance | 0.03 | p.u |
| The STATCOM voltage regulator gains Kp | 5 | - |
| The STATCOM voltage regulator gains Ki | 1000 | - |

| Parameters of protection system | | | |
|---------------------------------|------------------------|------------------------|----------------|
| Parameter | The minimum value (pu) | The maximum value (pu) | Delay time (s) |
| The AC under and over voltage | 0.75 | 1.1 | 0.1 |
| The under and over rotor speed | 1 | 1.05 | 5 |
| The AC current | - | 1.1 | 10 |
| The AC current unbalance | - | 0.4 | 0.2 |
| The Voltage unbalance | - | 0.05 | 0.2 |
| The DC voltage | - | 1900 | 0.001 |

5.3.1 Momentary fault

conditions without and with FACTS controllers

This section presents momentary fault circumstances to the network and conducts a comparison study between the network without FACTS controllers and the network with FACTS controllers attached to the grid. The grid is affected by line-to-ground, line-to-line, and three-phase faults. The complete simulation period is 20 s, and the findings are shown in the figures, followed by a discussion of the response of voltage, active and reactive power at B25.

5.3.1.1 Line-to-ground fault

A line-to-ground fault occurred at $t = 10$ s and was cleared after 88 ms at the timestamp $t = 10.088$ s. Three different graphs are illustrated, black is how the grid reacts to the fault without any FACTS controllers connected, blue with SVC connected, and red with STATCOM connected.

For statistical reference of comparing values, $t = 10.087$ s will be taken for readings just before the fault has been cleared.

Figure 5.9 illustrates that the active power delivered to the grid without FACTS controllers is 5.24 MW. With SVC and STATCOM connected, the power generated is 5.43 MW and 5.45 MW, respectively. STATCOM does have a slight advantage over SVC, but both FACTS controllers improve the active power delivery to the grid during the fault.

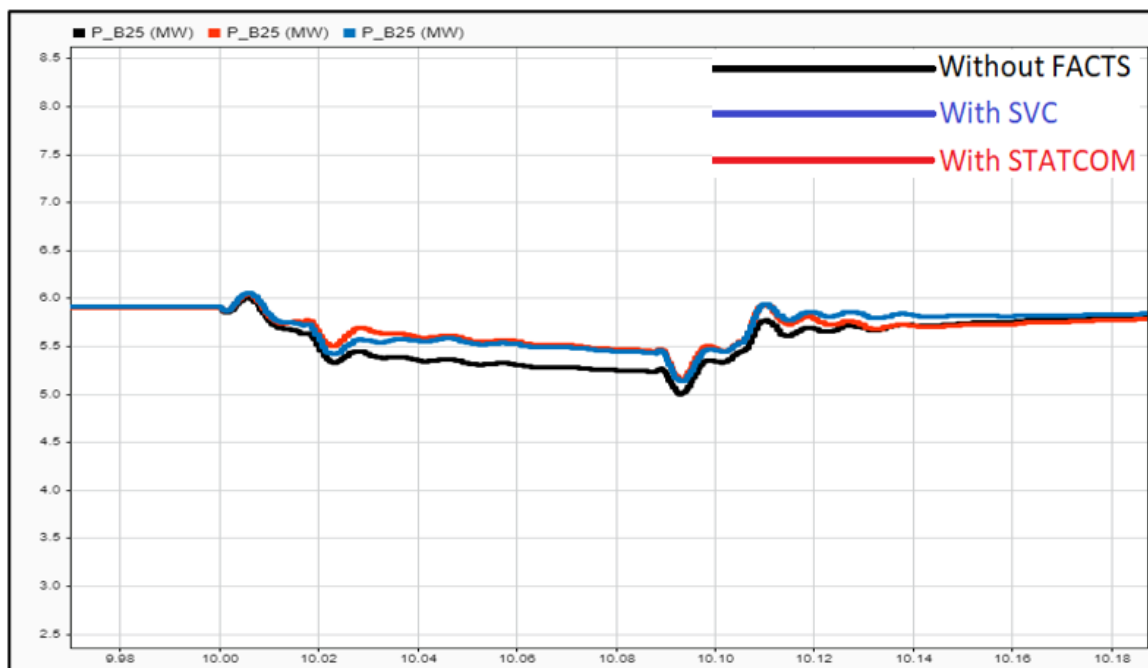


Figure 5.9: B25 active power – (line-to-ground fault) w/o and w/FACTS controllers

Figure 5.10 depicts that without FACTS controllers, the reactive power drawn from the grid is 1.9 MVar, but with SVC and STATCOM attached, the grid receives -0.5 MVar and -0.8 MVar, respectively. STATCOM has a slight advantage over SVC in supplying the network with more reactive power to lower the grid's reactive power consumption during a fault.

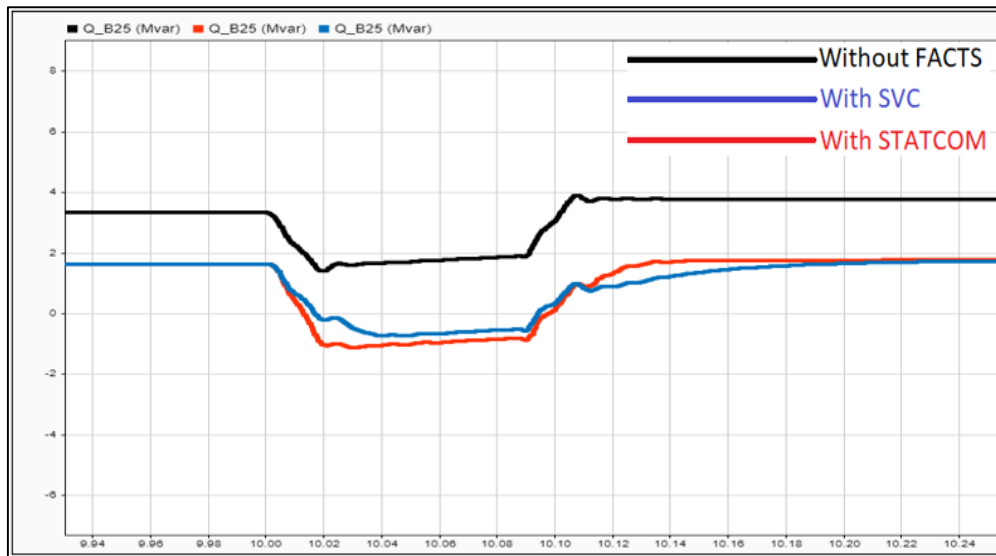


Figure 5.10: B25 reactive power – (line-to-ground fault) w/o and w/FACTS controllers

Figure 5.11 follows up on the STATCOM supplies greater reactive power than that of the SVC during the fault. As seen in Figure 5.10, the STATCOM maintained the grid more than the SVC since it supplied -2.55 MVAR whereas the SVC only supplied -2.14 MVAR. Additionally, it is evident that when reactive power is supplied, the STATCOM responds more quickly than the SVC.

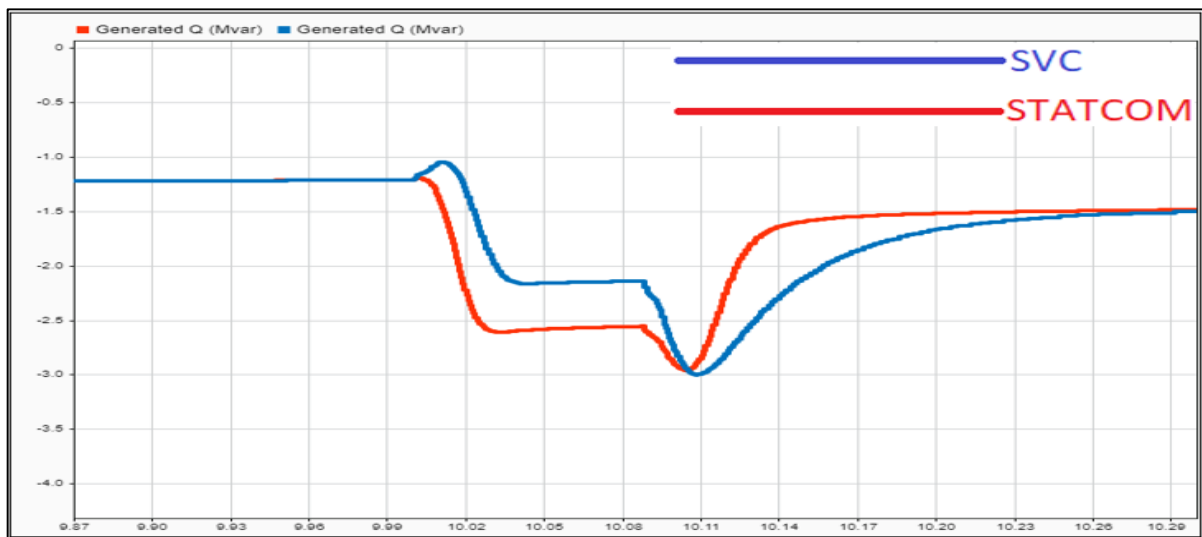


Figure 5.11: Reactive power provided by the SVC and STATCOM controller during fault condition (line-to-ground fault)

Figure 5.12 depicts the positive sequence bus voltage at B25. During the fault, the voltage at B25 decreased to 0.79 p.u without FACTS controllers, but 0.84 p.u and 0.85 p.u, respectively, when SVC and STATCOM were attached. Fortunately for the network without FACTS controllers installed, since the undervoltage threshold at B575 is set to 0.75 p.u, the wind turbine generators maintained connected to the grid and avoided any tripping of undervoltage. After the fault has been rectified, the FACTS controllers aid the network in

maintaining a voltage level of around 1 p.u. Due to their grid support for reactive power, both SVC and STATCOM deliver a voltage profile that is superior. Table 5.5 illustrates all the results discussed above in tabular form.

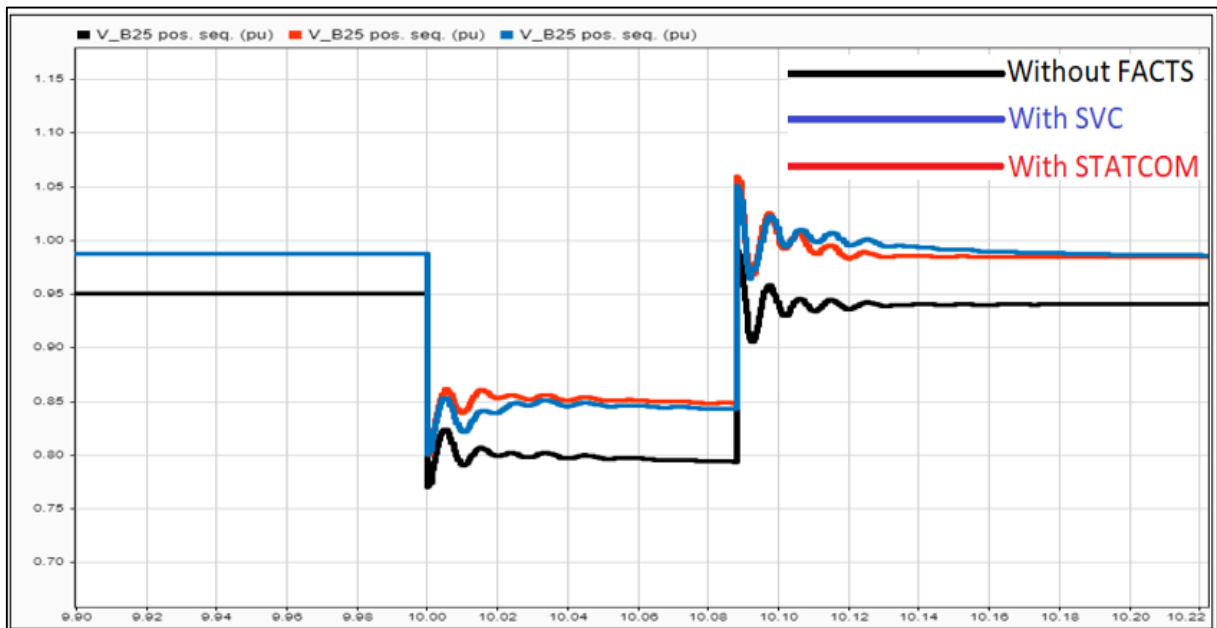


Figure 5.12: B25 positive sequence voltage – (line-to-ground fault) w/o and w/FACTS controllers

Table 5.5: Line-to-ground fault results

| Line-to-ground fault (measurements taken at t = 10.087 s during fault condition) | Tripping wind turbines | Reason for tripping condition | B25 Power | B25 Reactive power | B25 Voltage | Reactive power supplied by the FACTS controllers |
|--|------------------------|-------------------------------|-----------|--------------------|-------------|--|
| Without FACTS | - | - | 5.24 MW | 1.9 MVar | 0.79 p.u | - |
| With SVC | - | - | 5.43 MW | -0.5 MVar | 0.84 p.u | -2.14 MVar |
| With STATCOM | - | - | 5.45 MW | -0.8 MVar | 0.85 p.u | -2.55 MVar |

5.3.1.2 Line-to-line fault

A line-to-line fault occurred at t = 10 s and was cleared after 88 ms at the timestamp t = 10.088 s. Three different graphs are illustrated, black is how the grid reacts to the fault without any FACTS controllers connected, blue with SVC connected, and red with STATCOM connected.

For statistical reference of comparing values, $t = 10.087$ s will be taken for readings just before the fault has been cleared.

Figure 5.13 illustrates that the active power delivered to the grid without FACTS controllers is 2.76 MW. With SVC and STATCOM connected, the power generated is 2.85 MW and 2.83 MW, respectively. SVC does have a slight advantage over STATCOM, but both FACTS controllers improve the active power delivery to the grid during the fault.

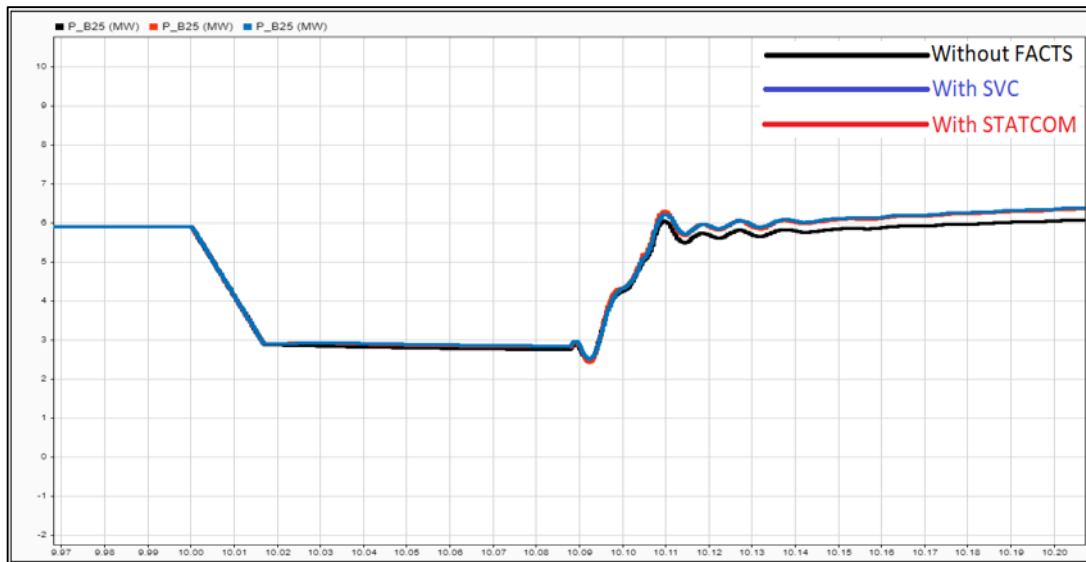


Figure 5.13: B25 active power – (line-to-line fault) w/o and w/FACTS controllers

Figure 5.14 demonstrates that without FACTS controllers, the reactive power drawn from the grid is 2.4 MVar, however with SVC and STATCOM attached, the reactive power drawn from the grid is 1.05 MVar and 1.03 MVar, respectively. STATCOM has a slight edge over SVC when it comes to supplying the grid with more reactive power to lower the grid's reactive power consumption during a fault.

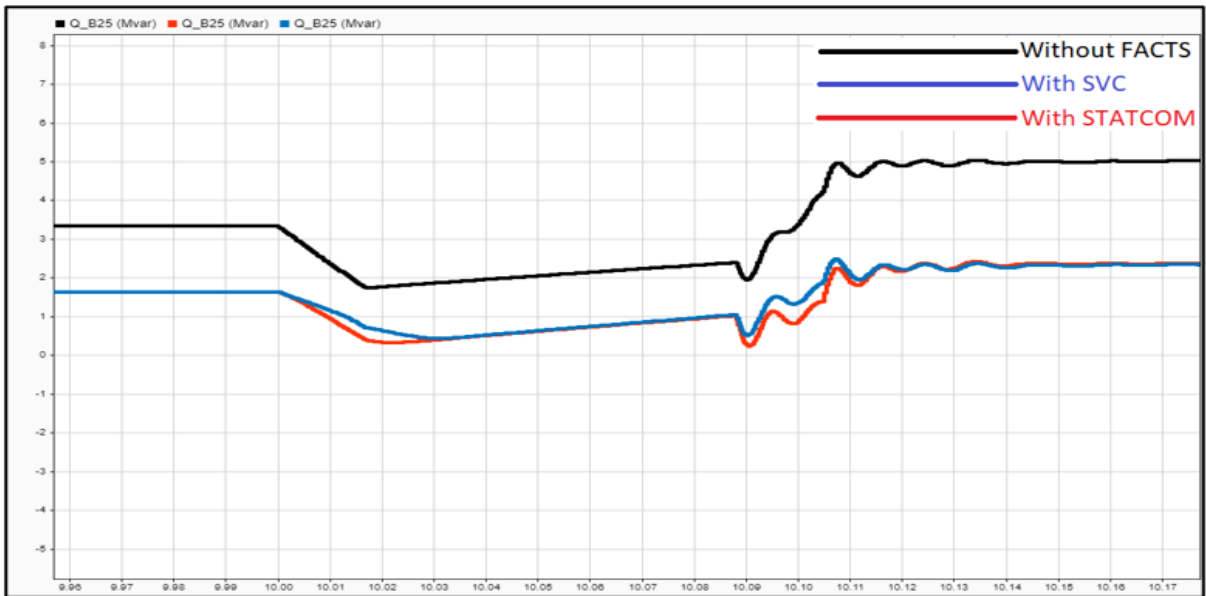


Figure 5.14: B25 reactive power – (line-to-line fault) w/o and w/FACTS controllers

Figure 5.15 is a continuation of Figure 5.14, which shows the STATCOM providing greater reactive power than the SVC controller during a fault condition. Figure 5.14 demonstrates that the STATCOM maintained the grid more effectively than that of the SVC since the STATCOM delivered -1.47 MVar while the SVC only delivered -0.72 MVar. STATCOM delivers more reactive power than SVC because its V-Q curve exhibits a linear relationship between reactive power and system voltage, while SVC's reactive power decreases according to the square of the power system voltage. As the system voltage recovers after clearing the fault, both FACTS controllers give the greatest amount of reactive power to assist the grid in recovering from the fault.

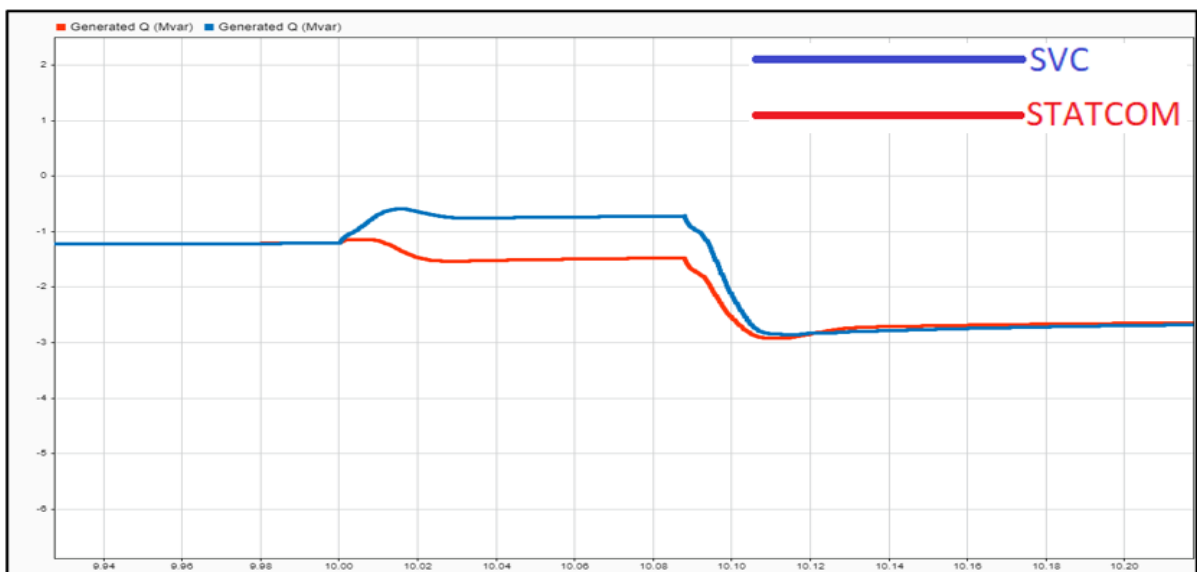


Figure 5.15: Reactive power provided by the SVC and STATCOM controller during fault condition (line-to-line fault)

The voltage of the positive sequence at bus B25 is shown in Figure 5.16. During the fault, the voltage at bus B25 declined to 0.456 p.u without FACTS controllers but decreased to 0.487 p.u and 0.488 p.u, respectively, with SVC and STATCOM attached. Fortunately, even if the p.u voltage is below the 0.75 p.u undervoltage thresholds established for B575, as seen in Figure 5.17, the wind farm generators maintained connected to the grid regardless of the presence or absence of FACTS controllers.



Figure 5.16: B25 positive sequence voltage – (line-to-line fault) w/o and w/FACTS controllers

Figure 5.17 depicts the voltages at bus B575 of each wind turbine inside the wind farm for both grid connections: without FACTS controllers and with FACTS controllers. The protective system monitors the voltages at B575, which are linked to the generator terminals' output. The 0.75 p.u. undervoltage protection has a delay of 0.1 seconds. When the voltage of each grid for both sets of wind turbines dropped below 0.75 p.u., the wind farms transitioned to low-voltage ride-through mode. Because the protection system's delay was set at 0.1 s, which is longer than the fault's clearing time, no wind turbines tripped and disconnected from the grid.

After the fault has been rectified, as seen in Figure 5.16, the FACTS controllers aid the grid in maintaining a voltage level at B25 that is near to 1 p.u. Even though the fault was severe, the magnitude of the voltage at bus B25 was improved with the SVC and STATCOM controllers attached to the grid, but the voltage profile was still affected.

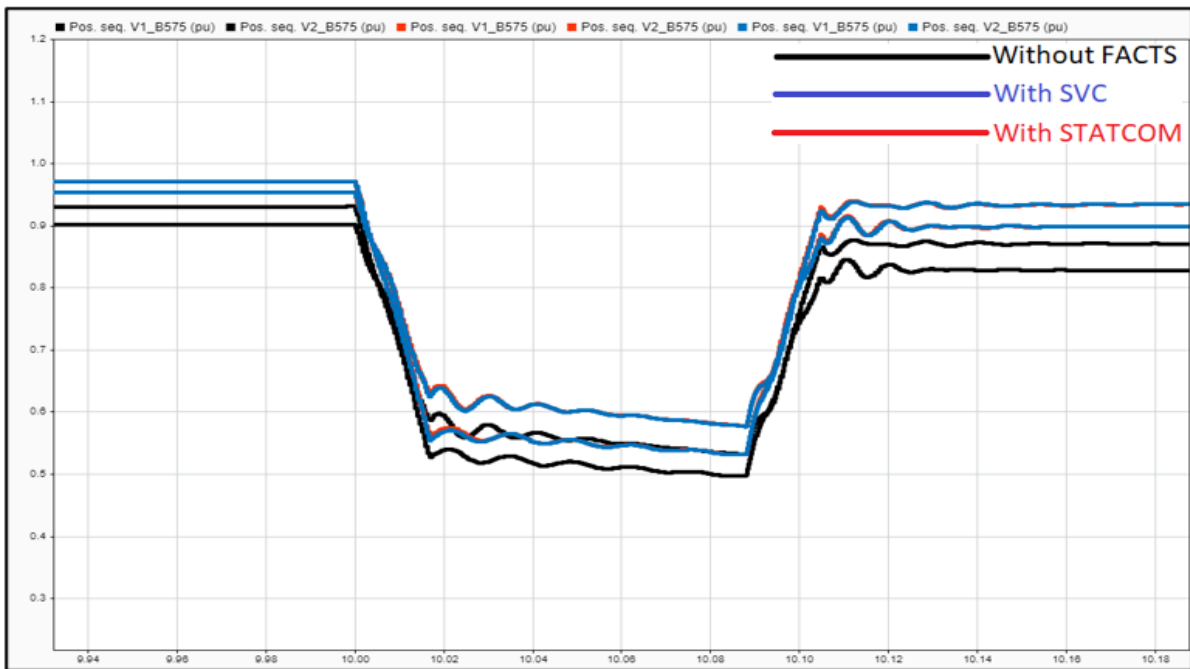


Figure 5.17: B575 voltage for wind turbine generator sets – (line-to-line fault) w/o and w/FACTS controllers

Table 5.6: Line-to-line fault results

| Line-to-line fault (measurements taken at t = 10.087 s during fault condition) | Tripping wind turbines | Reason for tripping condition | B25 Power | B25 Reactive power | B25 Voltage | Reactive power supplied by the FACTS controllers |
|--|------------------------|-------------------------------|-----------|--------------------|-------------|--|
| Without FACTS | - | - | 2.76 MW | 2.4 MVar | 0.456 p.u | - |
| With SVC | - | - | 2.85 MW | 1.05 MVar | 0.487 p.u | -0.72 MVar |
| With STATCOM | - | - | 2.83 MW | 1.03 MVar | 0.488 p.u | -1.47 MVar |

5.3.1.3 Three-phase fault

A three-phase fault occurred at $t = 10$ s and was cleared after 88 ms at the timestamp $t = 10.088$ s. Three different graphs are illustrated, black is how the grid reacts to the fault without any FACTS controllers connected, blue with SVC connected, and red with STATCOM connected.

For the three-phase fault, readings at $t = 10.087$ s will all be zero. Results will, however, be compared to how the grid responded after the fault had been cleared.

Figure 5.18 depicts the tripping state of wind turbine generator group 2 when no FACTS controllers are connected to the grid.

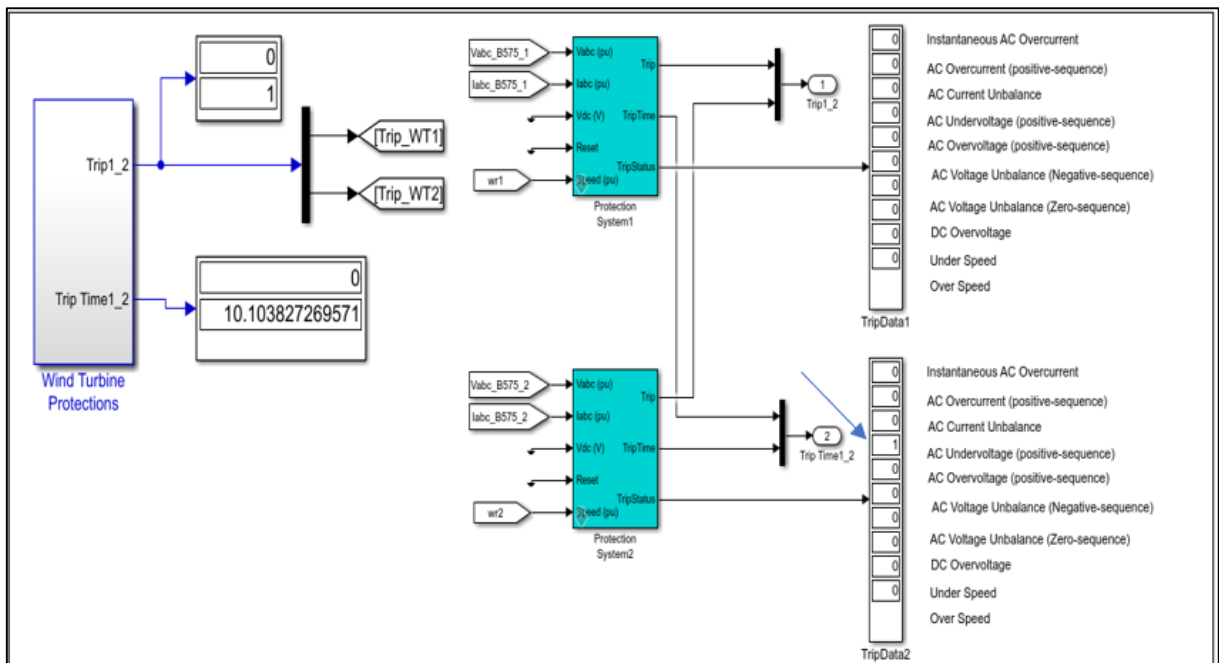


Figure 5.18: Tripping condition for the grid w/o FACTS controllers attached – (three-phase fault)

At $t = 10.104$ seconds, the protection detected an undervoltage condition at B575, resulting in a tripping condition. Due to one of the two sets of two 1.5 MW units tripping, the wind farm will only be able to provide the grid with half of its output capacity after the fault has been resolved.

The voltages levels for all three networks at bus B575 that are monitored by the protective system are shown in Figure 5.19. When no FACTS controllers are connected, the wind turbine generator group 2 voltage drops below the undervoltage threshold of 0.75 p.u. Due to the 0.1 s delay, the protection system disconnected the generator from the grid when wind turbine generator 2 failed to rise over 0.75 p.u with just 0.69 p.u. The increased voltage levels on the

grids that are linked to SVC and STATCOM indicate that both the SVC and STATCOM controllers have contributed to the increase in voltage.

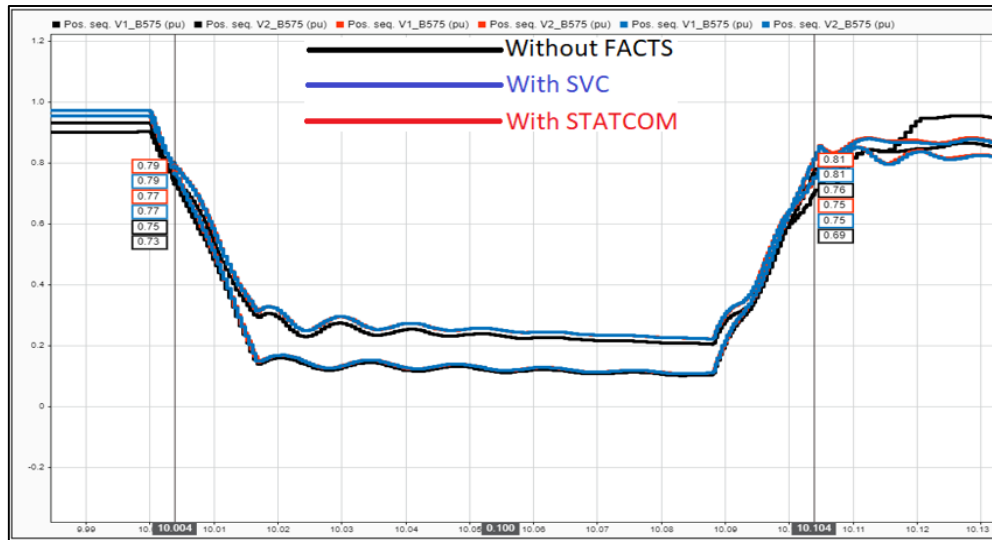


Figure 5.19: B575 voltage for wind turbine generator sets – (three-phase fault) w/o and w/FACTS controllers

Figure 5.20 depicts the active power supplied to the grid in the absence of FACTS controllers. As previously observed, the generator for the network without FACTS controllers experienced an undervoltage trip situation. After the fault has been rectified, the SVC and STATCOM networks continue to feed the grid with close to its 6 MW rating. Nonetheless, the network without FACTS controllers attached without wind turbine generator 2 can now only provide 3 MW. After the cleared fault, an increase in power generated by the generators occurs and only stabilizes at approximately $t = 11$ s.

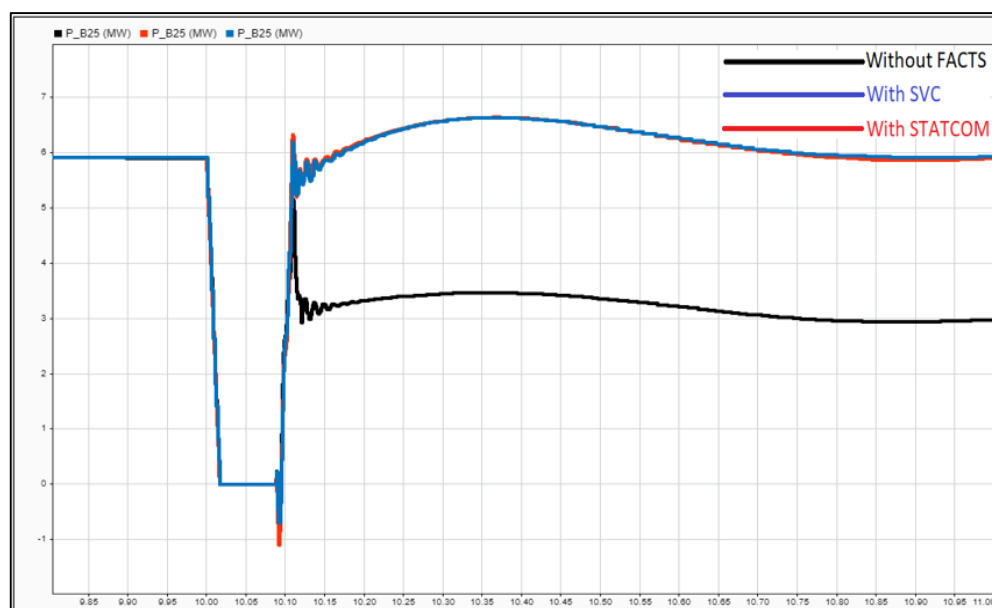


Figure 5.20: B25 active power – (three-phase fault) w/o and w/FACTS controllers

Figure 5.21 illustrates the generator rotor speeds of each grid's 2 sets of generators. After the fault has been cleared, the grids are unstable, causing the overspeed in generator rotors that caused the overpower generation, as seen in Figure 5.20. The rotor speed of the tripped generator is seen to increase as the generator is not connected to the grid anymore, whereas the rotor speeds of the generators that are still connected to the grid have to decrease to their nominal 1.005 p.u for their nominal power generation.

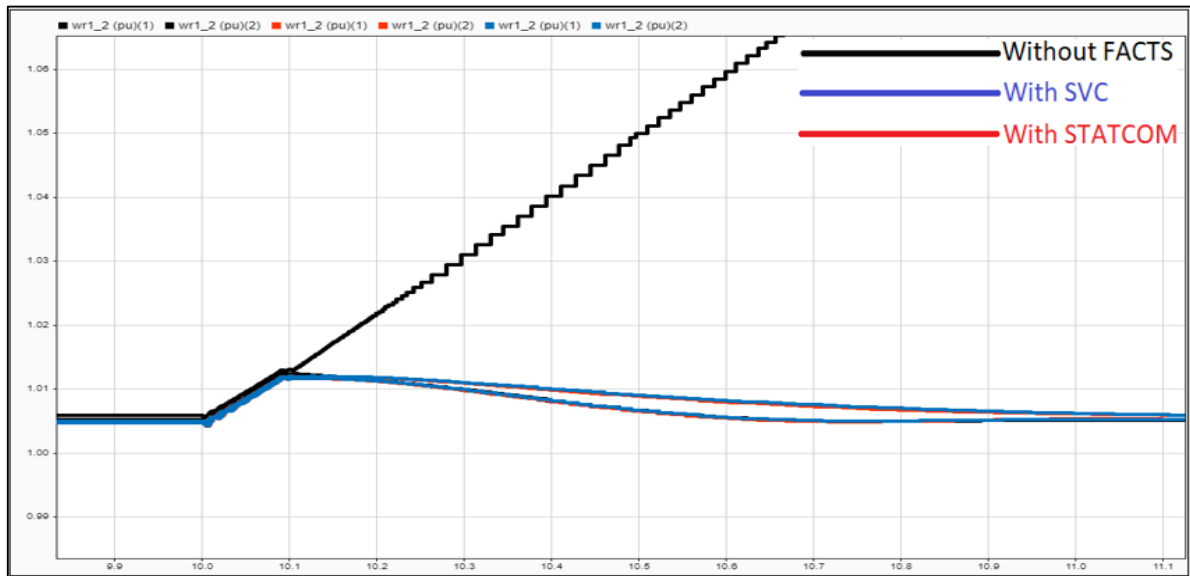


Figure 5.21: Sets of generator rotor speeds – (three-phase fault) w/o and w/FACTS controllers

The reactive power consumed drawn from the network without and with FACTS controllers is depicted in Figure 5.22. After the fault has been cleared, the reactive power drawn from the grid without FACTS controllers is 6.1 MVAR, but with SVC and STATCOM attached, it is 4.4 MVAR and 4.1 MVAR, respectively. The sudden rise in reactive power demanded from the network after the fault is caused by the increased power delivery brought on by the rotor speed increase and grid instability.

After some stability in the grids has been regained, the grid without FACTS controllers consumes less reactive power because of one less set of generators connected to the grid. STATCOM does have a slight advantage over SVC supporting the grid with more reactive power to reduce the reactive power consumption from the grid after the fault has been cleared.

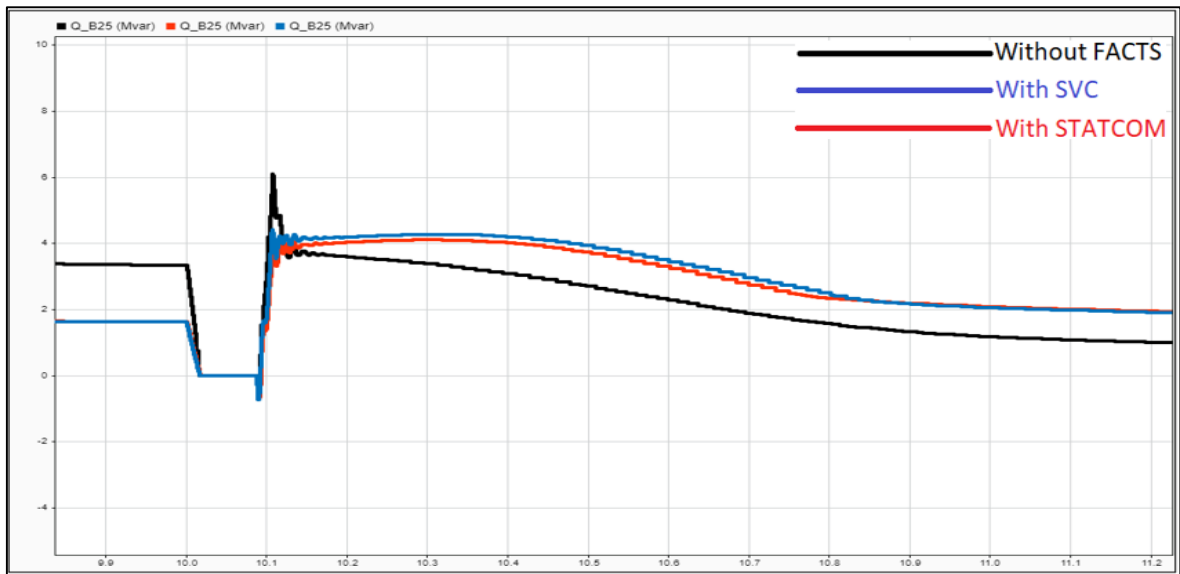


Figure 5.22: B25 reactive power – (three-phase fault) w/o and w/FACTS controllers

Figure 5.23 is a continuation of Figure 5.22, which shows the STATCOM delivering more reactive power than that of the SVC after the fault is resolved. As seen in Figure 5.22, the STATCOM supported the network better than the SVC by providing its rated capacity of -3 MVAR whilst the SVC only delivered -2.6 MVAR. STATCOM delivers more reactive power than SVC because its V-Q curve exhibits a linear connection between reactive power and system voltage, while SVC's reactive power decreases according to the square of the system voltage. As grid stability was restored after the fault and the B25 voltage rose, the reactive power of the FACTS controllers steadily reduced.

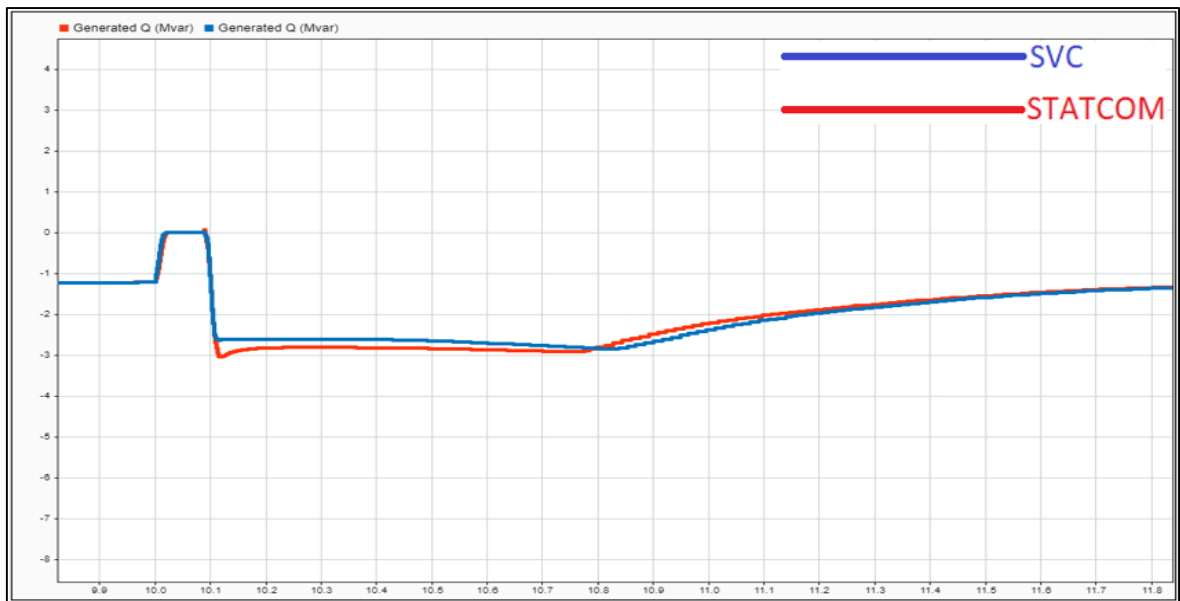


Figure 5.23: Reactive power provided by the SVC and STATCOM controller during fault condition (three-phase fault)

Figure 5.24 depicts the voltage of the positive sequence at B25. After the fault was rectified at $t = 10,088$ s, the bus voltage for the network without attached FACTS controllers rose to 1.18 p.u. The grid voltage increased to 1.21 p.u and 1.16 p.u when SVC and STATCOM were connected. STATCOM performed the best to quickly decrease its bus voltage by supplying less reactive power over the SVC as it performs faster where the SVC had a slight overshoot in voltage. The B25 voltages for all grids recovered over time as the FACTS controllers supported the voltage levels, and the grid with FACTS controllers connected also recovered as the set of generators that tripped consumed caused less reactive power to be drawn from the grid leading to a faster recovery time for stability in the grid.

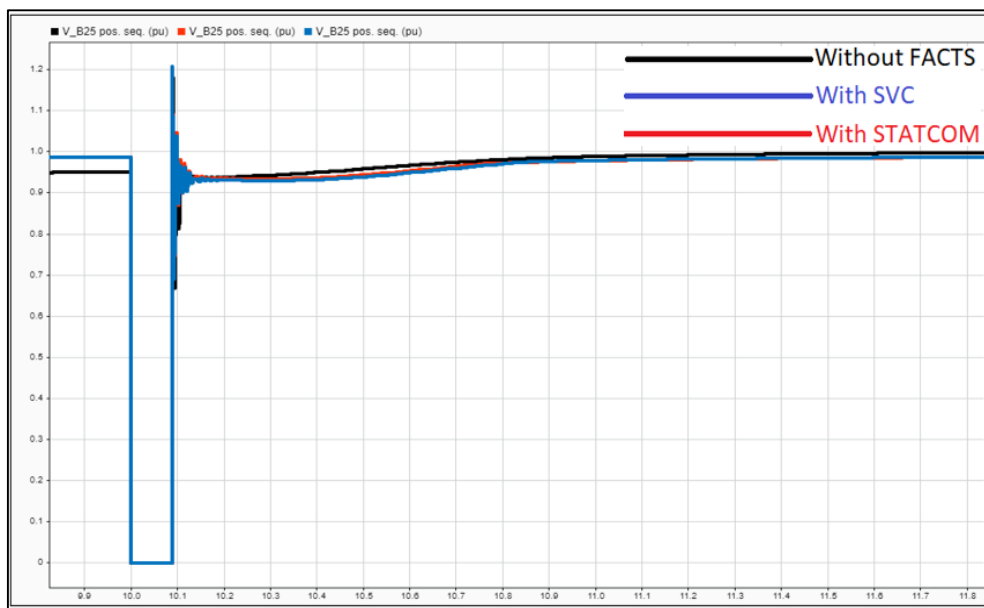


Figure 5.24: B25 positive sequence voltage – (three-phase fault) w/o and w/FACTS controllers

Table 5.7 is a tabular representation of the findings described before.

Table 5.7: Three-phase fault results

| Three-phase fault (measurements taken after fault is cleared) | Tripping wind turbines | Reason for tripping condition | B25 Power at t = 11 s | B25 Reactive power at t = 10.108 s | B25 Voltage at t = 10.088 s | B575 Voltage at t = 10.104 (turbine 1/turbine 2) | Reactive power supplied by the FACTS controllers at t = 10.117 s |
|---|--------------------------------------|---|-----------------------|------------------------------------|-----------------------------|--|--|
| Without FACTS | Wind turbine 2 tripped at t = 10.104 | Voltage remained below 0.75 p.u after the fault cleared. Undervoltage protection system disconnected the generator. | 2.99 MW | 6.1 MVar | 1.18 p.u | 0.76/0.69 p.u | - |
| With SVC | - | - | 5.93 MW | 4.4 MVar | 1.21 p.u | 0.81/0.75 p.u | -2.62 MVar |
| With STATCOM | - | - | 5.90 MW | 4.1 MVar | 1.16 p.u | 0.81/0.75 p.u | -3.03 MVar |

5.4 Summary and Conclusion

To study the influence of SVC and STATCOM controllers on the network under different fault scenarios, including line-to-ground, line-to-line, and three-phase faults, Chapter 5 offered simulations for a reference model and simulation results for momentary fault events.

Firstly, a reference model for each SVC and STATCOM controller was simulated. A line-to-line momentary fault was applied to the 2300 V feeder. Observations were that both FACTS controllers provided reactive power compensation and improved the voltage profile, with STATCOM being superior due to faster operation. The STATCOM also had a faster settling time than SVC. With the reference modeling completed by knowing the FACTS controllers were operating correctly, simulations for steady-state and transient-state were done.

Observations were conducted with a redesigned WECS network model that included FACTS controllers. SVC and STATCOM demonstrated their efficacy in several fault scenarios including momentary fault conditions. Neither with nor without linked FACTS controllers did the line-to-ground failure trigger any grid trip conditions. The B25 voltage rose from 0.79 p.u without FACTS controllers to 0.84 p.u for SVC and 0.85 p.u for STATCOM when FACTS controllers were included. With SVC and STATCOM providing the required reactive power power to the grid, the total reactive power drawn by the grid decreased, allowing the grid to

recover from the fault situation. Again, STATCOM has a slight edge over SVC in terms of voltage support and reactive power supply operating time. STATCOM provided greater reactive power than SVC because to its V-Q curve, in which reactive power declines linearly with system voltage, while SVC reactive power decreases according to the square of system voltage.

For the line-to-line fault scenario, similar outcomes were obtained. Again, there were no trip circumstances. However, the FACTS controllers' assistance increased the voltage at B25. Once more, the STATCOM outperformed the SVC in response time, demonstrating that the STATCOM can generate more reactive power than the SVC, which generates less reactive power.

During the three-phase fault, one of the two sets of wind turbine generators tripped on the network without any FACTS controllers, but none of the generators tripped on the networks with FACTS controllers attached. Owing to the absence of reactive power assistance from the FACTS controllers, the grid struggled to regain stability that caused the undervoltage tripping condition. SVC and STATCOM provided the required assistance to increase the voltage level at B575 and avoid undervoltage conditions for any generators. In addition, in order to provide vital reactive power support, the SVC and STATCOM controllers increased the voltage levels to roughly 1 p.u. Due to SVC and STATCOM, the active power distribution from both grids maintained its near-rated generating capacity to the grid after the fault condition. Again, it was evident that the STATCOM could create more reactive power and respond faster than the SVC.

When the SVC and STATCOM controllers are attached to the electrical grid, simulation results in the MATLAB/Simulink environment indicate that their reactive power support to the network during fault situations has a significant impact on the voltage profile and reduces the recovery time following any fault. Both the SVC and STATCOM controllers functioned well, with STATCOM functioning somewhat faster under fault circumstances than SVC and giving more reactive power in the event of severe faults when the bus voltage was lower due to its more extensive V-Q characteristics curve.

CHAPTER SIX: CONCLUSION AND FUTURE WORK

6.1 Introduction

Conclusions are made regarding the work done in this chapter with regard to the objectives stated in chapter 1 and how the objectives have been met. Additionally, suggestions for future research are also provided. This dissertation presents FACTS controllers for improving voltage quality in wind energy conversion systems. SVC and STATCOM are the only FACTS controllers WECS has chosen to use. Hence only those two are taken into account in this dissertation.

SVC is one of the shunt-connected FACTS controllers, a crucial component for enhancing grid stability and voltage regulation. The SVC can regulate the voltage profile with appropriate reactive power absorption and injection. A thyristor-controlled reactor (TCR) for absorbing reactive power and a thyristor-switched capacitor (TSC) for injecting reactive power are only two reactive power control components that make up an SVC device. These components function as a controlled shunt susceptance to provide the appropriate reactive current based on the system voltage to which the SVC is attached.

To help stabilize and rectify faults in wind farms, another FACTS device called STATCOM was designed for induction machines. The output of STATCOM, a shunt-connected reactive power compensation device, may be adjusted to regulate certain parameters, and it can produce or absorb reactive power from its associated system. STATCOM injects or absorbs reactive power during steady-state to maintain a constant bus voltage and reduce voltage swings. Additionally, during any transient-state activity, the STATCOM will inject the maximum amount of reactive power to support the grid and restore the voltage level.

6.2 Objective – Specific conclusions

In chapter 1, seven objectives for this work were stated. The objectives stated were:

1. Identify the existing voltage problems correlating to the IEC 61400-21 international standard.
2. Understand the problem by researching existing research papers.
3. Investigate existing mitigation techniques that are used to control the problems.
4. Provide a clear summary of the problem and mitigation technique.
5. Use MATLAB/Simulink to create a dynamic model to achieve waveforms and see the voltage quality effects of a fault present in the grid.

6. Include the mitigation technique in the model and see how the fault impact is lessened.
7. Compare own simulation results to existing literature based on the same research area using MATLAB/Simulink to confirm the simulation results.

6.2.1 Objectives 1,2,3 and 4

Chapters 1 and 2 have discussed objectives 1, 2, 3, and 4. The voltage problems presented by harmonic distortions, voltage flickering and fluctuations, voltage unbalance, voltage sags, voltage swells, and under and overvoltage are highlighted in Chapter 1 when wind turbine generators are connected to the electrical grid. As the IEC 61400-21 standard specifies the power quality characteristics of the wind turbine for power generation, including voltage quality, it served as the focus point of this research.

The issues with voltage quality related to the IEC 61400-21 standard were the subject of Chapter 2 Understanding why the power quality of wind turbines linked to the grid declines is vital for the sector's development. Therefore, this chapter reviewed previously published research articles on the many issues relating to voltage quality, such as harmonic distortions, voltage flickering and fluctuations, voltage unbalance, voltage sags, voltage swells, undervoltage, and overvoltage.

Based on the former, research into current solutions for mitigating the consequences of power quality degradation has been made. According to studies on mitigation strategies covered by the IEC 61400-21 standard, FACTS controllers like SVC and STATCOM are used to compensate for reactive power utilized for voltage support during steady-state and transient-state circumstances in the electrical grid. The chapter goes into further detail on how the FACTS controllers work and support voltage.

6.2.2 Objective 5

Objective 5 has been addressed in chapters 3 and 4. In chapter 3, the mathematical modeling of individual system components is given with mathematical equations. It is essential to understand how these individual system components work and then integrate the individual components to achieve a model for a complete system. The mathematical modeling for the FACTS controllers is also included, as these controllers are used for the mitigation technique to improve the voltage quality.

Chapter 4 focussed on computer modeling in MATLAB/Simulink. Modeling on individual system components was done to get a brief description of each of the components in the system with its set parameters. Two complete dynamic models were built, including an SVC

and STATCOM model. A comparative analysis of the results of the two models was done to analyze which FACTS controller provides more voltage support during fault conditions.

6.2.3 Objectives 6 and 7

Chapter 5 has discussed objectives 6 and 7. The analysis of the simulation results for the reference models revealed how the FACTS controllers injected or absorbed reactive power to keep the grid's voltage profile near the reference voltage profile.

With the modeling for the reference model completed by confirming the FACTS controllers operate correctly, the results of the complete model without any FACTS controllers and the complete model that included the FACTS controllers for the mitigation were analyzed.

Under momentary fault situations, the dynamic models for SVC and STATCOM controllers attached to WECS networks were simulated. Momentary fault scenarios, including line-to-ground, line-to-line, and three-phase faults, resulted in the production of faults. During fault condition operations, the usefulness of SVC and STATCOM was proved via a variety of fault circumstances. For instance, both with and without attached FACTS controllers, the line-to-ground fault did not cause any tripping conditions for wind turbine generators. In addition, the bus voltage at B25 was increased to a healthier level due to the FACTS controllers' voltage support.

The line-to-line fault scenario had similar results. There were no trip conditions, however the FACTS controllers assisted in increasing the voltage at B25. During the three-phase failure, the grids with attached FACTS controllers did not encounter tripping circumstances. However, the absence of FACTS controllers in the grids caused one of the two sets of wind turbine generators to trip. The lack of reactive power support from the FACTS controllers prevented the grid from regaining stability, which resulted in an undervoltage tripping situation. Again, the SVC and STATCOM controllers provided the support necessary to deliver reactive power to the network and improve the voltage at bus B575 in order to avoid any generators from experiencing undervoltage conditions.

In chapter 5, it was showed how connecting FACTS controllers to the grid mitigated the effect of the fault. When the SVC and STATCOM controllers are linked to the network, reactive power support during severe faults or any lack of reactive power has a significant influence on the voltage level, as determined by simulation findings. Additionally, SVC and STATCOM work with the network to maintain the maximum power production of wind farms to the grid. Both SVC and STATCOM performed well, with STATCOM being somewhat faster than the SVC

controller and supplying more reactive power in the event of severe faults when the bus voltage was low.

Objective 7 was to research existing literature from a similar research area that used the MATLAB/Simulink software environment with models integrating FACTS controllers with WECS to get a baseline reference on what simulation results to expect. The results in chapter 5 confirmed the expected results as in the literature by observing that both SVC and STATCOM successfully contributed to voltage and reactive power support during fault condition operation. STATCOM was superior to SVC because STATCOM supplied more reactive power during low system voltage and performed faster due to the absence of thyristor switching delays.

6.3 Future work

This work has focused on reactive power compensating controllers such as SVC and STATCOM. The modeling in this work only focused on one reactive power compensating controller for each model at the PCC where the wind farm is connected to the grid. Further studies can be done using multiple compensating controllers at the PCC and along the transmission line and should determine if this is feasible. In addition, technology constantly improves as time goes by, so constant research should continue to find better mitigation techniques that perform faster and cost-effectively.

REFERENCES

- Abdelwanis, M.I., Abaza, A., El-Sehiemy, R.A., Ibrahim, M.N. & Rezk, H. 2020. Parameter Estimation of Electric Power Transformers Using Coyote Optimization Algorithm With Experimental Verification. *IEEE Access*, 8: 50036–50044.
- Abdin, Khan, S., Ahmad, N., Khan, H.A., Ahmed, S. & Hussain, M. 2021. Real Time Comparative Analysis of Induction Generator Using Stand Alone (Capacitor Excitation) Scheme and Grid Connected Scheme under Different Load Scenarios. In *2021 16th International Conference on Emerging Technologies (ICET)*. IEEE: 1–6.
- Ahmed, I. 2017. *Comparative Evaluation of Different Power Quality Issues of Variable Speed Wind Turbines*. Doctor of Philosophy. London: Brunel University London.
- Ahmed, S.D., Al-Ismail, F.S.M., Shafiullah, M., Al-Sulaiman, F.A. & El-Amin, I.M. 2020. Grid Integration Challenges of Wind Energy: A Review. *IEEE Access*, 8: 10857–10878.
- Almohaimed, S.A. & Abdel-Akher, M. 2020. Power Quality Issues and Mitigation for Electric Grids with Wind Power Penetration. *Applied Sciences*, 10(24): 8852.
- Aluko, A.O. 2018. *Modelling and performance analysis of doubly fed induction generator wind farm*. Master of Engineering. Durban, South Africa: Durban University of Technology.
- Aluko, A.O. & Akindeji, K.T. 2018. Mitigation of Low Voltage Contingency of Doubly FED Induction Generator Wind Farm Using Static Synchronous Compensator in South Africa. In *2018 IEEE PES/IAS PowerAfrica*. IEEE: 13–18.
- Ameur, A., Berrada, A., Loudiyi, K. & Aggour, M. 2019. Analysis of renewable energy integration into the transmission network. *The Electricity Journal*, 32(10): 106676.
- Ashida Salim, N., Mohamad, H., Mat Yasin, Z., Ab Aziz, N.F. & Azzammudin Rahmat, N. 2019. Graphical user interface based model for transmission line performance implementation in power system. *Indonesian Journal of Electrical Engineering and Computer Science*, 16(1): 92.
- Bajaj, M. & Singh, A.K. 2020. Grid integrated renewable DG systems: A review of power quality challenges and state-of-the-art mitigation techniques. *International Journal of Energy Research*, 44(1): 26–69.
- Barrios-Martínez, E. & Ángeles-Camacho, C. 2017. Technical comparison of FACTS controllers in parallel connection. *Journal of Applied Research and Technology*, 15(1): 36–44.
- Belati, E.A., Nascimento, C.F., de Faria, H., Watanabe, E.H. & Padilha-Feltrin, A. 2019. Allocation of Static Var Compensator in Electric Power Systems Considering Different Load Levels. *Journal of Control, Automation and Electrical Systems*, 30(1): 1–8.
- Bollen, M.H. & Moreno-Munoz, A. 2017. The power grid as part of a 100% renewable energy system. In A. Moreno-Munoz, ed. *Large Scale Grid Integration of Renewable Energy Sources*. Institution of Engineering and Technology: 1–27. https://digital-library.theiet.org/content/books/10.1049/pbpo098e_ch1 22 January 2022.
- Calasan, M., Jovanovic, A., Rubezic, V., Mujicic, D. & Deriszadeh, A. 2020. Notes on parameter estimation for single-phase transformer. *IEEE Transactions on Industry Applications*: 1–1.
- Ćalasan, M., Kecojević, K., Lukačević, O. & Ali, Z.M. 2021. Testing of influence of SVC and energy storage device's location on power system using GAMS. In A. F. Zobaa & S. H. E. Abdel Aleem, eds. *Uncertainties in Modern Power Systems*. Elsevier: 297–342.
- Čerňan, M., Müller, Z., Tlustý, J. & Valouch, V. 2021. An improved SVC control for electric arc furnace voltage flicker mitigation. *International Journal of Electrical Power & Energy Systems*, 129: 106831.
- Chamundeswari, V., Niraimathi, R., Shanathi, M. & Mahaboob Subahani, A. 2021. Renewable Energy Technologies. In M. Kathiresh, A. Mahaboob Subahani, & G. R. Kanagachidambaresan, eds. *Integration of Renewable Energy Sources with Smart Grid*. John Wiley & Sons, Ltd: 1–18.
- Chen, J. & Hu, W. 2021. MATLAB Simulation Research on Static Var Compensator. *E3S Web of Conferences*, 256: 01022.

- Cherkaoui, N., Haidi, T., Belfqih, A., Mariami, F. el & Boukherouaa, J. 2018. A Comparison Study of Reactive Power Control Strategies in Wind Farms with SVC and STATCOM. *International Journal of Electrical and Computer Engineering (IJECE)*, 8(6): 4836.
- Cisneros-Magaña, R., Medina, A. & Anaya-Lara, O. 2018. Time-Domain Voltage Sag State Estimation Based on the Unscented Kalman Filter for Power Systems with Nonlinear Components. *Energies*, 11(6): 1411.
- Davidson, C. & de Oliveira, M.M. 2020. Technical Description of Static Compensators (STATCOM). In B. R. Andersen & S. L. Nilsson, eds. *Flexible AC Transmission Systems*. Cham: Springer International Publishing: 207–251.
- Dey, R.S., Purkait, T., Kamboj, N. & Das, M. 2019. *Carbonaceous Materials and Future Energy*. Boca Raton: CRC Press.
- Du, P., Baldick, R. & Tuohy, A. 2017. *Integration of Large-Scale Renewable Energy into Bulk Power Systems*. Cham: Springer International Publishing.
- Ezhiljenekha, GB. & MarsalineBeno, M. 2020. Review of Power Quality Issues in Solar and Wind Energy. *Materials Today: Proceedings*, 24: 2137–2143.
- Fan, Z. & Zhu, C. 2019. The optimization and the application for the wind turbine power-wind speed curve. *Renewable Energy*, 140: 52–61.
- Fang, J. 2021a. Power Quality Conditioning. In *More-Electronics Power Systems: Power Quality and Stability*. Singapore: Springer Singapore: 93–134.
- Fang, J. 2021b. Power Quality Problems and Standards. In *More-Electronics Power Systems: Power Quality and Stability*. Singapore: Springer Singapore: 71–92.
- Fang, J. 2021c. Stability Problems. In *More-Electronics Power Systems: Power Quality and Stability*. Singapore: Springer Singapore: 135–182.
- Gandoman, F.H., Ahmadi, A., Sharaf, A.M., Siano, P., Pou, J., Hredzak, B. & Agelidis, V.G. 2018. Review of FACTS technologies and applications for power quality in smart grids with renewable energy systems. *Renewable and Sustainable Energy Reviews*, 82: 502–514.
- Ganthia, B.P., Barik, S.K. & Nayak, B. 2020. Shunt Connected FACTS Devices for LVRT Capability Enhancement in WECS. *Engineering, Technology & Applied Science Research*, 10(3): 5819–5823.
- Gianto, R. 2020. Steady State Model of Wind Power Plant for Load Flow Study. In *2020 International Seminar on Intelligent Technology and Its Applications (ISITIA)*. IEEE: 119–122.
- Gianto, R. & Purwoharjono, P. 2022. Two-port network model of wind turbine generator for three-phase unbalanced distribution system load flow analysis. *Bulletin of Electrical Engineering and Informatics*, 11(1): 9–19.
- Gupta, G. 2018. *An analysis and improvement of selected features of power quality of grid-tied alternative energy systems*. Bellville.
- Gupta, S. & Shukla, A. 2022. Improved dynamic modelling of DFIG driven wind turbine with algorithm for optimal sharing of reactive power between converters. *Sustainable Energy Technologies and Assessments*, 51: 101961.
- Haddadi, A., Farantatos, E., Kocar, I. & Karaagac, U. 2021. Impact of Inverter Based Resources on System Protection. *Energies*, 14(4): 1050.
- Hepsiba, D., Anand, L.D.V., Granty, R.E.J., Shajilin, J.B. & Shirley, D.R.A. 2021. Mitigation Measures for Power Quality Issues in Renewable Energy Integration and Impact of IoT in Grid Control. In M. Kathiresh, A. Mahaboob Subahani, & G. R. Kanagachidambaresan, eds. *Integration of Renewable Energy Sources with Smart Grid*. John Wiley & Sons, Ltd: 306–326.
- Hernández, M.R. 2012. Transmission Line Parameters. In L. L. Grigsby, ed. *Electric Power Generation, Transmission, and Distribution*. Florida: CRC Press: 14.1-14.35.
- Hossain, E., Tur, M.R., Padmanaban, S., Ay, S. & Khan, I. 2018. Analysis and Mitigation of Power Quality Issues in Distributed Generation Systems Using Custom Power Devices. *IEEE Access*, 6: 16816–16833.
- Hu, Y.-L., Wu, Y.-K., Chen, C.-K., Wang, C.-H., Chen, W.-T. & Cho, L.-I. 2017. A Review of the Low-Voltage Ride-Through Capability of Wind Power Generators. *Energy Procedia*, 141: 378–382.

- Infield, D. & Freris, L. 2020. *Renewable Energy in Power Systems*. 2nd ed. John Wiley & Sons Ltd.
- Jena, R., Swain, S.C. & Dash, R. 2021. Power flow simulation & voltage control in a SPV IEEE-5 bus system based on SVC. *Materials Today: Proceedings*, 39: 1934–1940.
- Jerin A, R.A., Kaliannan, P. & Subramaniam, U. 2018. Testing of low-voltage ride through capability compliance of wind turbines – a review. *International Journal of Ambient Energy*, 39(8): 891–897.
- Kamel, B.K., Omran, W.A. & Attia, M.A. 2021. Enhancement of Wind Energy Conversion System Voltage Stability by Using STATCOM with Different Controllers. In *2021 16th International Conference on Computer Engineering and Systems (ICCES)*. IEEE: 1–6.
- Kannan, R. & Ali, J.S. 2017. Power quality definitions. In A. F. Zobaa & S. H. Abdel Aleem, eds. *Power Quality in Future Electrical Power Systems*. Institution of Engineering and Technology: 1–27.
- Kaushal, J. & Basak, P. 2020. Power quality control based on voltage sag/swell, unbalancing, frequency, THD and power factor using artificial neural network in PV integrated AC microgrid. *Sustainable Energy, Grids and Networks*, 23: 100365.
- Lee, H., Bae, M. & Lee, B. 2017. Advanced Reactive Power Reserve Management Scheme to Enhance LVRT Capability. *Energies*, 10(10): 1540.
- Liang, X. 2017. Emerging Power Quality Challenges Due to Integration of Renewable Energy Sources. *IEEE Transactions on Industry Applications*, 53(2): 855–866.
- Mahela, O.P., Gupta, N., Khosravy, M. & Patel, N. 2019. Comprehensive Overview of Low Voltage Ride Through Methods of Grid Integrated Wind Generator. *IEEE Access*, 7: 99299–99326.
- Mahela, O.P. & Shaik, A.G. 2016. Comprehensive overview of grid interfaced wind energy generation systems. *Renewable and Sustainable Energy Reviews*, 57: 260–281.
- Melkebeek, J.A. 2018. *Electrical Machines and Drives*. Cham: Springer International Publishing.
- Mikkili, S. & Panda, A.K. 2016. *Power Quality Issues*. 1st ed. Boca Raton: CRC Press.
- Mikwar, A. 2017. *Modeling of Hybrid STATCOM in PSSE*. Masters Thesis. Stockholm, Sweden: KTH Royal Institute of Technology.
- Misak, S. & Prokop, L. 2017. *Operation Characteristics of Renewable Energy Sources*. Cham: Springer International Publishing.
- Mishra, S., Sharma, D., Singh, S.N., Lee, K.Y., Farsangi, M.M., Nezamabadi-pour, H., Voumvoulakis, E.M., Hatziargyriou, N.D., Wu, X. & Ma, L. 2020. POWER SYSTEM AND POWER PLANT CONTROL. In K. Y. Lee & Z. A. Vale, eds. *Applications of Modern Heuristic Optimization Methods in Power and Energy Systems*. John Wiley & Sons: 227–380.
- Moghadas, A., Sarwat, A. & Guerrero, J.M. 2016. A comprehensive review of low-voltage-ride-through methods for fixed-speed wind power generators. *Renewable and Sustainable Energy Reviews*, 55: 823–839.
- Molina-Garcia, A., Hansen, A.D., Muljadi, E., Gevorgian, V., Fortmann, J. & Gomez-Lazaro, E. 2017. International requirements for large integration of renewable energy sources. In A. Moreno-Munoz, ed. *Large Scale Grid Integration of Renewable Energy Sources*. Institution of Engineering and Technology: 29–57. https://digital-library.theiet.org/content/books/10.1049/pbpo098e_ch2 22 January 2022.
- Morshed, M.J. 2018. *Fault Ride-Through Control Paradigms for DFIG-Based Wind Turbines*. Doctor of Philosophy . University of Louisiana at Lafayette.
- de Moura, A.P., de Moura, A.A.F. & da Rocha, E.P. 2020. *Transmission of Electrical Energy*. Boca Raton, FL: CRC Press.
- Murali, M., Gokhale, A., Pandey, A.V. & Sharma, E. 2016. Modelling, design and comparison of PI and PID controllers for Static Synchronous Compensator (STATCOM). In *2016 IEEE 1st International Conference on Power Electronics, Intelligent Control and Energy Systems (ICPEICES)*. IEEE: 1–6.
- Musoni, N.E. 2018. *Analysis of the effect of renewable generation on the power quality of the grid, modelling and analysis of harmonic and voltage distortion*. Master of Engineering. Bellville: Cape Peninsula University of Technology.

- Naderi, Y., Hosseini, S.H., Ghassem Zadeh, S., Mohammadi-Ivatloo, B., Vasquez, J.C. & Guerrero, J.M. 2018. An overview of power quality enhancement techniques applied to distributed generation in electrical distribution networks. *Renewable and Sustainable Energy Reviews*, 93: 201–214.
- Nhlapo, B. & Awodele, K. 2020. Review and comparison of the South African grid code requirements for wind generation with the European countries' grid codes. In *2020 International SAUPEC/RobMech/PRASA Conference*. IEEE: 1–6.
- Nobela, O.N., Bansal, R.C. & Justo, J.J. 2019. A review of power quality compatibility of wind energy conversion systems with the South African utility grid. *Renewable Energy Focus*, 31: 63–72.
- Noussi, K., Abouloifa, A., Katir, H. & Lachkar, I. 2019. Modeling and Control of a Wind Turbine Based On a Doubly Fed Induction Generator. In *2019 4th World Conference on Complex Systems (WCCS)*. IEEE: 1–5.
- Omran, A.S., Abbasy, N.H. & Hamdy, R.A. 2018. Enhanced performance of substation dynamics during large induction motor starting using SVC. *Alexandria Engineering Journal*, 57(4): 4059–4070.
- Ouyang, J., Tang, T., Yao, J. & Li, M. 2019. Active Voltage Control for DFIG-Based Wind Farm Integrated Power System by Coordinating Active and Reactive Powers Under Wind Speed Variations. *IEEE Transactions on Energy Conversion*, 34(3): 1504–1511.
- Paredes, L.A., Molina, M.G., Pozo, M. & Serrano, B.R. 2021. Improvement of Dynamic Voltage Stability in a Resilient Microgrid based on Smart Inverters & SVC. In *2021 IEEE Fifth Ecuador Technical Chapters Meeting (ETCM)*. IEEE: 1–6.
- Park, C. & Jang, G. 2016. Voltage quality assessment considering low voltage ride-through requirement for wind turbines. *IET Generation, Transmission & Distribution*, 10(16): 4205–4212.
- Pekdemir, A. & Yildiz, A.B. 2018. Analysis and modelling of FC-TCR based on static VAR compensator. In *2018 5th International Conference on Electrical and Electronic Engineering (ICEEE)*. IEEE: 115–118.
- Perera, S. & Elphick, S. 2023. Impact and management of voltage fluctuations, flicker and rapid voltage changes. In *Applied Power Quality*. Elsevier: 131–146.
- Ponce, P., Molina, A., Mata, O., Ibarra, L. & MacCleery, B. 2017. *Power System Fundamentals*. CRC Press.
- Popavath, L. & Kaliannan, P. 2018. Photovoltaic-STATCOM with Low Voltage Ride through Strategy and Power Quality Enhancement in a Grid Integrated Wind-PV System. *Electronics*, 7(4): 51.
- Rahmouni, A. 2020. Impact of static reactive power compensator (SVC) on the power grid. *WSEAS TRANSACTIONS ON ELECTRONICS*, 11: 96–104.
- Rezaie, H. & Kazemi-Rahbar, M.H. 2019. Enhancing voltage stability and LVRT capability of a wind-integrated power system using a fuzzy-based SVC. *Engineering Science and Technology, an International Journal*, 22(3): 827–839.
- Rini Ann Jerin, A., Kaliannan, P., Subramaniam, U. & Shawky El Moursi, M. 2018. Review on FRT solutions for improving transient stability in DFIG-WTs. *IET Renewable Power Generation*, 12(15): 1786–1799.
- Rosin, A., Drovtar, I. & Kilter, J. 2017. Solutions and active measures for wind power integration. In A. Moreno-Munoz, ed. *Large Scale Grid Integration of Renewable Energy Sources*. Institution of Engineering and Technology: 87–129. https://digital-library.theiet.org/content/books/10.1049/pbpo098e_ch4 22 January 2022.
- Roy, N.K. & Das, A. 2018. Prospects of Renewable Energy Sources. In Md. R. Islam, N. K. Roy, & S. Rahman, eds. *Renewable Energy and the Environment*. Singapore: Springer Singapore: 1–39.
- Salam, Md.A. 2020. *Fundamentals of Electrical Power Systems Analysis*. Singapore: Springer Singapore.
- Sallam, A.A. & Malik, O.P. 2020. *Power Grids with Renewable Energy: Storage, integration and digitalization*. A. A. Sallam & O. P. Malik, eds. London, United Kingdom: Institution of Engineering and Technology.

- Satpathy, A., Kastha, D. & Kishore, N.K. 2021. Vienna Rectifier-Fed Squirrel Cage Induction Generator Based Stand-Alone Wind Energy Conversion System. *IEEE Transactions on Power Electronics*, 36(9): 10186–10198.
- Shakeri, S., Esmaeili, S. & Rezaeian Koochi, M.H. 2020. Determining accurate area of vulnerability for reliable voltage sag assessment considering wind turbine ride-through capability. *International Journal of Electrical Power & Energy Systems*, 119: 105875.
- Sharma, J., Rangarajan, S.S., Srikanth, V.S.S., Sundarabalan, C.K., Kothari, D.P. & Senjyu, T. 2021. Transient Stability Enhancement Using FACTS Devices in a Distribution System Involving Distributed Generation Systems. In M. J. B. Reddy, D. Kr. Mohanta, D. Kumar, & D. Ghosh, eds. *Advances in Smart Grid Automation and Industry 4.0, Lecture Notes in Electrical Engineering*. Singapore: Springer Singapore: 507–515.
- Siahpoosh, M.K. 2019. *Issues with the delivery of power quality in wind farms*. Doctor of philosophy. Sydney: University of technology Sydney.
- Silva, E.O., Vanco, W.E. & Guimaraes, G.C. 2020. Capacitor Bank Sizing for Squirrel Cage Induction Generators Operating in Distributed Systems. *IEEE Access*, 8: 27507–27515.
- Singh, B. & Agrawal, G. 2018. Enhancement of voltage profile by incorporation of SVC in power system networks by using optimal load flow method in MATLAB/Simulink environments. *Energy Reports*, 4: 418–434.
- Sivaraman, P. & Sharmeela, C. 2021. Power quality and its characteristics. In P. Sanjeevikumar, C. Sharmeela, J. Bo Holm-Nielsen, & P. Sivaraman, eds. *Power Quality in Modern Power Systems*. Elsevier: 1–60.
- Solanki, S. & Mittal, S.C. 2017. Study of 6MW wind farm with and without STATCOM using MATLAB/SIMULINK. In *2017 International Conference on Information, Communication, Instrumentation and Control (ICICIC)*. IEEE: 1–7.
- Tawfiq, K.B., Abdou, A.F. & EL-Kholy, E.E. 2018. Wind Energy System with Matrix Converter. In Md. R. Islam, N. K. Roy, & S. Rahman, eds. *Renewable Energy and the Environment*. Singapore: Springer Singapore: 143–174.
- Todeschini, G. 2017. Shunt flexible a.c. transmission. In A. F. Zobaa & S. H. Abdel Aleem, eds. *Power Quality in Future Electrical Power Systems*. Institution of Engineering and Technology: 165–204.
- Vetoshkin, L., Votava, J., Kyncl, J. & Muller, Z. 2019. Improvement of transient stability using STATCOM combined with optimization. In *2019 20th International Scientific Conference on Electric Power Engineering (EPE)*. IEEE: 1–5.
- Vishnupriyan, J. & Dhanasekaran, A. 2021. Challenges in Planning and Operation of Large-Scale Renewable Energy Resources Such as Solar and Wind. In M. Kathiresan, A. Mahaboob Subahani, & G. R. Kanagachidambaresan, eds. *Integration of Renewable Energy Sources with Smart Grid*. John Wiley & Sons, Ltd: 263–279.
- Wang, K., Gao, S., Shi, Z., Liu, L., Ren, A., Wang, Y., Tian, L. & Gao, J. 2020. Research on Reactive Power Coordinated Control Strategy of Doubly-Fed Wind Farm Considering STATCOM. In *2020 IEEE 4th Conference on Energy Internet and Energy System Integration (EI2)*. IEEE: 1275–1279.
- Weber, G.H. 2018. *Characterization of transmission lines based on frequency-domain and time-domain measurement techniques*. Parana. Curitiba: Federal University of Technology.
- Xu, L., Tang, Y.-H., Pu, W. & Han, Y. 2014. Hybrid electromechanical-electromagnetic simulation to SVC controller based on ADPSS platform. *Journal of Energy in Southern Africa*, 25(4): 112–122.
- Zare Oskouei, M. & Mohammadi-Ivatloo, B. 2020. *Integration of Renewable Energy Sources Into the Power Grid Through PowerFactory*. Cham: Springer International Publishing.
- Zobaa, A.F., Ahmed, I. & Abdel Aleem, S.H.E. 2019. A Comprehensive Review of Power Quality Issues and Measurement for Grid-Integrated Wind Turbines. *Recent Advances in Electrical & Electronic Engineering (Formerly Recent Patents on Electrical & Electronic Engineering)*, 12(3): 210–222.
- Zohuri, B. 2019a. Electricity Production and Renewable Source of Energy, Economics. In *Small Modular Reactors as Renewable Energy Sources*. Cham: Springer International Publishing: 229–245.

- Zohuri, B. 2019b. Energy Storage Technologies and Their Role in Renewable Integration. In *Small Modular Reactors as Renewable Energy Sources*. Cham: Springer International Publishing: 247–290.
- Zohuri, B. 2018. Types of Renewable Energy. In *Hybrid Energy Systems*. Cham: Springer International Publishing: 105–133.

APPENDIX A: Computer modeling components

8.1 Three-phase programmable voltage source

The three-phase programmable voltage source block has a programmable function to set the time variation of the amplitude, phase, frequency, and harmonics of the fundamental component of the source. Figure 8.1 and Figure 8.2 illustrate the icon of the component used in the computer modeling and the setup of this block, where the time variation of amplitude will be discussed later. This voltage and frequency have been set at 120 kV and 60 Hz, respectively.

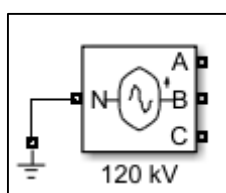


Figure 8.1: Three-phase programmable voltage source icon

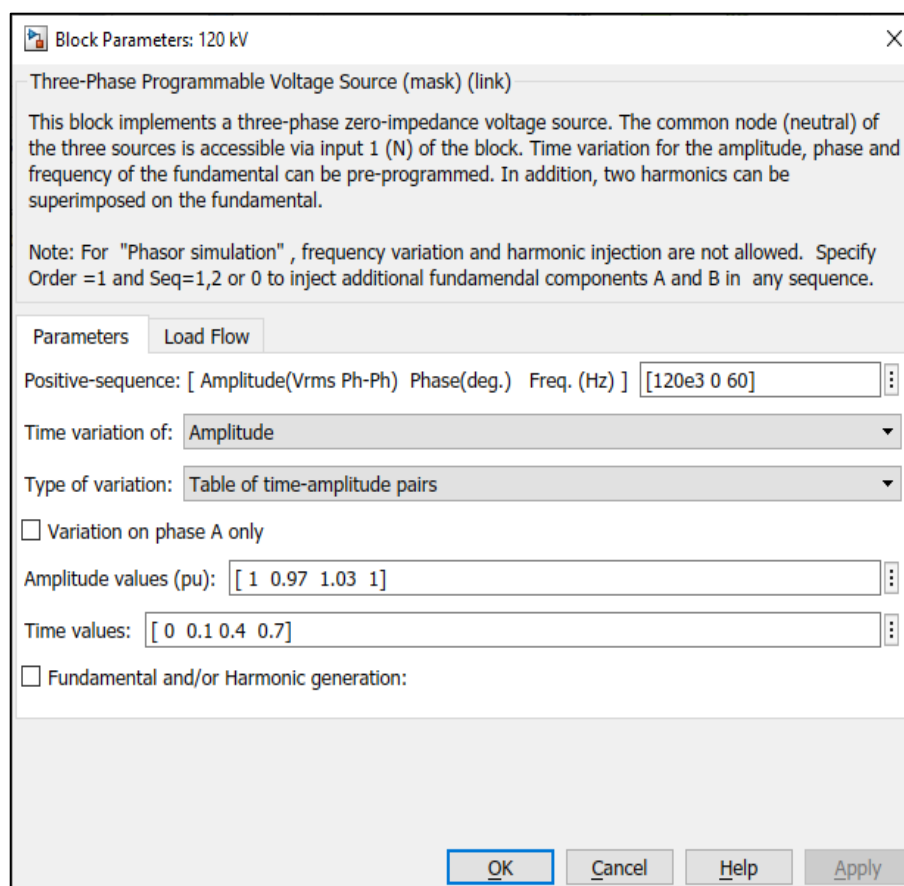


Figure 8.2: Three-phase programmable voltage source setup

8.2 Three-phase mutual inductance Z1-Z0

The three-phase mutual inductance block performs the same as the three-winding inductance block that provides a set of three coupled inductors or windings to implement balanced three-phase inductive and resistive impedance to the grid with mutual coupling between the three phases. For a balanced three-phase system, the positive- and zero-sequence resistances and inductances are entered in this block. Figure 8.3 and Figure 8.4 illustrate the icon of the component used in the computer modeling and the setup of this block.

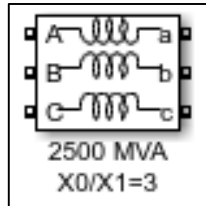


Figure 8.3: Three-phase mutual inductance Z1-Z0 icon

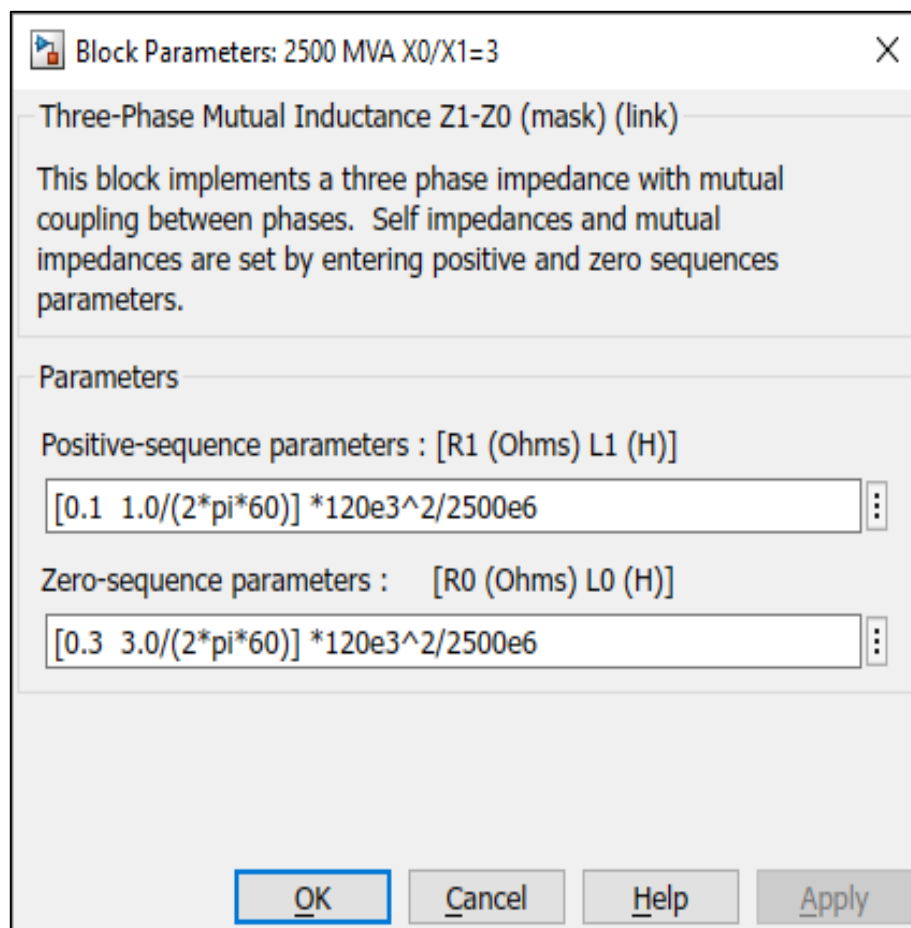


Figure 8.4: Three-phase mutual inductance Z1-Z0 setup

8.3 Three-phase transformer

The three-phase transformer block is used to implement a three-phase transformer that uses three single-phase transformers. This transformer is used as a step-down transformer that transforms the grid voltage from 120 kV to 25 kV, where the nominal power and frequency are set at 47 Mega volt-ampere (MVA) and 60 Hz, respectively. Figure 8.5 and Figure 8.6 illustrate the icon of the component used in the computer modeling and the setup of this block.

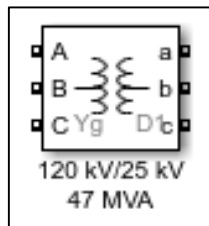


Figure 8.5: Three-phase transformer icon

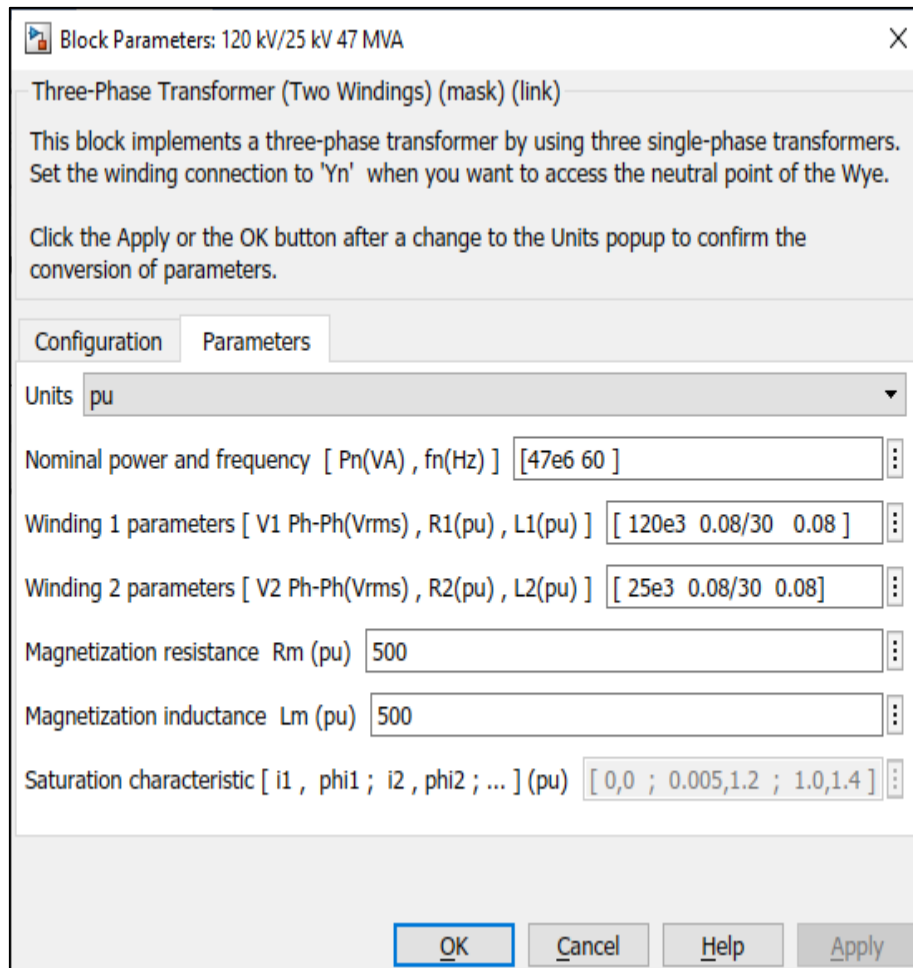


Figure 8.6: Three-phase transformer setup

8.4 Grounding transformer

The grounding transformer creates a ground path for the delta-connected step-down transformer. The terminal voltage for the grounding transformer is 25 kV, where the nominal power and frequency are set at 100 MVA and 60 Hz, respectively. Figure 8.7 and Figure 8.8 illustrates the icon of the component used in the computer modeling and the setup of this block.

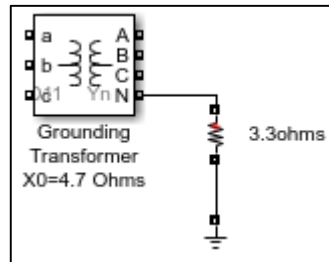


Figure 8.7: Grounding transformer icon

Figure 8.8: Grounding transformer setup

8.5 Three-phase PI Section

The three-phase pi section line block implements a balanced three-phase transmission line model where the resistance, inductance, and capacitance are uniformly distributed along the transmission line in a pi section. The line length is considered to be 25 km. Figure 8.9 and Figure 8.10 illustrate the icon of the component used in the computer modeling and the setup of this block.

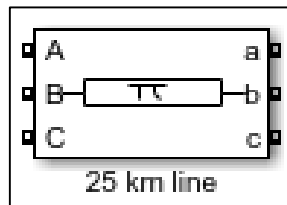


Figure 8.9: Three-phase PI Section icon

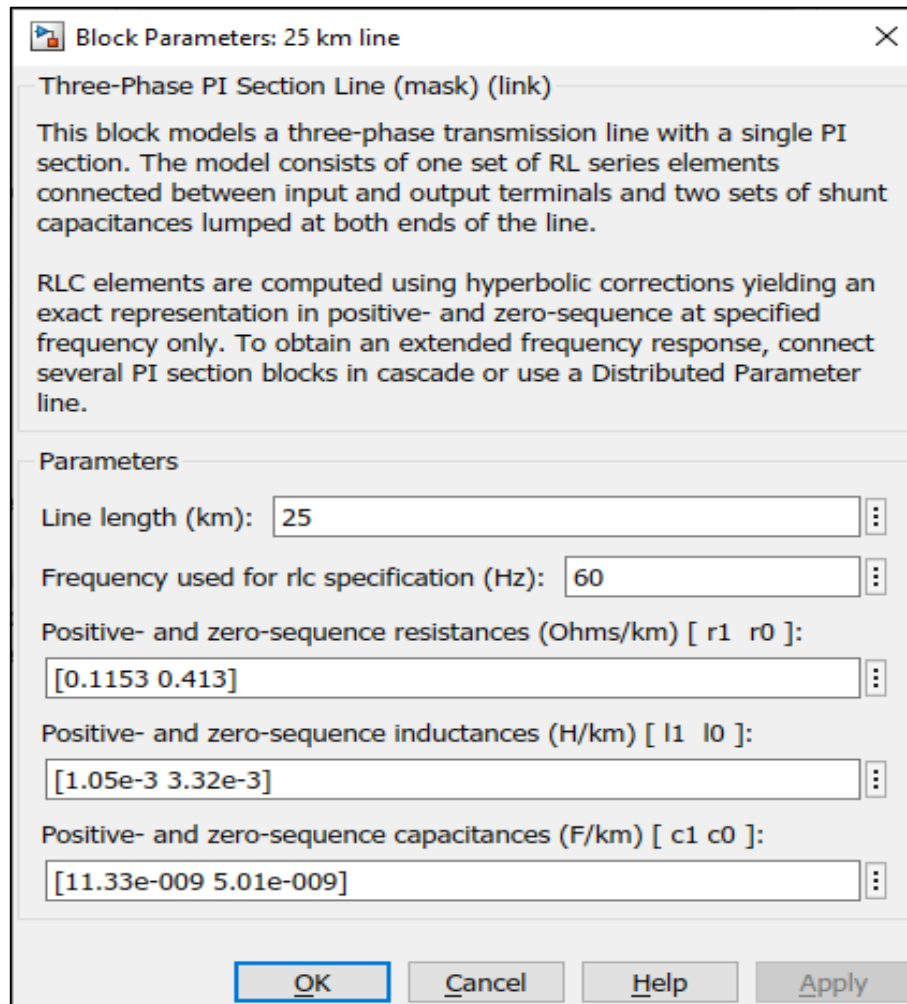


Figure 8.10: Three-phase PI section setup

8.6 Three-phase parallel RLC load

The three-phase parallel RLC load block implements a balanced three-phase load as a parallel combination of resistance, inductance, and capacitance elements. The nominal phase-to-phase voltage is 25 kV, with the 2 MW load at 60 Hz grid frequency. Figure 8.11 and Figure 8.12 illustrate the icon of the component used in the computer modeling and the setup of this block.

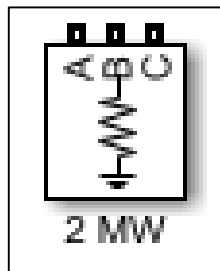
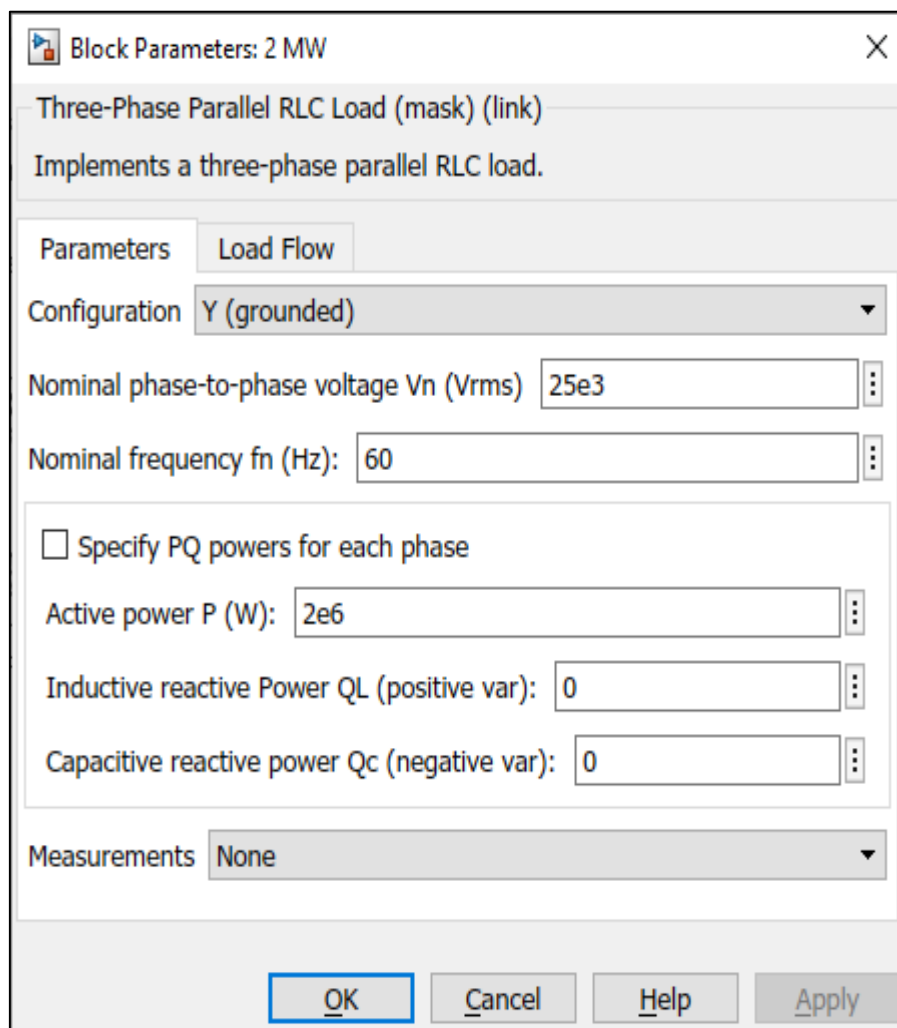


Figure 8.11: Three-phase parallel RLC load icon



Block Parameters: 2 MW

Three-Phase Parallel RLC Load (mask) (link)

Implements a three-phase parallel RLC load.

Parameters Load Flow

Configuration Y (grounded)

Nominal phase-to-phase voltage V_n (Vrms) 25e3

Nominal frequency f_n (Hz): 60

Specify PQ powers for each phase

Active power P (W): 2e6

Inductive reactive Power Q_L (positive var): 0

Capacitive reactive power Q_c (negative var): 0

Measurements None

OK Cancel Help Apply

Figure 8.12: Three-phase parallel RLC load setup

8.7 Three-phase V-I measurement

The three-phase V-I measurement block measures three-phase voltage and current within the electrical grid and returns the measured values. This block can be connected in series with three-phase elements. The block returns measured three-phase, phase-to-ground, or phase-to-phase voltages with all phase line currents. A base power of 3 MVA and 25 kV are considered for the per-unit measurements. Figure 8.13 and Figure 8.14 illustrate the icon of the component used in the computer modeling and the setup of this block.

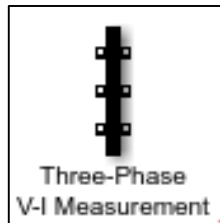
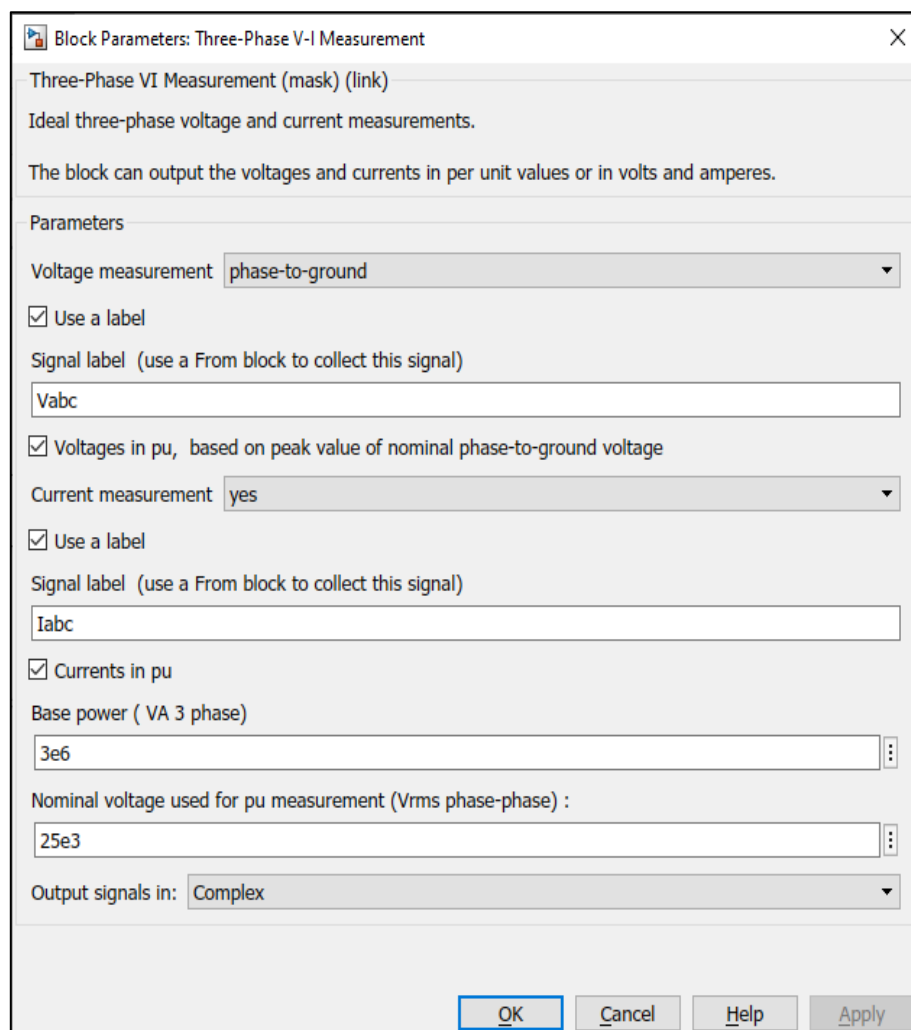


Figure 8.13: Three-phase V-I measurement icon



Block Parameters: Three-Phase V-I Measurement

Three-Phase VI Measurement (mask) (link)

Ideal three-phase voltage and current measurements.

The block can output the voltages and currents in per unit values or in volts and amperes.

Parameters

Voltage measurement: phase-to-ground

Use a label

Signal label (use a From block to collect this signal): Vabc

Voltages in pu, based on peak value of nominal phase-to-ground voltage

Current measurement: yes

Use a label

Signal label (use a From block to collect this signal): Iabc

Currents in pu

Base power (VA 3 phase): 3e6

Nominal voltage used for pu measurement (Vrms phase-phase): 25e3

Output signals in: Complex

OK Cancel Help Apply

Figure 8.14: Three-phase V-I measurement setup

8.8 Three-Phase Fault

The three-phase fault block is used to implement a short-circuit fault between any of the three phases of the electrical grid, either phase-to-phase or phase-to-ground. Switching time is presented when the fault should occur and when the fault should be cleared. Figure 8.15 and Figure 8.16 illustrate the icon of the component used in the computer modeling and the setup of this block.

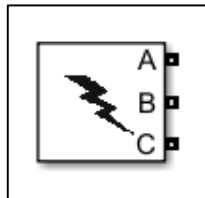


Figure 8.15: Three-phase fault block icon

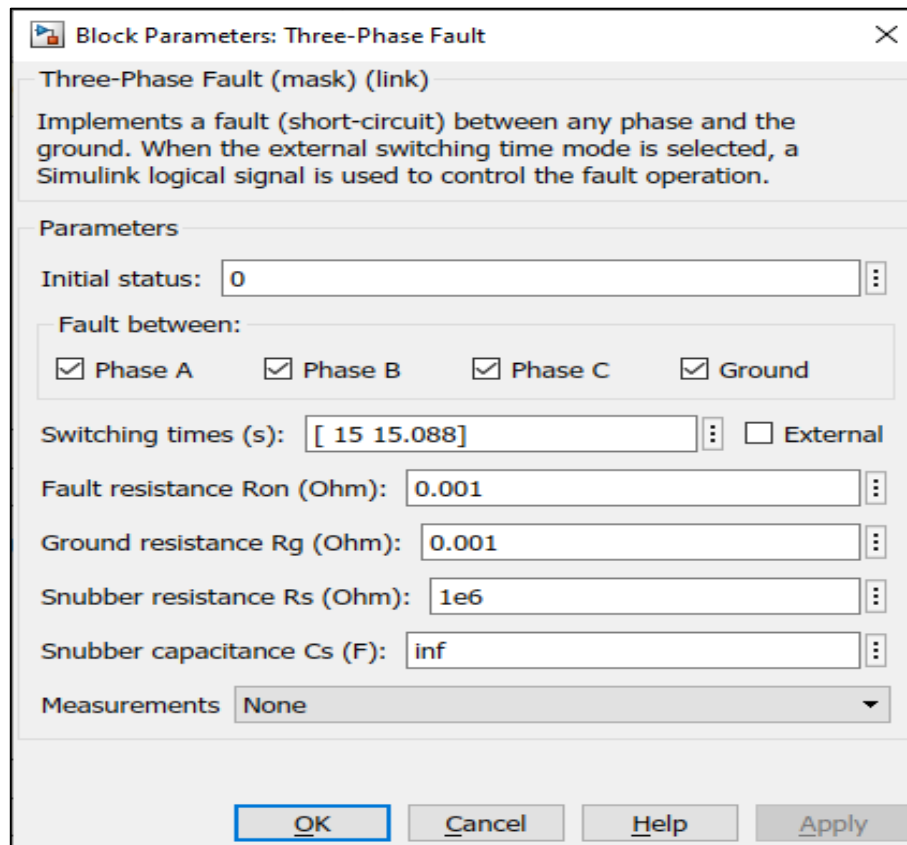


Figure 8.16: Three-phase fault block setup

8.9 Three-Phase Series RLC Load

The three-phase series RLC load block implements a balanced three-phase load as a parallel combination of resistance, inductance, and capacitance elements. The nominal phase-to-phase voltage is 575 V, with the load being a capacitor supplying reactive power of 400 kilovolt-ampere reactive (kVAR) at 60 Hz grid frequency. Figure 8.17 and Figure 8.18 illustrate the icon of the component used in the computer modeling and the setup of this block.

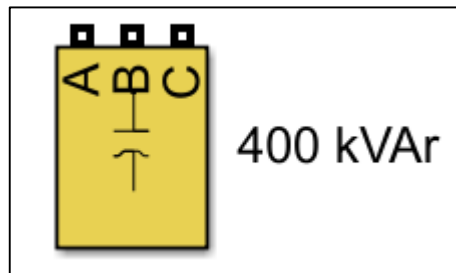


Figure 8.17: Three-Phase series RLC Load block icon

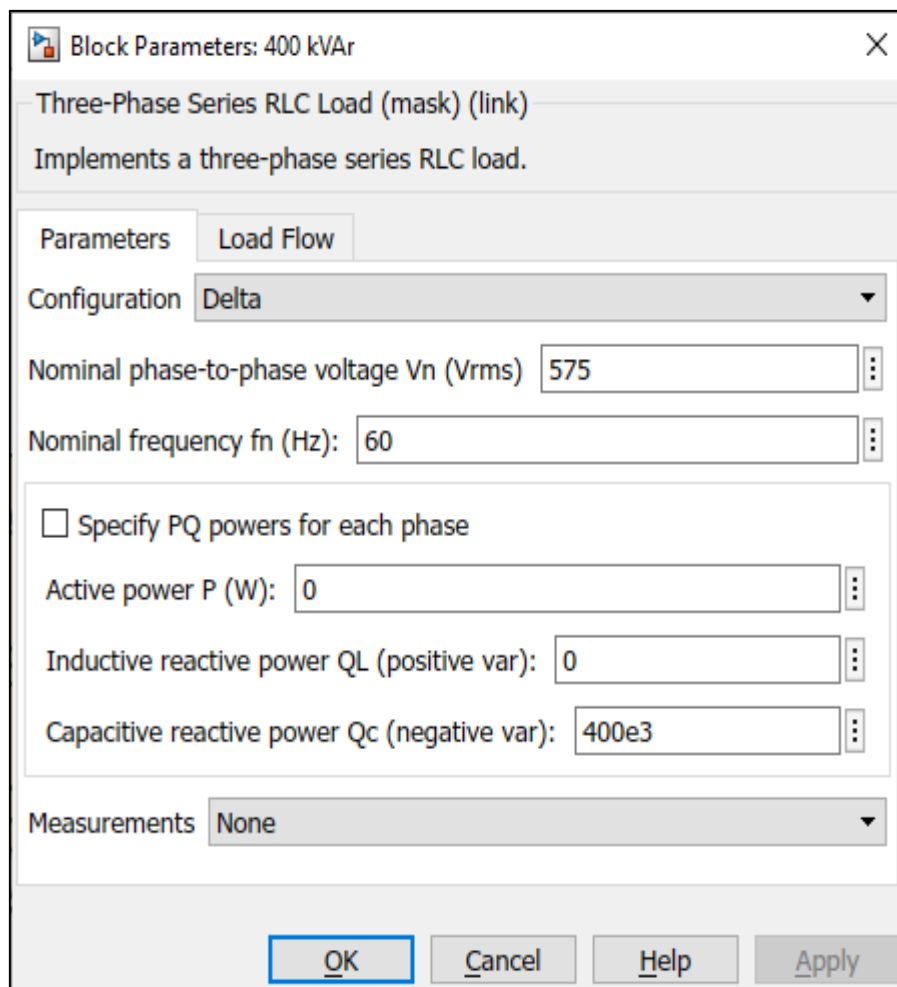


Figure 8.18: Three-Phase series RLC Load setup block

APPENDIX B: Reference model parameters and computer model

Table 9.1: Parameters of the reference WECS model

| Parameters of the electrical grid | | | | |
|-------------------------------------|------------|-----------|--------------------|------|
| Parameter | | Value | Unit | |
| Rated voltage | | 69 | kV | |
| Frequency | | 60 | Hz | |
| Parameters of transformers | | | | |
| Parameter | Value | Unit | Value | Unit |
| Transformer | 69/13.8 | kV | 15 | MVA |
| Transformer | 13.8/0.575 | kV | 6 | MVA |
| Transformer | 13.8/2.3 | kV | 3 | MVA |
| Transformer | 2.3/0.480 | kV | 1 | MVA |
| Parameters of the transmission line | | | | |
| Parameter | | Value | Unit | |
| Positive-sequence resistances | | 0.1153 | Ω/km | |
| Positive-sequence inductances | | 1.05 e-3 | H/km | |
| Positive-sequence capacitances | | 11.33 e-9 | F/km | |
| Length of transmission line | | 2.05 | km | |
| Length of transmission line | | 3.05 | km | |
| Parameters of the loads | | | | |
| Parameter | | Value | Unit | |
| Three-phase load | | 500 | kW | |
| Three-phase load | | 200 | kW | |
| Three-phase load | | 570 | kW | |
| Three-phase load | | 470 | k Ω | |
| 2300V Three-phase electrical motor | | 1.68 | MW | |
| Parameters of the capacitor | | | | |
| Parameter | | Value | Unit | |
| Rated voltage | | 2300 | V | |
| Capacitive reactive power | | 800 | kVar | |
| Parameters of the wind farm | | | | |
| Parameter | | Value | Unit | |
| Rated wind farm power | | 4.5 | MW | |
| Base wind speed | | 12 | m/s | |
| Rated power of wind turbine | | 1.5 | MW | |
| Number of wind turbines | | 3 | - | |
| Generator type | | DFIG | - | |
| Rated voltage | | 575 | V | |
| Stator resistance | | 0.00706 | pu | |
| Stator inductance | | 0.171 | pu | |
| Rotor resistance | | 0.005 | pu | |
| Rotor inductance | | 0.156 | pu | |
| Magnetizing inductance | | 2.9 | pu | |
| Pole pairs | | 3 | - | |
| Inertia constant | | 5.04 | s | |

Table 9.2: Parameters of the reference FACTS controllers

| Parameters of the SVC | | |
|--------------------------------|--------------------|------|
| Parameter | Value | Unit |
| Rated voltage | 13.8 | kV |
| Frequency | 60 | Hz |
| Rated power | 3 | MVar |
| Thyristor switching delay time | 4 e-3 | s |
| Mode | Voltage regulation | - |
| Voltage reference | 1 | p.u |
| Drop reactance | 0.03 | p.u |
| Voltage Regulator gains Kp | 0 | - |
| Voltage Regulator gains Ki | 500 | - |
| Parameters of the STATCOM | | |
| Parameter | Value | Unit |
| Rated voltage | 13.8 | kV |
| Frequency | 60 | Hz |
| Rated power | 3 | MVar |
| DC link voltage | 4000 | V |
| DC link equivalent capacitance | 1125 | uF |
| Mode | Voltage regulation | - |
| Voltage reference | 1 | p.u |
| Drop reactance | 0.03 | p.u |
| Voltage Regulator gains Kp | 5 | - |
| Voltage Regulator gains Ki | 1000 | - |

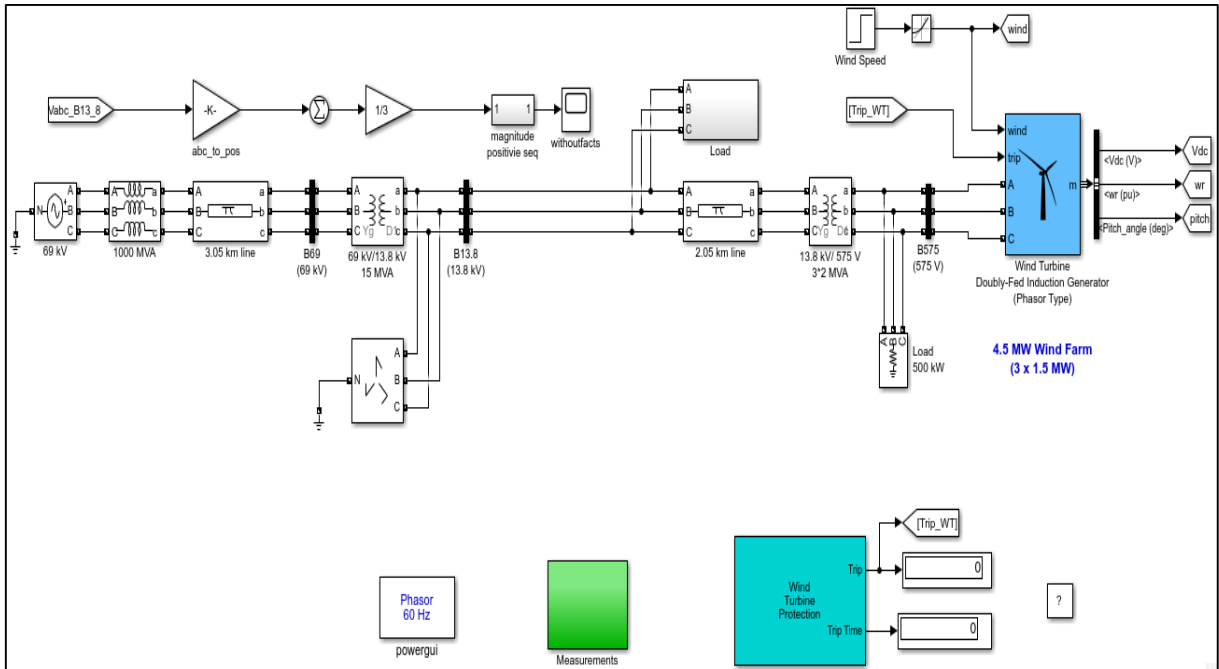


Figure 9.1: Complete reference model without FACTS controller